EXPERIMENTAL STUDY AND IMPROVEMENT ON TRIBOLOGICAL BEHAVIORS OF AUTOMOTIVE LUBRICANTS WITH DILUTION OF VARIOUS GASOLINE-BIOETHANOL BLENDS

LEANG SO KHUONG

FACULTY OF ENGINEERING
UNIVERSITY OF MALAYA
KUALA LUMPUR

2017

EXPERIMENTAL STUDY AND IMPROVEMENT ON TRIBOLOGICAL BEHAVIORS OF AUTOMOTIVE LUBRICANTS WITH DILUTION OF VARIOUS GASOLINE-BIOETHANOL BLENDS

LEANG SO KHUONG

DISSERTATION SUBMITTED IN FULFILMENT OF THE REQUIREMENTS FOR THE DEGREE OF MASTER OF ENGINEERING SCIENCE

FACULTY OF ENGINEERING
UNIVERSITY OF MALAYA
KUALA LUMPUR

2017

UNIVERSITY OF MALAYA
ORIGINAL LITERARY WORK DECLARATION

Name of Candidate: **LEANG SO KHUONG**

Registration/Matric No: **KGA150041**

Name of Degree: **Masters of Engineering Science**

Title of Project Paper/Research Report/Dissertation/Thesis ("this Work"):

EXPERIMENTAL STUDY AND IMPROVEMENT ON TRIBOLOGICAL BEHAVIORS OF AUTOMOTIVE LUBRICANTS WITH DILUTION OF VARIOUS GASOLINE-BIOETHANOL BLENDS

Field of Study: Energy, Tribology

I do solemnly and sincerely declare that:

(1) I am the sole author/writer of this Work;
(2) This Work is original;
(3) Any use of any work in which copyright exists was done by way of fair dealing and for permitted purposes and any excerpt or extract from, or reference to or reproduction of any copyright work has been disclosed expressly and sufficiently and the title of the Work and its authorship have been acknowledged in this Work;
(4) I do not have any actual knowledge nor do I ought reasonably to know that the making of this work constitutes an infringement of any copyright work;
(5) I hereby assign all and every rights in the copyright to this Work to the University of Malaya ("UM"), who henceforth shall be owner of the copyright in this Work and that any reproduction or use in any form or by any means whatsoever is prohibited without the written consent of UM having been first had and obtained;
(6) I am fully aware that if in the course of making this Work I have infringed any copyright whether intentionally or otherwise, I may be subject to legal action or any other action as may be determined by UM.

Candidate's Signature Date:

Subscribed and solemnly declared before,

Witness's Signature Date:

Name:

Designation:

ABSTRACT

Concerns over depleting fossil fuel reserves and climate change have resulted in stringent legislation demanding automobiles use more renewable fuels in particular bioethanol, which is being considered as a long-term gasoline replacement. However, the piston ring and cylinder wall interface, which is the largest contributor to engine friction, suffers the highest levels of fuel dilution into the lubricant from unburned fuel, especially bioethanol that has high heat of vaporization to enhance the tendency of fuel dilution in the crankcase. Recently, bioethanol is blended with gasoline at increasingly higher concentrations and the accumulation of fuel in the crankcase is significant. Therefore, it is crucial to study the effect of various bioethanol-gasoline blends on properties degradation and tribological characteristics of engine oil as well as improving friction and wear behaviors of bioethanol-diluted engine oil. This research provides insight into using higher bioethanol blend and bioethanol-resistance lubricant formulation.

In this study, three objectives were achieved to understand properties degradation and tribological behaviors and improvement of lubricant with bioethanol dilution. In the first study, five bioethanol-gasoline blends are formulated, namely, pure gasoline (E0), and gasoline blended with ethanol at different percentage volumes (10, 20, 30 and 85%, designated as E10, E20, E30, and E85, respectively). These fuels are then blended with synthetic oil (SO) at a dilution rate of 6 vol.%. These fuel-oil mixtures were then tested in four-ball wear tester according to ASTM D4172 standard test. The four-ball machine enables to investigate friction and wear of bioethanol-diluted oils. The second objective was carried out for the purpose of improving friction and wear losses from bioethanol-diluted oils, the nanocomposite of tungsten disulfide and graphene (GP/WS_2) was added to the fuel-oil blends as an antiwear additive at three concentrations of 0.01wt%, 0.02wt%, and 0.04wt%, respectively, and tested using the same conditions. The third objective aims to observe the combined effect of ta-C coating and antiwear additive (GP/WS_2) on tribological behavior of bioethanol-diluted engine oil under boundary lubrication using high frequency reciprocating ring (HFRR).

The result shows that the addition of gasoline-bioethanol blend decreases the oil viscosity, and increases the acidity of the oil because bioethanol is more acidic in nature compared to gasoline. All fuel-diluted oil samples have higher friction and wear losses, compared to the fresh synthetic oil. After adding the additive, the result reveals that GP/WS_2 performs lower friction and wear in all blends, compared to bioethanol-diluted oils without additive. The wear losses reduce with the increase of nanocomposite concentrations from 0.01%-0.04wt%. It is shown that E10-SO and E20-SO need 0.01-0.02wt% GP/WS_2 to improve wear performance to below baseline oil (SO). However, E30-SO and E85-SO performance lower friction and wear than pure SO when 0.04wt% GP/WS_2 is dispersed to the blends. The combined effect of ta-C coating and GP/WS_2 performs a significant reduction of friction and wear losses of bioethanol-diluted oil. From this study, it is suggested that 0.01%-0.02wt%. GP/WS_2 should be added to commercial engine oil used with the bioethanol-fueled engine to improve the lubricating efficiency of the engine and hamper the effect of bioethanol dilution on engine oil.

ABSTRAK

Kebimbangan terhadap kekurangan rizab bahan api fosil dan perubahan iklim telah menggesa penguatkuasaan undang-undang yang lebih ketat terhadap kenderaan untuk menggunakan bahan api boleh diperbaharui terutamanya bioetanol. Walaubagaimanapun, perantaramukaan gegelang omboh dengan dinding silinder mengakibatkan kadar pencairan minyak pelincir tertinggi daripada bahan api belum terbakar, terutamanya bioetanol yang mempunyai daya pengewapan yang tinggi dan boleh meningkatkan kecenderungan terhadap pencairan minyak pelicir di dalam takungan minyak. Mutakhir ini, bioetanol telah dicampur bersama petrol pada komposisi yang tinggi dan telah menyebabkan pengumpulan bahan api di dalam takungan minyak pelincir semakin bertambah. Oleh itu, adalah penting untuk mengkaji kesan pelbagai campuran bioetanol-petrol terhadap sifat-sifat degradasi dan ciri-ciri tribologi minyak pelincir. Disamping itu, kajian ini juga mengkaji peningkatan tingkah laku geseran dan hausan bagi minyak pelincir yang dicairkan dengan bioetanol.

Dalam kajian ini, tiga objektif telah dicapai untuk memahami sifat-sifat degradasi dan tingkah laku tribologi dan penambahbaikan pelincir yang dicairkan dengan bioetanol. Pada kajian pertama, lima campuran bioetanol-petrol telah diformulasikan iaitu petrol tulen (E0), dan campuran petrol bersama bioetanol pada jumlah peratusan yang berbeza (10, 20, 30 dan 85%, yang masing-masing dilabelkan sebagai E10, E20, E30 dan E85). Campuran bahan api ini kemudiannya dicampur dengan minyak enjin komersial (minyak sintetik: SO) pada kadar pencairan 6%. Campuran minyak-bahan api ini kemudiannya diuji mengunakan penguji tribo empat bola mengikut standard ujian ASTM D4172. Penguji tribo empat bola ini digunakan untuk menyiasat geseran dan hausan bagi setiap minyak pelicir yang dicairkan dengan campuran bahan api tersebut. Objektif kedua telah dijalankan bagi tujuan mengurangkan geseran dan hausan menggunakan minyak pelincir yang dicairkan oleh bioetanol, komposit nano disulfida tungsten dan *graphene* (GP/WS$_2$).

Bahan-bahan ini telah ditambah bersama campuran minyak-bahan api pada tiga kepekatan yang berbeza iaitu 0.01wt %, 0.02wt% dan 0.04wt% sebagai bahan tambahan penyahhausan dan seterusnya diuji menggunakan keadaan yang sama. Objektif ketiga bertujuan untuk melihat kesan gabungan salutan ta-C dan bahan tambahan penyahhausan (GP/WS_2) ke atas tingkah laku tribologi minyak enjin yang dicairkan dengan bioetanol pada pelinciran rejim sempadan menggunakan mesin salingan frekuensi tinggi (HFRR).

Hasil kajian menunjukkan bahawa penambahan campuran bioetanol-petrol dapat mengurangkan kelikatan minyak, sementara jumlah asid meningkat kerana bioetanol secara asalnya adalah lebih berasid berbanding petrol. Semua sampel minyak yang dicairkan dengan bahan api mempunyai geseran dan hausan yang tinggi, berbanding minyak sintetik. Selepas bahan tambahan penyahhausan ditambah, hasil menunjukkan bahawa GP/WS_2 menunjukkan geseran dan hausan yang lebih rendah untuk semua campuran, berbanding minyak enjin baru. Hausan dapat dikurangkan dengan peningkatan kepekatan nano-komposit daripada 0.01% sehingga 0.04wt%. Hal ini dapat dilihat apabila E10-SO dan E20-SO memerlukan sebanyak 0.01-0.02wt% GP/WS_2 untuk mengurangkan haus berbanding minyak sintetik (SO). Walau bagaimanapun, prestasi geseran dan hausan E30-SO dan E85-SO adalah lebih rendah berbanding SO tulen apabila 0.04wt% GP/WS_2 ditambah ke dalam campuran. Kesan gabungan salutan ta-C dan GP/WS_2 juga menunjukkan pengurangan yang amat ketara terhadap geseran dan hausan untuk minyak yang dicairkan dengan bioetanol. Hasil kajian ini mencadangkan bahawa 0.01% - 0.02wt% GP/WS_2 perlu ditambah ke dalam minyak enjin yang menggunakan bahan api bioetanol-petrol bagi meningkatkan kecekapan pelincir enjin dan menghalang kesan pencairan bioetanol terhadap minyak enjin.

ACKNOWLEDGEMENTS

First, I would like to express the deepest appreciation and gratitude to my supervisors, Prof Dr. Masjuki Bin Haji Hassan, Dr. Nurin Wahidah Binti Mohd Zulkifli, and Dr. Edzrol Niza Bin Mohamad, who have shown the attitude and the substance of genius. They continually and persuasively conveyed their constant guidance, valuable advice, and spirit of adventure and inspiration in regard to research. Without their supervision and constant help, this dissertation would not have been possible.

I would like to extend my gratitude to all faculty members in the Department of Mechanical Engineering of University of Malaya, Kuala Lumpur, who cooperatively helped provide the facility regarding this research.

In addition, a thank you to M.H. Mosarof and A. Arslan for their assistance during my laboratory works. I also would like to thank all my colleagues of Center for Energy Sciences who always make me encouraged.

In particular, I would like to extend my special thank and gratitude to my beloved parents, Mr. Leang Sokhon and Mrs. Thuok Masy, as well as my brother, Mr. Leang Sokheng for their priceless and endless love and encouragement and for their supports throughout my academic life.

Last but not least, I would like to greatly indebted to the Japan International Cooperation Agency (JICA) and AUN/Seed-Net for funding the author’s postgraduate study as well as providing the research grant under the ‘Collaborative Research’ program. I amiably thank the Ministry of Higher Education Malaysia and University of Malaya, Malaysia for funding this study through the Grand Challenge Project (GC001-14AET), and Fundamental Research Grant Scheme (FP063-2015A).

TABLE OF CONTENTS

LIST OF FIGURES

LIST OF TABLES

LIST OF SYMBOLS AND ABBREVIATIONS

AISI : American Iron and Steel Institute

ASTM : American Society for Testing Materials

C.L.A : Central Line Average

DLC : Diamond-Like Carbon

EDS : Energy Dispersive X-Ray Spectroscopy

COF : Coefficient of Friction

FFV Flex Fuel Vehicle

FTP Flash Temperature Parameter

GP/WS$_2$: Graphene/Tungsten Disulfide

HFRR : High Frequency Reciprocating Ring

MoDTC : Molybdenum Dithiocarbamate

RON : Research Octane Number

SAE : Society of Automotive Engineers

SEM : Scanning Electron Microscope

SO : Synthetic Oil

TAN : Total Acid Number

TBN : Total Base Number

TGDI : Turbocharged Gasoline Direct-Injection

VI : Viscosity Index

WSD : Wear Scar Diameter

ZDDP : Zinc Dialkyl Dithiophosphate

LIST OF APPENDICES

CHAPTER 1: INTRODUCTION

1.1 Overview

Bioethanol has gained much attention from governments all over the world and this is spurred by the availability of feedstocks and facilities for bioethanol production. Much effort is being made to improve the quality and quantity of bioethanol for use in engines (Balat & Balat, 2009). S. Kim and Dale (2004) reported that the total production of bioethanol from lignocellulose materials is approximately 442 billion liters, which is roughly 16 times greater than the global production of bioethanol in 2004. The world's leading producers of bioethanol are USA and Brazil, followed by Germany, France, Spain, Italy, and UK. Bioethanol is increasingly used in USA and Brazil over the years. The bioethanol produced by the USA and Brazil constitutes 86% of the world's bioethanol in 2010. Bioethanol production has been increasing steadily in Europe ever since the biofuel directive was enforced in 2003. European countries produced approximately 576000 m^3 of bioethanol in 2004 and bioethanol production reached 4.6 million m^3 in 2013, whereby 19% was produced in Germany. Bioethanol consumption is expected to rise annually in Europe with the implementation of the 'Renewable Energy Directive' which prescribes a mandatory bioethanol blending rate of 10% in the transportation sector by 2020 (SUDZUCKERGroup, 2016). There is also a great potential for bioethanol production in China, India, Japan and Indonesia due to the availability of various feedstocks. Asia is now the largest potential producer of bioethanol from crop wastes and residues. The favorable feedstocks for bioethanol production in Asia are rice straws, rice husk, wheat straws and corn stover (S. Kim & Dale, 2004). It has been recorded that the world's bioethanol production for fuel application reached 22966.87 million gallons in 2011 (Koçar & Civaş, 2013). Figure 1.1 shows the global production of bioethanol from 2007 to 2015. It is evident that there is a gradual increase in the global bioethanol production within this period, whereby the total production of bioethanol is more than 25 billion of gallons in 2015. It is projected that the total bioethanol production may reach or exceed 125 billion liters by 2020 owing to the new targets set by the governments in America, Brazil, Asia and Europe (Demirbas, 2007).

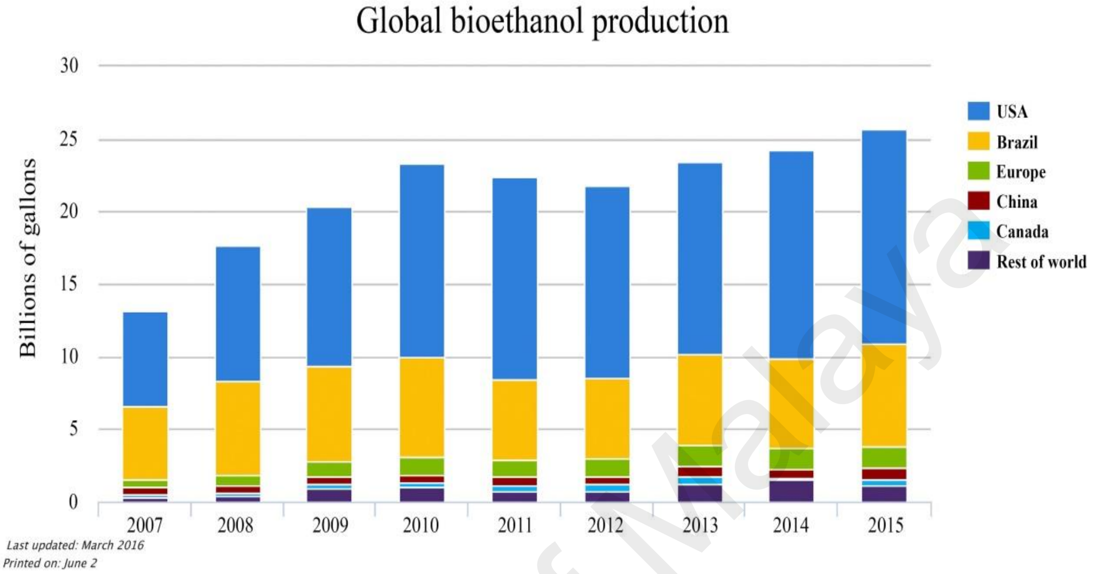

Figure 1.1: Global bioethanol productions from 2007 to 2015 [Retrieved from Alternative Fuels Data Center (AFDC, 2016)]

Bioethanol can be produced from renewable feedstocks such as corn, sugar cane, cassava, waste biomass, molasses, starch, and cellulose. The feedstocks used for bioethanol production are shown in figure 1.2. In general, there are three types of bioethanol based on the feedstock used for bioethanol production, namely first-generation bioethanol, second-generation bioethanol and third-generation bioethanol (REBEL, 2011). First-generation bioethanol is produced from edible feedstocks such as seeds, grains, corn, wheat, and sugar cane, which have high sugar or starch content. The sugar or starch is converted into bioethanol through the fermentation process. However, it is also known that the production of bioethanol from edible feedstocks is undesirable since food sources are used for fuel production and this leads to food scarcity, especially in developing countries. For this reason, second-generation bioethanol is produced from non-edible feedstocks such as lignocellulosic biomass and crop waste residues including rice husk, straws, grasses, and wood. These materials are in demand for biofuel production owing to the rising need for energy production from renewable sources. Third-generation bioethanol, however, is produced from algae, which are microorganisms that convert sunlight, water, and carbon dioxide into energy via photosynthesis. Algae require these components for high algal growth. Algae are desirable for bioethanol production because they require low input and they give high yields of up to 30–100 times more as well as their high oil/lipid, carbohydrate and protein content (REBEL, 2011).

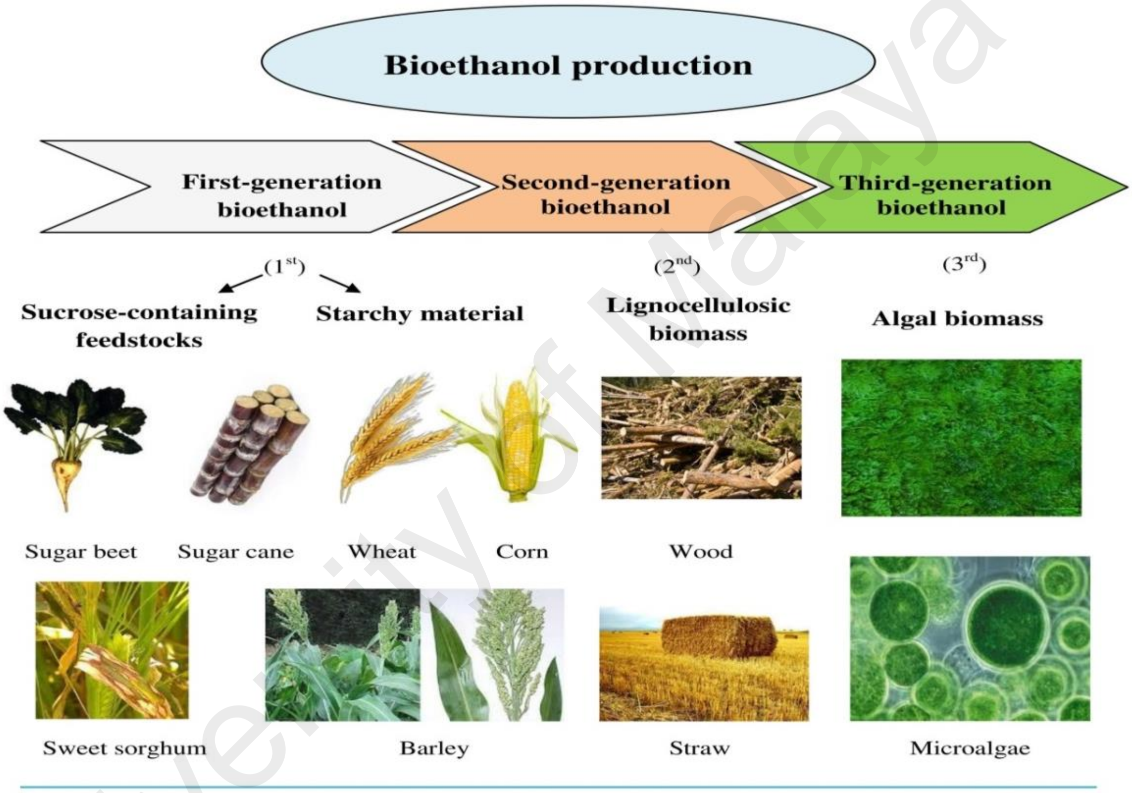

Figure 1.2: Feedstocks used for bioethanol productions

1.2 Background

Nowadays, various methods are used to improve the performance of automotive engines such as coatings (Quazi et al., 2016b), laser texturing (A Arslan et al., 2016; A Arslan et al., 2015; Ahmed Arslan et al., 2016; Quazi et al., 2016a), reducing the weight of components and modifying the composition of automotive lubricants (M. Mosarof et al., 2016). Lubricants serve a variety of purposes and one of them is to lubricate the metal-to-metal contact surfaces of moving parts inside engines. Lubricants protect engine components such as bearings, pistons, piston rings, cylinder liner and valve train against wear by forming a protective film over the surface. Lubricants protect engine components against corrosion by neutralizing acids through an alkaline agent and transporting waste products or sludge away from the site where they are generated. Lubricants improve fuel economy due to the reduction of friction in the engine (Erdemir, 2005; Simon C. Tung & McMillan, 2004). However, lubricants and fuels interact with each other in the engine lubrication system. During engine operations, unburned fuel always finds its way to reach the oil sump via the piston ring-cylinder liner system and eventually contaminates the lubricant. The accumulation of fuel and combustion products can dilute into the lubricant in certain driving conditions such as start-and-stop driving and cold-start conditions (Chui & Baker, 1980; Tze-Chi Jao, 2008). The fuel diluting into the crankcase through the cylinder liner degrades the performance of the lubricant in reducing friction and protecting the engine components against wear (Ferrarese et al., 2010a). Fuel dilution deteriorates the concentration of oil additives such as dispersants, detergents as well as wear, corrosion and oxidation inhibitors. This makes the lubricant thinner and more volatile, which decreases the viscosity and total base number of the oil (Hu et al., 2015b). Moreover, water maybe presents in the lubricant at significant amounts during short-trip and cold-start conditions, since bioethanol is hygroscopic in nature and attracts water from the atmosphere (Boons et al., 2008).

Blending bioethanol with gasoline can affect the performance of the lubricant, and consequently, decrease fuel economy and engine durability. The addition of bioethanol into gasoline increases the tendency of the fuel to reach the crankcase of the lubricant, which increases the rate of fuel dilution due to the higher boiling point and heat of vaporization (Chui & Baker, 1980; Wattrus, 2013a). Significant amounts of diluted bioethanol (6–25%) have been found in the lubricant crankcase after field tests (Boons et al., 2008) and bench sequence tests (Chui & Baker, 1980; Chui & Millard, 1981). This affects the viscosity, total acid number (TAN) and total base number (TBN) of the lubricant (among other properties) due to the higher concentration of bioethanol dilution. Consequently, this reduces the performance of the lubricant to protect the engine components against friction, wear and formation of deposits resulting from oxidation and corrosion of oxygenated bioethanol (Boons et al., 2008; Dhar & Agarwal, 2014; Ljubas et al., 2010). A number of users of flex-fuel engines (of various sizes and models) have reported that the accumulation of bioethanol affects the lubrication and friction characteristics as well as causing severe wear (Ferrarese et al., 2010b). An investigation on the effects of low and high-temperature conditions revealed that the addition of 5% of either anhydrous or hydrated bioethanol into a fully formulated oil containing ZDDP anti-wear additive degrades the pre-formed anti-wear tribofilm between sliding surface. The thickness of the tribofilm decreases significantly when bioethanol is blended with both types of oils (Costa & Spikes, 2016). The degradation of the lubricant (in terms of the lubricating capacity, viscosity and oxidation stability) was assessed in one study. The experiments were carried out using four motorcycles of a similar build and age, running using four combinations of fuels and lubricants: (1) gasoline and mineral oil, (2) gasoline and synthetic oil, (3) gasohol and mineral oil, and (4) gasohol and synthetic oil. The results showed that the viscosity decreases by 20–45% after a mileage of 3000 km. The mineral oil results in a larger scar area compared with synthetic oil. For the same type of engine oil, the scar areas from the gasohol-run engine were about 10% larger than those from the gasoline-run engine. The results showed that the properties of the lubricant change with respect to the operating time because of oxidation, thermal degradation, reaction with the sliding surface and engine blow-by contamination as well as depletion of oil additives (Tippayawong & Sooksarn, 2010). Some researchers have also investigated the effect of fuel dilution on the properties of the automotive lubricant. Hu, Teng, Luo, and Chen (2015a) proved that the turbocharged direct injection engine fueled with gasoline has a significant effect on fuel dilution, especially at higher engine torque values. The fuel dilution rate is up to 9% during cyclic-load engine testing, resulting in a significant drop in the oil viscosity as well as an increase in the fuel consumption and formation of carbon deposits on the piston ring area. Ajayi et al. (2016) investigated the effect of fuel dilution on the friction and wear characteristics of the lubricant. They prepared three fuel-oil mixtures (*i.e.* pure gasoline (E0), gasoline-10% bioethanol blend (E10), gasoline-16% isobutanol blend (i-B16)), whereby each was blended with the lubricant. Each fuel-oil mixture was tested in a marine machine operated in on-water condition using a start-and-stop cycle protocol. The bioethanol fuel showed the least rate of fuel dilution among all fuel blends whereas isobutanol (i-B16) blend showed the highest rate of fuel dilution. This difference was due to the higher evaporation of bioethanol at higher temperatures. They observed that fuel dilution increases with an increase in engine speed, resulting in a significant drop in the oil viscosity. However, there was a slight decrease in friction when the oil viscosity was low. In addition, the fuel-diluted lubricant samples produce larger wear scars compared to fresh oil. A couple of studies showed that there is a slight reduction in friction when bioethanol was used, particularly when the water in the bioethanol was exposed to the lubricant (P. De Silva et al., 2011a, 2011b).

1.3 Problem statement and motivation

It can be described that bioethanol is commonly used at the increasing rates as a substitute for fossil fuels in gasoline engines due to its production availability and significant performance and properties. Mostly, bioethanol is blended into gasoline at the concentration range from 5–30% for SI engine and up to 85% for flex-fuel engines. Bioethanol and its blends reduce the emission and enrich engine performance with a little higher fuel consumption compared to fossil fuels. Bioethanol blends, however, exhibits a few major problems concerning material compatibility and immiscibility with other fuels such diesel and biodiesel blends. The high amount of water and organic acid in bioethanol enhance corrosion on the contact of sliding surfaces, especially fuel injector and injection pump. Another main problem of bioethanol is its possibility to contaminate automotive lubricant through fuel dilution. The diluted fuel in particular bioethanol provokes further oxidation and causes serious problems such as wear, sludge and deposit formation for lubricant and engine. In a bioethanol-fueled engine, the piston ring and cylinder wall interface which is the largest contributor to engine friction suffers the highest levels of fuel dilution into the lubricant from unburned fuel because bioethanol has high heat of vaporization which enhances the tendency of fuel dilution in the oil sump. Therefore, it is crucial to study the effect of various bioethanol-gasoline blends on degradation of properties and tribological behaviors of engine oil. There have not been many researchers investigating thoroughly into the lubricating effect of bioethanol as well as the enhancement of lubricating performance of bioethanol-diluted lubricant yet. Since bioethanol dilution is known as undesirable factor destroying friction and wear behaviors of engine oil, the addition of nano-additive and the use of coating can be applied to solve the aforementioned problem of bioethanol-fueled engines, particularly bioethanol-diluted engine oil. This study was conducted to provide the useful insights for researchers and practitioners in this field of fuel dilution.

1.4 Objectives

This experimental study concerns the effect of bioethanol fuel dilution on tribological behavior of commercial engine oils, which play a very important role to determine friction and wear losses of sliding engine components. Formulated fuels were blended into the engine oils. These fuel-oil mixtures were then tested with four-ball machine and high frequency reciprocating ring. The goals of the study are as follows:

- To investigate the effects of various bioethanol blends on the degradation of properties and friction and wear behaviors of the lubricant using four-ball wear tester
- To enhance the lubricating performance of bioethanol-diluted lubricant using an antiwear nanocomposite additive, graphene with tungsten disulfide (GP/WS_2)
- To understand the combined effect of GP/WS_2 and ta-C coating on friction and wear behaviors of bioethanol-diluted oil using High Frequency Reciprocating Ring

1.5 Scope of the study

This experimental study aims to observe the effect of five formulated fuel (E0, E10, E20, E30, and E85) on commercial engine oil. Friction and wear characteristics of the contaminated lubricants are obtained using four-ball machine operated under varied conditions of two different loads. From the observation of the effect of bioethanol fuel on lubricant, it is understood that bioethanol worsens the friction and wear prevention of the engine oil as indicated by higher friction and wear losses. Therefore, this study aims to reduce the friction and wear losses of bioethanol-diluted engine oil using antiwear nanocomposite of tungsten disulfide and graphene. Finally, the author continues to evaluate the tribological performance of GP/WS_2-bioethanol-lubricant tested with ta-C using high frequency reciprocating ring (HFRR). E10 is selected to blend with the lubricant as this blend has already been widely used in gasoline-fueled engines. The results of friction and wear behaviors of WS_2/GP-bioethanol-lubricant tested with ta-C are discussed accordingly in this current study

1.6 Organization of the thesis

This dissertation contains five chapters, which are chronologically organized as follows:

Chapter 1 provides the overview of the global bioethanol production and its implementation as transportation fuels as well as the agricultural feedstocks for bioethanol production. This chapter is followed by the background, which describes the effect of bioethanol dilution on engine components and lubricating oil. Then, the problem statement and motivation of this study are explained. Finally, the objectives and scopes of the study are described.

Chapter 2 aims to evaluate previous studies and to identify relation, contradiction, gaps and inconsistencies in the existing literature. Section 1 gives the overall introduction of the fossil fuel and biofuel relation. Section 2 describes the properties of bioethanol blend with gasoline. Section 3 and 4 explain engine oil additive and nanomaterial while section 5 and 6 explain the fundamental of engine tribology and coating. Section 7 and 8 describe the characteristic of fuel dilution into engine oil as well as its effect on engine oil. This chapter includes the summary and the research gap.

Chapter 3 explains the tentative methodology of this experimental study in order to achieve the set objectives. It starts with the research guideline, then followed by the material and equipment, tribological testing (four-ball wear tester/high frequency reciprocating ring), surface analysis techniques and statistical and error analysis.

Chapter 4 shows all results of friction and wear behavior of fuel diluted engine oil that has been obtained from the experiment. It presents all the finding of the study followed by a clear discussion. This chapter also analyzes these findings and compares them to the existing result of previous researchers in this field.

Chapter 5 provides a detailed conclusion of the key findings and reflects these finding to the set objectives of the study. It also put forward some recommendations for the future studies.

CHAPTER 2: LITERATURE REVIEW

2.1 Introduction

Bioethanol offers a variety of benefits and is being used as engine fuel around the world. Table 2.1 shows the use of bioethanol around the world. Firstly, bioethanol can be derived from various feedstocks such as sugar cane, corn and wheat (*i.e.* first-generation bioethanol), lignocellulosic materials (*i.e.* second-generation bioethanol) and algal biomass (*i.e.* third-generation bioethanol) (Akponah E, 2013). Secondly, bioethanol burns with a smokeless blue flame and it has a low auto-ignition temperature. The auto-ignition temperature is the temperature at which the bioethanol will ignite spontaneously in ambient conditions without an external source of ignition such as flame or spark (Kevin Fisher, 2006). Thirdly, bioethanol is miscible with water and most organic solvents such as acetic acid, acetone, ether, ethylene glycol, glycerol and toluene (Lide, 2000; Windholz, 1979). Lastly, the addition of bioethanol into gasoline or diesel reduces the concentration of particulate mass in the exhaust and this helps reduce carbon oxide emissions due to the high octane number and oxygen content.

Table 2. 1: Use of bioethanol fuel around the world

Countries	Blending percentages	References
United States	MTBE, E10, E15, E85, E95	(Australia, 2017; Woo, 2017)
Brazil	E5, E15, E20, E22, E23, E24, E25, E100	
Europe	E5, E50, E85, E100	
Australia	E10, E20, E85	
Japan	N/A	
China	Ratio: 1:9 (E10)	
India	E5, E10	
Philippines	E20 (2020-2030)	
Malaysia	B10, B20 (Bioethanol has not been used)	
Thailand	E10, Thai government is planning to use E20	
Vietnam	E5 and planning to boost the use of E10	

However, bioethanol is corrosive to engine components due to its high oxygen content (Tandon et al., 2011). The presence of water in the chemical structure of alcohol has a corrosive effect on fuel systems, which results in phase separation, and this is undesirable for engine operations (Hazar & Temizer, 2012). Corrosion causes damage to the components in the fuel system since these components are made of metals such as steel and zinc-aluminum alloys. One study was carried out to investigate the corrosion of metals using weight loss (immersion test) and electrochemical impedance stereoscopy (EIS), and the results showed that the addition of bioethanol into gasoline corrodes the metal components in the fuel system (Jafari et al., 2010). Baena et al., (2012) studied the corrosion of various metallic materials used in the automotive industry. They conducted immersion test using 20% bioethanol-gasoline fuel. The results revealed that copper and carbon steel have higher tendency towards corrosion.

Using bioethanol as engine fuel also causes tribological issues. When bioethanol is used as the fuel, there is a possibility that the engine oil will be contaminated with bioethanol. One of the causes of bioethanol dilution is partial combustion of the fuel, whereby the reactive compounds produced from the combustion process dilute into the crankcase through the cylinder liner and mix with the lubricant. This is undesirable since bioethanol dilution significantly alters the properties of the automotive lubricant (Boons et al., 2008). The immiscible alcohol forms a thick emulsion with the lubricant, which will likely increase wear in bioethanol-fueled engines (Schwartz et al., 1988).

2.2 Bioethanol as an alternative fuel

2.2.1 Physicochemical properties of bioethanol

Bioethanol is ethyl alcohol or grain alcohol biofuel having the following chemical formula, CH_3–CH_2–OH. Bioethanol has shown great potentials for use as an alternative fuel in spark-ignition and compression-ignition engines due to its favorable physicochemical properties. The physicochemical properties of bioethanol are summarized in Table 2.2. Bioethanol is an oxygenated fuel and therefore, it can reduce particulate emissions from engines. Bioethanol also has higher octane number, higher heat of vaporization and broader flammability limits, which enhance fuel combustion, increase the compression ratio and shorten ignition timing compared to gasoline and diesel. In brief, bioethanol is more efficient compared to gasoline and diesel.

Table 2. 2: Physicochemical properties of bioethanol

Fuel property	**Unit**	**Bioethanol [C_2H_5OH]**
Density at 15°C	kg/m^3	790.00
Kinematic viscosity at 40°C	mm^2/s	1.13
Oxygen	mass%	34.70
Cetane number	–	5.00
Octane number	–	110.00
Latent heat of vaporization	MJ/kg	0.91
Lower calorific value	MJ/kg	25.22, 26.70
Auto-ignition temperature	°C	332.80, 366.00
Water content	mg/kg	2024.00
Stoichiometric fuel/air ratio	-	1/9.01
References	(Avinash & Sasikumar, 2015; Balat, 2011; Lapuerta et al., 2010)	

2.2.2 Bioethanol blends

Bioethanol can be blended with gasoline, diesel, and biodiesel, and these blends can be used to fuel gasoline and diesel engines without any engine modifications or with minor engine modifications (Ajav & Akingbehin, 2002). However, the addition of bioethanol into gasoline and diesel alters the properties of the fuel blend, which in turn affects engine operations. In general, the presence of bioethanol reduces the physicochemical properties of the fuel blend in diesel engines (Degang Li et al., 2005). The physicochemical properties of several biodiesel–diesel blends, bioethanol–gasoline blends and bioethanol–diesel–biodiesel blends are summarized in Table 2.3, 2.4 and 2.5, respectively. It can be seen that blending various fuels alters the kinematic viscosity, density, cetane number, calorific value, and other properties of the fuel blend (Alptekin & Canakci, 2009; Kwanchareon et al., 2007; Degang Li et al., 2005). This affects the lubricity, engine performance, exhaust emissions of the fuel blend (Xu et al., 2007).

Table 2. 3: Physicochemical properties of bioethanol–diesel blends

Fuel property	**Unit**	**Bioethanol–diesel blends**				
		E5D95	**E10D90**	**E15D85**	**E20D80**	**E25D75**
Density at 15°C	kg/m^3	834.30	831.70	829.40	815.00	–
Kinematic viscosity at 40°C	mm^2/s	2.53	2.31	2.19	3.00	–
Cetane number	–	–	44.60	44.10	36.00	–
Calorific value	MJ/kg	43.63	43.19	42.74	41.87	41.00
Flash point	°C	24.00	25.00	27.00	25.00	25.00
References	(Ajav & Akingbehin, 2002; Chen et al., 2013; Matuszewska et al., 2013; Torres-Jimenez et al., 2011)					

Table 2. 4: Physicochemical properties of bioethanol–gasoline blends

Fuel property	Unit	Bioethanol–gasoline blends					
		E0	**E10**	**E15**	**E20**	**E25**	**E30**
Density at 15.6°C	kg/m^3	740.00	739.60	749.50	754.10	757.10	761.30
Kinematic viscosity at 30°C	mm^2/s	0.48	0.54	0.56	0.60	0.63	0.66
Octane number	–	93.20	97.10	98.60	100.40	99.50	102.50
Heat of combustion	MJ/kg	34.84	33.19	32.91	32.43	31.70	31.53
Flash point	°C	–	29.00	29.40	29.50	30.00	29.20
References	(Koçar & Civaş, 2013; Rahman et al., 2014; Yücesu et al., 2006)						

Table 2. 5: Physicochemical properties of bioethanol–diesel–biodiesel blends at various compositions (Kwanchareon et al., 2007)

%D	%B	%E	Cetane number	Flash point (°C)	Pour point (°C)	Density (g/ml)	Heat of combustion (MJ/kg)
90	10	0	47.99	71.00	6.00	0.838	44.70
90	5	5	47.31	17.50	3.00	0.831	44.50
90	0	10	46.05	14.50	3.00	0.826	43.40
85	15	0	48.52	73.50	6.00	0.841	44.20
85	10	5	47.70	14.00	3.00	0.833	43.70
85	5	10	46.67	13.50	3.00	0.831	43.60
85	0	15	45.81	13.00	3.00	0.824	42.50
80	15	5	48.66	16.00	3.00	0.837	43.30
80	10	10	46.85	15.00	3.00	0.833	43.5
80	5	15	46.25	13.00	3.00	0.829	42.8
100	0	0	47.64	69.00	6.00	0.835	45.0
0	100	0	55.40	122.00	9.00	0.878	39.6
0	0	100	5.00–8.00	13.00	-117.30	0.794	27.0

Note: D, B, and E denote diesel, biodiesel, and bioethanol, respectively.

2.3 Engine oil additives

Nowadays, most modern lubricants contain chemical additives which enhance the quality and properties of the lubricants and extend service life and performance. There are a variety of oil additives which play different roles in the lubricating system of engine oil components. Table 2.6 shows different types of lubricant additives and their roles in lubrication. Engine oil additives play a major role to protect the surface of engine sliding components, minimize the change in viscosity at high temperature, and provide high anti-friction characteristic and maximum resistance to oxidation. The engine oil containing anti-wear additive prevents the contact surface against high wear losses by forming a chemical film on the rubbing surface.

Table 2. 6: Automotive lubricant additives: role and chemical compound (Smith et al., 2005)

Additive	Chemical compound	Role(s)
Deposit control additives		
Detergent	Succinimides	To reduce insoluble deposits formed on surfaces at high temperatures
Dispersant	PIB-succinimide	To limit engine sludge and varnish
Anti-oxidant	ZDDP	To prevent oxidation of engine oil
Anti-wear and EP additives		
Properties Modifiers:	ZDDP	To reduce wear from corrosion and limit mechanical wear To prevent scuffing of rubbed surfaces under shock and very high loads.
Friction Modifiers	MoDTC	To reduce friction of metal-to-metal contact surface
Viscosity index enhancers	Olefin copolymer	To limit variation of oil viscosity at high temperature
Anti-foaming	Silicone	To reduce the formation of foam in engine oil
Pour point depressant	Polyalkylmethacrylates	To reduce pour point of oil containing paraffinic compound
Corrosion inhibitor	Alkyl sulphonates	To neutralize acid number caused by oxidation of engine oil

ZDDP = Zinc dialkyl dithiophosphate, MoDTC = Molybdenum Dithiocarbamate

2.4 Nanomaterial

The study of tribology, including friction, wear, and lubrication, has recently attracted significant attention because numerous mechanical system failures originate from wear and friction. The most effective approach to controlling or reducing friction and wear is to formulate high-quality engine oil by employing micro/nanomaterial as lubricating oil additives thanks to their facile preparation and tiny nano-size dimension. A variety of nanostructured metals and metallic oxides, such as copper, nickel, silver and their oxides were reported as excellent additives in liquid lubricants. Recent studies are also focusing on the tribological behavior of graphene (the two dimensional material as engine oil additive) because it has a significant reduction in friction and wear losses and increases load carrying capacity. Moreover, the studies of nanocomposite are being carried out to explore the excellent friction and wear-reducing behaviors.

2.4.1 Nanoparticles

Nanoparticles are nano-size particles that have one dimension that measures 100nm or less. The properties of many conventional materials change when formed from nanoparticles due to the fact that nanoparticles have a greater surface area per weight than larger particle which causes them to be more reactive to some other molecules. Over a few decades, nanoparticles have been used, or are being used in many fields including medicine application, energy, and electronics, manufacturing, and material as well as petroleum engineering. Recently, a variety of nanoparticles such as diamond, silicon dioxide (SiO_2), copper oxide (CuO), titanium dioxide (TiO_2), aluminum oxide (Al_2O_3), zinc oxide (ZnO) and molybdenum disulfide (MoS_2) as well as graphene have been employing as engine oil additive in order to investigate the tribological behavior of engine oil. Wu et al. (2007) investigated the effect of additives CuO, TiO2, and Nano-Diamond nanoparticles on the tribological properties of two different lubricating oils and observed that with CuO additive, oils significantly exhibited good friction-reduction and anti-wear properties. Battez et al. (2008) investigated the effect of CuO, ZnO and ZrO_2 nanoparticles as an antiwear additive in engine oil. The result illustrated that all nanoparticle suspension exhibited a reduction in friction and wear compared to the base oil. Xie et al. (2016) studied the effects of the base lubricant with and without MoS_2 and SiO_2 nanoparticles on the tribological behavior of magnesium alloy/steel contacts were investigated using a reciprocating sliding ball-on-flat tribometer. The results showed that the tribological properties of the base lubricant have been improved by adding the nanoparticles. The MoS_2 nano lubricant is more pronounced in terms of the load carrying capacity and the lubrication film stability as compared with SiO_2.

2.4.2 Nanocomposite

Nanocomposite is the combination of two nanoparticles to obtain a homogenous material working as engine oil additive. It is well-known that the nanocomposite has excellent and greater lubricating performance than the compositional nanoparticle alone. However, the study of nanocomposite as engine oil additive is still limitedly carried out. Meng et al. (2016a) studied the tribological application of silver nanoparticle-decorated graphene in engine oil. The result revealed that Ag/GP outperformed Ag and GP nanoparticle alone. Ag/GP formed a greater protective film on the friction pairs and significantly reduced the surface roughness of the sliding balls. Recently, organically modified GP and GP-inorganic nanocomposite have attracted much attention. Gusain et al. (2016) synthesized graphene oxide modified with ionic liquid and ethylene glycol to integrate the friction-reducing properties of both ionic liquid and graphene nanosheets because graphene can improve the anti-wear performance whereas ionic liquids facilitate the dispersion of the Gr-IL in the polyethylene glycol. Moreover, Meng et al. (2016b) prepared Ni and Ag nanoparticle-decorated GP nanocomposite. The result showed that Ni-Ag/GP provided greater lubricating performance than GP alone. More recently, Zheng et al. (2017) investigated the tribological properties of graphene and tungsten disulfide

(GP/WS_2) nanocomposite as engine oil additives. It shows that GP/WS_2 dispersed oil yield lower friction and wear losses than lubricant dispersed with GP and WS_2 alone. Figure 2.1 shows SEM images of graphene (GP), tungsten disulfide (WS_2), and GP/WS_2 nanocomposite. It can be notified that GP presents thin layer with tiny wrinkled morphology on its surface (figure 2.1a), whereas WS_2 image has nanoscale patchy particles (figure 2.1b). When the two nanoparticles were dispersed together, the image of the combined nano-composite (GP/WS_2) in figure 2.1c illustrates the overlapping layer of GP and WS_2. This confirms that graphene and tungsten disulfide were well-dispersed and well-combined with each other.

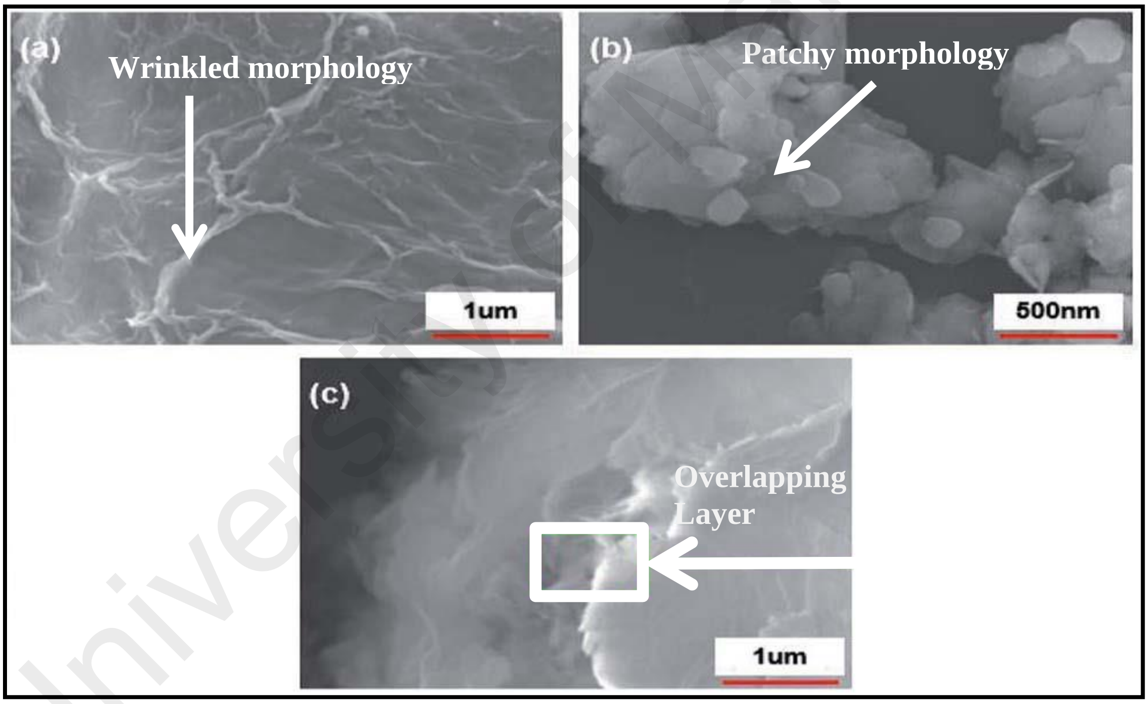

Figure 2. 1: SEM images of (a) GP, (b) WS_2, and (c) GP/WS_2 (Zheng et al., 2017)

2.5 Fundamental of engine tribology and coating technology

The study of engine tribology serves the purpose to reduce mechanical losses of main sliding components such as piston, piston ring, pistons skirt, cylinder bore, camshaft, valve train, and journal bearing. This has led to enormous advanced researches in the field of tribology such as lubricant formulation, material, and surface technology. Currently, many coatings have been used to prevent elevated wear rates of metal-to-metal contacts (Kalin et al., 2008). These coatings include nitrides (titanium nitride (TiN), titanium carbonitride (TiCN), and chromium nitride (CrN), carbides (metallic carbides), hydrogenated amorphous carbon (a-C:H), hydrogen-free amorphous carbon (a-C), hydrogenated tetrahedral carbon (ta-C:H) and diamond-like carbon (DLC) films (Schamel et al., 1997). Among these coatings, DLCs offers reliable surface coatings due to their unique blend of mechanical, chemical, and tribological properties (Bewilogua & Hofmann, 2014; Deng et al., 2014; Tasdem et al., 2014). However, the interaction between oil additives and coated surfaces become complicated. Oil additives may react with the surface material during oil lubricated sliding contact to form tribochemical surface films while other types of additives affect coating deposition as well as the metal surface. The use of higher levels (current level, 10%) of bioethanol fuel in the current gasoline engines leads to high fuel dilution of engine oil and causes oil degradation and accelerated wear due to its acidic nature. These complicated effects need more advanced researches to study the interactive effect of biofuel on oil additives and contact surfaces, especially coating deposition, which has not been widely studied in the current trend of using higher levels of bioethanol. Therefore, new engine lubricants and coating depositions techniques for friction reduction below the current levels must suit the high use of bioethanol fuel to protect the engine component surfaces from the chemical interaction of fuel and oil causing accelerated wear.

2.5.1 Lubrication of the engine

The lubrication system in IC engines is primarily important to reduce the friction of the following areas: (i) the power cylinder (piston and rings), (ii) valve train components (cam, tappets, rods), and (iii) crank bearings. Power cylinder components contribute to approximately half of the total friction. The lubrication regimes of each component are also generally understood: bearing (hydrodynamic), valve train (mostly boundary), and piston/ring-liner lubrication mostly in hydrodynamic mode except near the end strokes where piston sliding speed is near zero at which mixed or boundary contacts occur. Most frictional power loss occurs at mid-stroke due to the large sliding speed. Figure 2.2 shows the schematic representation of stribeck curve.

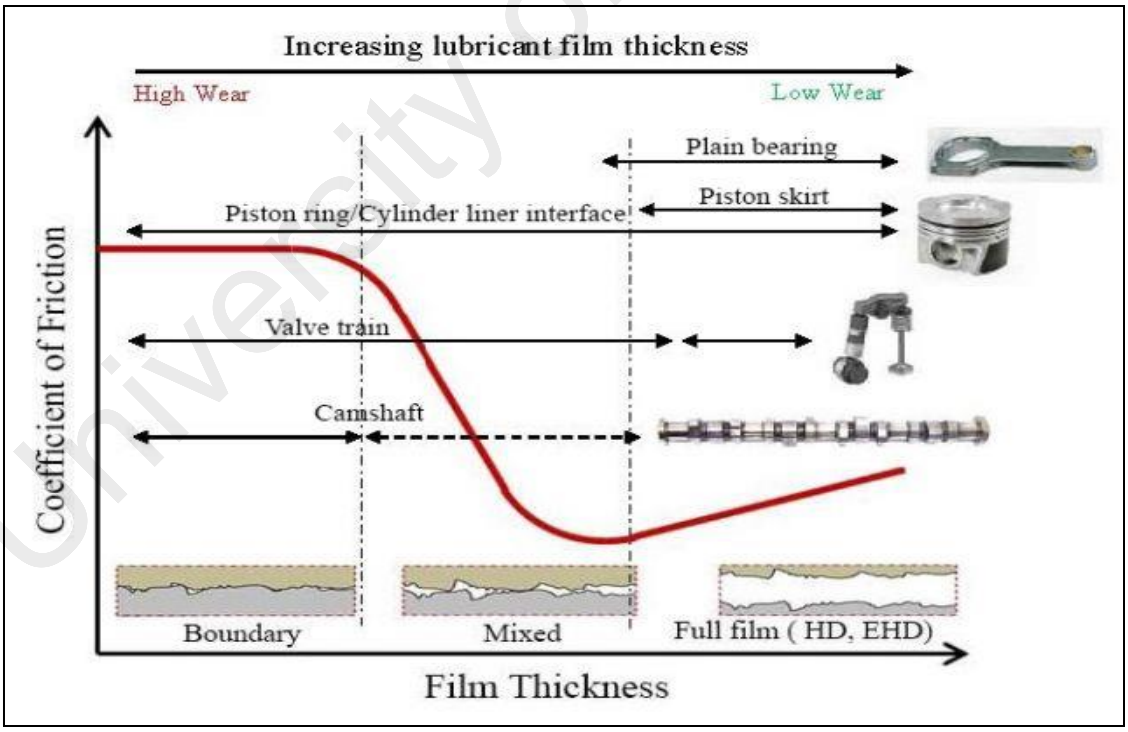

Figure 2.2: Schematic representation of stribeck curve (Robinson et al., 2016)

2.5.1.1 Boundary lubrication

Boundary lubrication is the condition when the fluid films are negligible and there is considerable asperity contact. The physical and chemical properties of thin surface films are of significant importance while the properties of the bulk fluid lubricant are insignificant. The surfaces are in normal contact with behavior characterized by the chemical (and physical) actions of thin films of molecular proportions. Generally, valve train and cam follower are operated in the boundary condition and may be influenced by Elastohydrodynamic lubrication.

2.5.1.2 Mixed lubrication

Mixed lubrication is the condition when the speed is low, the load is high, or the temperature is sufficiently large to reduce lubricant viscosity. When any of these conditions occurs, the highest asperities of the bounding surfaces will protrude through the film and occasionally come in contact. There is a surface asperity interaction and the Elastohydrodynamic and boundary lubrication are influential because the generated lubricating film is not enough to separate the bodies completely. Most of the components such as piston ring/liner, valve train, and camshaft operate in this regime.

2.5.1.3 Elastohydrodynamic lubrication

Elastohydrodynamic lubrication occurs when a lubricant is introduced between surfaces that are in rolling contacts, such as ball and rolling element bearings. Piston ring/liner also experiences this lubrication regime during mid-stroke condition. In this regime, the load is sufficiently high enough for the surfaces to deform elastically during the hydrodynamic action. The effect of pressure on viscosity is important.

2.5.1.4 Hydrodynamic lubrication

Hydrodynamic lubrication is the condition when a thick film of lubricant separates the load carrying surfaces. The lubricant pressure is self-generated by the moving surfaces drawing the lubricant into the wedge formed by the bounding surfaces at a high enough velocity to generate the pressure to completely separate the surfaces and support the applied load. Therefore, the dynamic viscosity of the lubricant is its most important property. The plain bearing works in this regime, in which metal-to-metal contact of the bearing does not occur during the steady state operation.

2.5.2 Friction analysis and energy distribution

For an IC engine, 10~15% of the energy is lost to friction from piston assembly, bearings, and valve train. Friction is a function of engine speed and load (Allmaier et al., 2015). Friction could be 10% or less at high loads and 30% or more at lighter loads. A fraction of total fuel energy used for gasoline engines is shown in figure 2.3 (Richardson, 2000a), in which mechanical friction is approximately 4%−15% of the total fuel energy. This general estimate reflects typical in-use engine conditions and does not apply to unique extreme conditions such as at idling and very light loads where most of the fuel energy is consumed to overcome friction. Thermal efficiencies of modern engines vary between 38%−50%. Accordingly, mechanical friction is typically 10%−30% of engine power output, although it could be 100%, at idling, at the extreme. The above estimate of mechanical friction is consistent with other estimates of total mechanical losses in an engine, which include pumping and accessory losses in addition to mechanical friction itself, at up to 40% of the gross (indicated) power output from the engine (Stachowiak & Batchelor, 2005). Most of the mechanical losses, about 75%, are rubbing friction (Heywood, 1988).

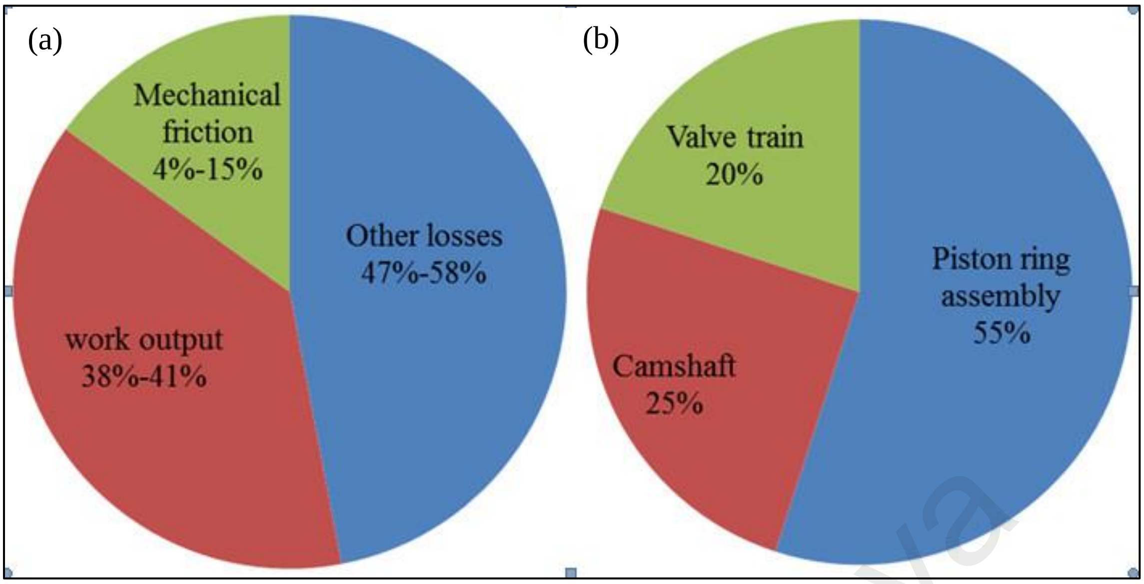

Figure 2. 3: Image of (a) distribution of total energy, (b) distribution of friction in a fired engine (Richardson, 2000b)

2.5.3 Wear analysis of engine components

Wear analysis of engine components is the study of damaged surface caused by metal-to-metal contact. Generally, working conditions affecting wear of engine components include load, speed, temperature, and lubrication. There are four main types of wear such as adhesive wear, abrasive wear, fatigue wear, and corrosive and oxidative wear, which usually occur to engine sliding component as shown in figure 2.4.

2.5.3.1 Abrasive wear

Abrasive wear occurs between the harder and softer surfaces. Particle contamination causes abrasive groove and damage to a mating surface that is in relative motion. As plowing takes place in the sliding portion, a certain volume of surface material is removed. There are two main mechanisms of abrasive wear. Two-body abrasion occurs when metal asperities on one surface cut directly into a second metal surface. The contact occurs in the boundary lubrication regime due to inadequate lubrication. Three-body abrasion occurs when a particle or wear debris becomes embedded in one metal surface and is squeezed between the two surfaces. When the particle size is greater than the fluid film thickness, scratching and plowing can occur.

2.5.3.2 Adhesive wear

Adhesive wear is the transfer of material from one contacting surface to another. It occurs when high loads, temperatures, or pressures cause the asperities on two contacting metal surfaces to spot-weld together and then immediately tear apart the metal in small, discrete areas. The adhesive wear is caused by the relative motion, plastic deformation, and direct contact between the rubbing surfaces.

2.5.3.3 Fatigue wear

This phenomenon occurred when a processed metal removed by cracking and pitting, or when the surface of the material is weakened due to cyclic elastic loading or stress during rolling and sliding. Fatigue wear particles will be generated when worn-off surface is separated by the cyclic growth of microcracks on the surface.

2.5.3.4 Corrosive and oxidative wears

The chemical interactions corrode the surface forming corrosion products on the contact surface exposed to corrosive gas or liquids (i.e. bioethanol). Wear mechanism is formed by the interactions of solid materials with the corrosive environment. A reaction layer formed on the surface by the tribochemical reaction destroys the chemical bonding of the material and then such layer is removed by friction. Oxidative wear is a similar process that occurs on unlubricated metal surfaces rubbing in air or oxygen. The main difference between corrosive and oxidative wear is that in oxidative wear oxide particles mix with metal and form a debris layer. The adoption of bioethanol as a fuel for vehicles creates many problems of corrosive wear in engines. Bioethanol is hygroscopic and absorbs water. Concentrations of water as low as 1% can cause significant increases in wear (Gwidon & Andrew, 1993).

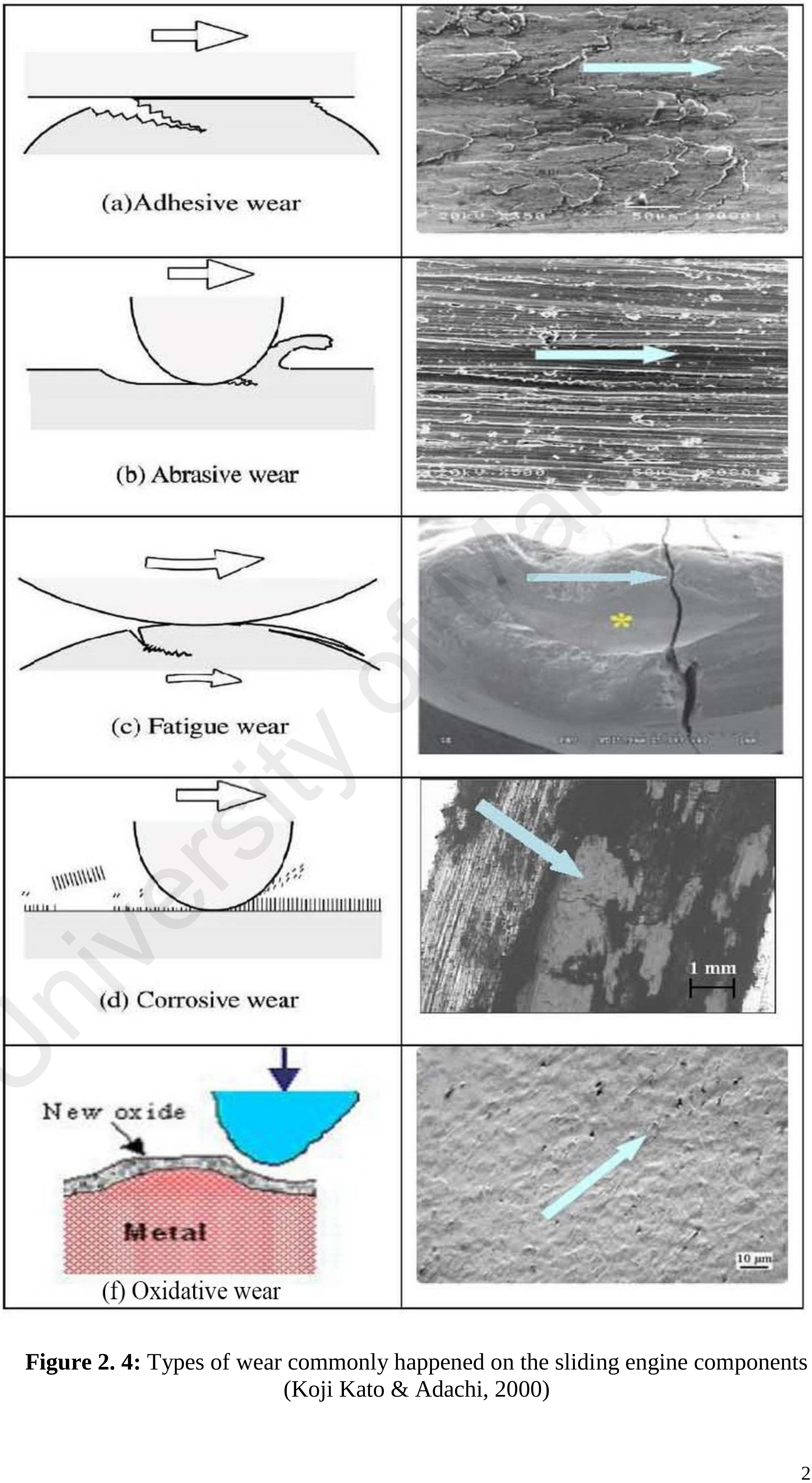

Figure 2. 4: Types of wear commonly happened on the sliding engine components (Koji Kato & Adachi, 2000)

2.5.4 Coating for sliding engine components

This section aims to show the material and coating techniques for contact surface that have been applied to sliding engine components. Many coating techniques exist to reduce wear and friction between metallic surfaces, and the demand for advanced coating deposition of engine components needs to match the new formulation of engine oil and biofuels, which may interact with coated surface thus increasing friction and wear losses. Moreover, the use of bioethanol fuel causes higher fuel dilution into the engine oil. The fuel-oil mixture may interact with coating deposition and cause chemical reactions, resulting in elevated wear and friction rates. Therefore, understanding the behavior of coating under lubricated conditions is important. The following subsections describe the materials and surface technology as well as coating techniques applied on the main sliding components such as piston ring, piston skirt, cylinder liner, and camshaft. The detailed literature of coatings was reviewed in (Zahid et al., 2016) and the study of coating behavior can be found in (Al Mahmud et al., 2014; Mutafov et al., 2014; Neville et al., 2007; Simon C Tung & Gao, 2003; Vengudusamy et al., 2011). These coatings may include nitrides (titanium nitride (TiN), titanium carbonitride (TiCN), and chromium nitride (CrN)), carbides (metallic carbides), hydrogenated amorphous carbon (a-C: H), hydrogen-free amorphous carbon (a-C), hydrogenated tetrahedral carbon (ta-C: H), Hydrogenated diamond-like carbon coatings doped with tungsten (W-doped a-C:H or W-DLC-H) (Mutafov et al., 2014) and diamond-like carbon (DLC) films (Schamel et al., 1997). Figure 2.5 shows the use of DLC coating for sliding component. DLC coatings have been deposited on different sliding components including piston ring, piston skirt (Cho & Lee, 2009; Y. Kim et al., 2011; Simon C Tung & Gao, 2003), cylinder liner (Rejowski et al, 2012) and valve train (Johnston & Hainsworth, 2013; Mutafov et al., 2014).

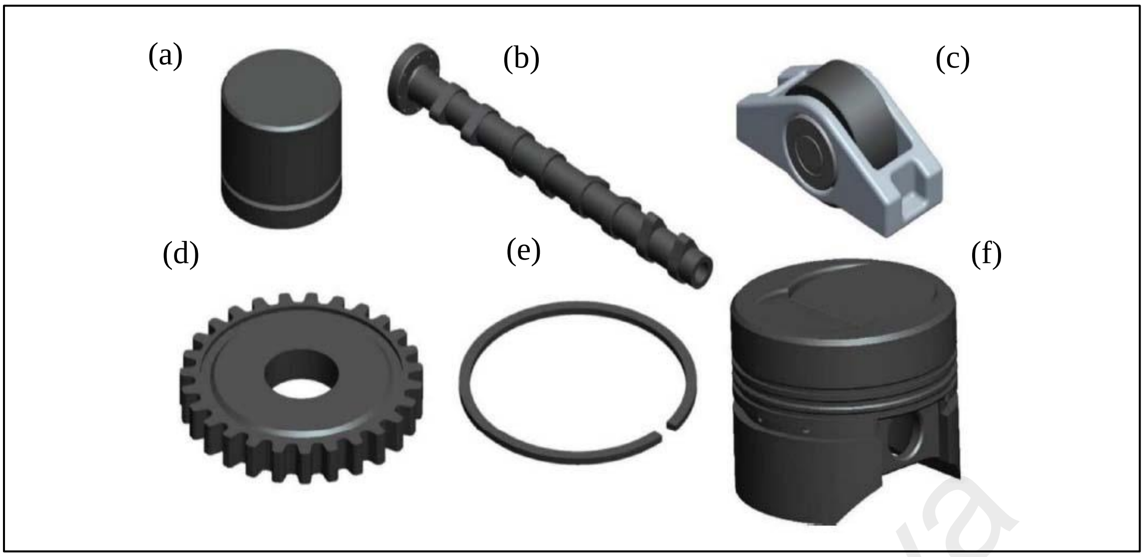

Figure 2. 5: Use of DLC coatings for (a) tappet, (b) camshaft, (c) finger roller follower, (d) camshaft sprocket, (e) piston ring, and (f) piston (Zahid et al., 2015)

2.5.4.1 Camshaft

Gray cast irons and hardened alloy CI are commonly used to make camshafts due to their low cost. Recently, there have been moves to replace some of these with forced steel, light forged aluminum, and composite materials (Nakamura et al., 1996). Several surface treatment techniques such as induction hardening or flame hardening of cast iron, carburizing of low carbon steel and induction hardening of medium carbon steel are performed to prevent cam failures. To prevent high wear rates, shim material such as high chromium cast iron, silicon nitride, and ferrous based powder have been used to make the cam/follower components (Kano & Tanimoto, 1991). Ion-plated Cr–N and Cr2N on shims give excellent scuffing resistance under boundary lubrication (Eyre & Crawley, 1980). The use of DLC coating on steel shim can remarkably reduce the friction loss in cam/follower arrangement (Schamel et al., 1997).

2.5.4.2 Cylinder wall

Monolithic gray cast iron and cast aluminum-silicon alloys are used to make cylinder wall (Enomoto & Yamamoto, 1998). However, Al-Si alloys have poor scuffing and the hard Si particles in the Al matrix can act as abrasive particles, thus causing fatigue crack initiation (Yoshida et al., 1990). Aluminum alloy is then used to make cylinder bore which can retain 30% reduction of weight (Enomoto & Yamamoto, 1998). Therefore, hyper-eutectic Al-Si alloys are being coated with the electrolytic iron coating or thermal-sprayed coatings. The cylinder inner surface is modified by SiC dispersed Ni-P plating, and plasma sprayed coating by hard ferrous or non-ferrous alloys (Yoshida et al., 1990). To ensure high cylinder pressure, the development of Compacted Graphitic Iron (CGI) has been evolved as an emerging material that gives 75% higher tensile strength and doubles the fatigue strength of unalloyed gray CI and aluminum.

2.5.4.3 Piston and piston ring

Gray cast iron has been widely used as a piston material, but recently, because of high thermal conductivity, cast iron piston materials are being replaced by different kinds of lightweight and high strength aluminum alloys. The aluminum alloys experience high thermal expansion, which requires maintaining high clearance between piston skirt and cylinder bore. The copper and nickel-based aluminum alloy (Al 336) provides 13% lower thermal expansion coefficient than pure Al and thus helps to maintain low clearance between piston skirt and cylinder liner (Becker, 2004). One major limitation of piston skirts made of aluminum alloys sliding against cast iron cylinder liners is high friction. The nickel–ceramic composite coatings or molybdenum coatings on aluminum alloys have also been recommended for piston skirts due to their improved thermal and friction resistance (Becker, 2004).

Gray cast iron (CI), carbidic CI and malleable CI were used as piston ring materials due to its low cost while nitride stainless-steel and tool steel are widely used as piston ring materials because of its high strength and good fatigue properties (Becker, 2004; Enomoto & Yamamoto, 1998). Arc-ion plating of Cr–N or Cr on steel or CI compression rings has been reported to give wear resistance and low friction losses during high temperature (Simon C. Tung & McMillan, 2004). However, Cr–N plating gives much lower friction compared to Cr plating resulting in 90% and 15% reduction in ring wear and bore wear, respectively (Enomoto & Yamamoto, 1998). This is because the Cr coatings give poor oil entrapment which is difficult to maintain oil film at the sliding interface (Taylor & Eyre, 1979). Recently, to reduce friction and engine failure, plasma sprayed molybdenum, cermet, ceramics and diamond-like carbon have been used for coating the piston ring (Simon C. Tung & McMillan, 2004).

2.6 Fuel/lubricant/coating interactions

Coatings have been deposited on engine components in order to reduce friction and wear rates and are becoming a desirable strategy to cope with the new challenge faced by the automotive industry. Obtaining optimum durability (low wear) and fuel economy (low friction) of tribological systems, especially where new materials and surface treatments and coatings are used relies on compatibility between the surface and the lubricant, lubricant additive, and biofuel. It is known that wear and friction in the boundary lubrication regime are controlled mainly from the lubricant additives, which form tribofilms in the contact surfaces. Surface treatments and coating have an important role in providing an improved tribological performance, and they can eliminate the benefits of the additive. Therefore, understanding the details of how surfaces and additive react is essential in order to achieve optimal lubrication in the boundary (and mixed) regimes. Nowadays, the coatings having most attention in the automotive industry are diamond-like carbon (DLC) coatings and the studies of DLC coating interaction with engine oil, and oil additive, as well as biofuels, are important to understand tribological behaviors (friction and wear) of coated surface with fuel diluted engine oil. It has been reported that DLC coatings are inert to engine oil and its additives in comparison with uncoated steel surfaces (Al Mahmud et al., 2014). Some studies have reported positive chemical interactions between DLC coatings and oils (Kržan et al., 2009; Mistry et al., 2011), whereas some others found negative interaction (Equey et al., 2008; Podgornik et al., 2003). It has been understood that hydrogen content in coating influences the interaction between DLC coating and lubricant additives under lubricated conditions. Amorphous non-hydrogenated (a-C) DLC yields lower friction than amorphous hydrogenated (a-C: H) DLC under lubricated (engine oil 5W-30, SJ grade) conditions (Yasuda et al., 2003). Higher surface energy allows better interaction with a-C DLC. Surface energy is low for a-C: H because of the differences in their molecular structure. Simon C Tung and Gao (2003) studied the friction and wear performance of coatings on nitrided stainless steel (NSS) piston rings and chrome plated stainless steel rings sliding against cast iron cylinder liner segments in fully formulated engine oils using a high frequency reciprocating tribometer. The impacts of E85 fuel (a fuel blend of 85% bioethanol and 15% unleaded gasoline) on scuffing of the chrome-coated piston ring and cast-iron cylinder liner segment were studied with different fuels varying in their degree of acidity. The tribological characteristics due to surface interactions between piston ring coatings and energy-conserving engine oils containing molybdenum dithiocarbamate (MoDTC) or an organic friction modifier were compared and analyzed. The test results show that the DLC coating produces the lowest wear on the cylinder liner segment and has a similar ring wear to nitrided and CrN coated piston rings. With MoDTC present in the engine oil, friction and wear are effectively reduced. Table 2.7 shows previous studies of coatings with engine oil.

Table 2. 7: Previous studies of coated material lubricated with engine oils

Authors	Experiment	Fuel/lubricant/material	Results
(Simon C Tung & Gao, 2003)	**Test**: High frequency reciprocating ring **Load**: 80N-120N **Velocity**: 0.138m/s **Frequency**: 10Hz-20Hz **Slide distance**: 6.9mm **Time/Temp**: 10 h/60°C for fuel-oil blend test & 20 h/125°C for fresh engine oil	- Synthetic oil 5W20, 5W-30 - Mineral oil 5W-30, 10W40 -Ethanol - Counter body: Steel piston ring -Ring coating Nitrided steel, CrN, DLC, Chrome -Organic friction modifier, molybdenum	-The friction and wear increase when lubricant diluted with lubricant. -DLC has lowest friction and wear. - The more acidity in the fuel-oil sample, the more severe wear
(Banerji et al, 2016)	**Test**: Ball-on-disc **Load**: 5 N **Velocity**: 0.05m/s **Slide cycles**: more than 8000 cycles **Temp**: RT, 25°C	-Gray cast iron cylinder liner -AISI 52100 Steel Ball, diameter:6mm - Coating: NH-DLC -Synthetic oil: SAE 5W-30 (ILSAC GF-5) -E85 (85%ethanol + 15%gasoline) - Dilution ratio: 1:1 (by volume)	-NH-DLC coating results in lower friction and wear losses -It is found that dilution of E85 is beneficial to reduce more friction and wear
(Al Mahmud et al., 2014)	**Test:** Pin-on-plate **Load**: 392N **Velocity**: 0.64m/s **Frequency**: 4Hz **Stoke length**: 80mm **Temp**: 50°C, 100°C, 150°C **Time**: 3600s	- Counter body: AISI 440C steel ball -Substrate AISI 316-grade stainless steel - Coating: ta-C & a-C:H -Engine oil: SAE 40 -Additive: ZDDP	-COF and wear (coated layer and counter surface) are mostly influenced by coating graphitization - ta-C DLC has lower wear than a-C: H DLC
(Tasdemir et al., 2014)	**Test**: Pin-on-disc configuration **Load**: 5N **Velocity**: 0.1m/s **Hertzian contact pressure**: 0.15 GPa **Stoke length**:5mm **Temp**: 80°C **Time**: 60 min	- Material: high carbon chrome bearing steel (JIS SUJ2) - Coating: a-C, ta-C, a-C: H1, a-C: H2, Si-DLC, Cr-DLC -Lubricant: Base oil (PAO), PAO+ZnDTP	- ZnDTP greatly influences the tribological performance of DLC coating and reduces wear, but seems to promote high COF. - Hydrogenated and doped DLC coatings were more reactive with the ZnDTP additive

2.7 Fuel dilution in automotive lubricant

Figure 2.6 shows the effect of fuel on the engine and the lubricant in piston ring-cylinder system. Fuel dilution is a serious issue for automotive lubricants, particularly for direct-ignition engines. Fuel dilution is the condition in which unburned fuel accumulates in the engine crankcase through the cylinder walls. In reality, the fuel does not burn completely inside the combustion chamber of gasoline and diesel engines for various reasons. A high proportion of unburned fuel leaves the engine as exhaust while a small proportion of the unburned fuel impinges on the cold walls of the combustion chamber, which will then be scrapped to the oil pan and mix with the lubricant (S. Shanta et al., 2011). It has been identified that the causes of fuel dilution are the mode of injection and the properties of the fuel (Gu, 2014; Wattrus, 2013a). It has been shown in previous studies that even a low level of fuel dilution can degrade the physicochemical properties of the lubricant such as viscosity, total base number (TBN), total acid number (TAN), flash point, oxidation stability as well as the concentration of the engine oil additive. This, in turn, affects the lubricating properties of the lubricant (S. Shanta et al., 2011; Uy et al., 2011).

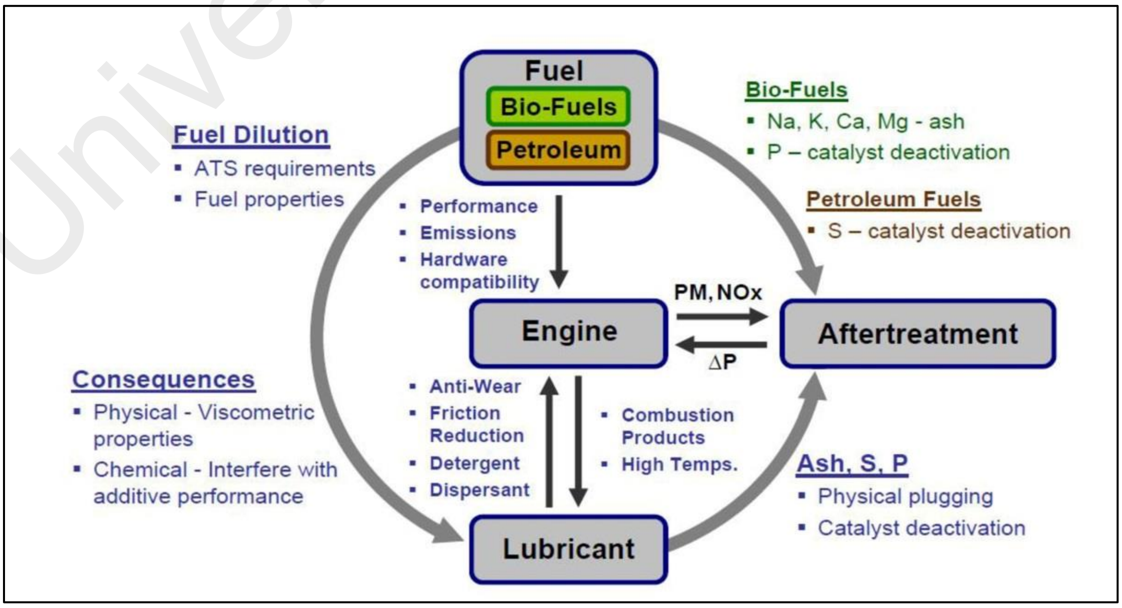

Figure 2. 6: Effect of biofuel and lubricant on the engine (Gili et al., 2011)

2.7.1 Primary cause of fuel dilution

One of the serious side-effects of the pre-injection and post-injection strategy in direct-injection gasoline and diesel engines is the increase in fuel dilution of the lubricant (Martyr & Plint, 2012). The post-injection of fuel used for regeneration of the diesel particulate filter accelerates fuel dilution. Filter regeneration increases fuel dilution in the lubricant because it involves the periodic injection of a small quantity of fuel with the burned fuel in order to increase the exhaust temperature and burn off all unburned hydrocarbons at the exhaust (S. M. Shanta, 2011). Uy et al. (2011) discovered that post-injection results in 20wt% fuel dilution before the oil was drained. Therefore, the fuel was not suitable for use in the engine. A direct injection engine has a fuel injector in the combustion chamber, whereby the fuel is injected directly towards the upper side of the piston and cylinder wall. Consequently, the fuel mixes with the oil film on the cylinder wall. In general, greater fuel dilution occurs at low temperatures in multi-point injection (MPI) engines, which reduces the viscosity of the lubricant. Late injection also affects the level of fuel dilution (Sagawa et al., 2002). The main disadvantage of late injection is that it increases the amount of lubricant exposed to the fuel. Unlike normal combustion, late-injected fuels do not atomize and evaporate easily. Hence, a portion of this fuel dilutes through the cylinder wall and washes down with the lubricant into the sump. This degrades the quality of the lubricant, which leads to significant wear losses (Wattrus, 2013b). If the fuel is injected late during the power stroke, there is a higher chance that the fuel spray will hit the oil on the cylinder liner rather than the piston bowl, resulting in an increase in fuel dilution (Gu, 2014). Figure 2.7 shows the fuel dilution based on the modes of injection such as (a) normal injection timing, and (b) late post-injection timing. One study proved that the turbocharged gasoline direct injection (TGDI) engine operated at high-speed end torque results in significant fuel dilution. This is due to the increased injection timing, which results in large fuel drops impinging on the top of the piston. The results also showed that the higher the torque rate-power, the greater the level of fuel dilution (Hu et al., 2015c).

The fuel properties are also the cause of fuel dilution. It is worth noting that the effect of bioethanol on the fuel dilution differs from that of gasoline. Based on this literature review, it is found that most of the studies related to the effect of fuel properties on fuel dilution highlight that bioethanol has higher final boiling point and latent heat of vaporization. Both of these properties increase the tendency of the fuel to reach the crankcase and increase the rate of fuel addition to the lubricant (Wattrus, 2013b). In addition, the presence of bioethanol affects the lubricant in the ring pack in cold-start, warm-up, and short-trip conditions due to its higher heat of evaporation compared to gasoline. One study was focused on investigating accelerated oil dilution using an engine test bench, and the results showed that fuel with low viscosity, density, surface tension and high front-end volatility is correlated to the fuel addition rate rather than the droplet size of the fuel spray and in-cylinder droplet evaporation rate (Wattrus, 2013b). The distillation temperature, and penetrating and solvency properties also have a significant effect on the fuel dilution in the long term (S. M. Shanta, 2011). Other factors causing fuel dilution are leaking fuel injectors, excessive idle time, incomplete combustion, cold engine operating conditions, frequent short-trip driving and worn piston ring or excessive blow-by. Hence, the mode of injection (i.e. pre-injection and post-injection), late injection and fuel properties are the factors which influence the fuel dilution rate of lubricants.

As seen in the above literature, fuel properties also contribute to fuel dilution, which is one of the main causes of lubricating oil degradation. During cold condition, engine fueled with bioethanol will encounter significant starting problem because of its high boiling point. If the temperature of lubricant does not reach operating temperature of 70°C or over, bioethanol existing in the sump will not evaporate. Hence, based on this literature, the study on the optimization of fuel blends such as gasoline-bioethanol and diesel-biodiesel blends at different blending concentrations should be encouraged to include the investigation into fuel properties like boiling point, heat of vaporization, distillation temperature, and penetrating and solvency properties because they are factors influencing the increase in fuel dilution rates of engine oil.

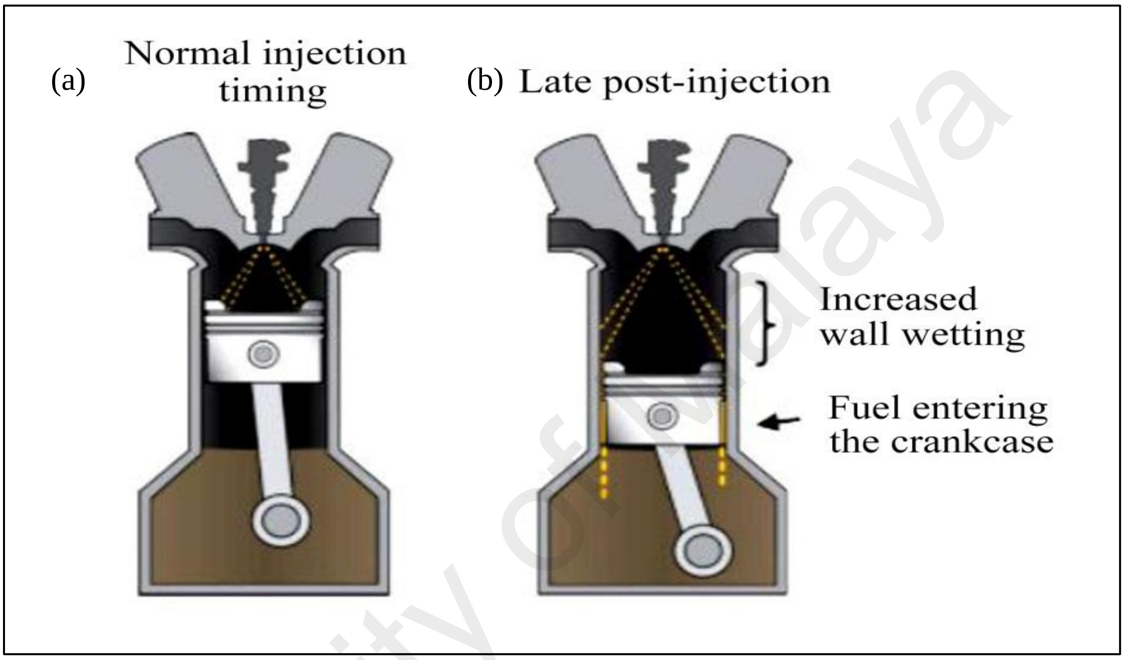

Figure 2. 7: Fuel dilution of lubricants based on the modes of injection (Wattrus, 2013b)

2.7.2 Fuel dilution rate of lubricant

A high level of fuel dilution in the lubricant indicates that there is serious contamination of the lubricant. It is known that fuel dilution degrades the quality of the lubricant and it is worth noting that it is crucial to maintaining the quality of the lubricant in order to ensure optimum lubrication performance during engine operations. The design limit for fuel dilution is typically less than 5 wt.% and a higher level of fuel dilution is unacceptable because this results in a significant reduction in the oil viscosity as well as the concentration of the oil additive. This, in turn, reduces the film thickness of the lubricant (Gu, 2014). A number of researchers have investigated the effect of fuel dilution rate on the properties of automotive lubricants. One study showed that the properties of mineral oils degrade significantly at 1% fuel dilution, and the wear protection properties of these oils were totally deteriorated at 7% fuel dilution. In contrast, the stability resistance of synthetic oils improves at 1% fuel dilution but these oils lose almost all of their lubrication properties at 7% fuel dilution (Gur’yanov, 2007). Other researchers discovered that the maximum fuel dilution is 4% for gasoline engines, whereas 5% fuel dilution is sufficient enough to decrease the viscosity and flash point of the oil considerably and weakens the film stability of the oil (Cerny & Vaclavickova, 2006). There are two mechanisms which influence the level of fuel dilution, the rate of fuel leaving the oil and the rate of fuel entering the oil. This occurs when the fuel fails to vaporize and remains in the cylinder in liquid form. The rate of evaporation from the oil plays a critical role in determining the overall dilution rate. It is important to determine the level of fuel dilution and keep it less than 5% to ensure that the lubricant remains effective.

2.8 Effect of fuel dilution on the physicochemical properties and performance of automotive lubricants

Even though bioethanol is widely accepted as an alternative fuel for gasoline engines, there are still issues concerning the effect of bioethanol dilution on the tribological behaviors of automotive lubricants which need to be addressed. In general, bioethanol dilution decreases the viscosity and TBN of the lubricant while it increases the TAN of the lubricant. The accumulation of bioethanol in the lubricant reduces the lubricating performance of the lubricant to protect the engine components against friction and wear. For this reason, it is important to highlight the effects of bioethanol dilution on the physicochemical properties and performance of automotive lubricants, which is the focus of this section. Table 2.8 lists the previous studies of the effect of bioethanol fuel on tribological characteristics of engine oil.

Table 2. 8: Previous studies of lubricant diluted with fuel contaminant

Authors	Methods/Material	Conditions	Results
Assessment of lubricating oil degradation in small motorcycle engine fueled with gasohol			
(Tippayawong & Sooksarn, 2010)	- Engine Testing - Bench Wear tester - Mineral oil - Synthetic oil - Gasoline/Gasohol	- Mileage: 3000km - Load: 33N - Speed: 500rpm - Temp:25°C	-Viscosity drop: 20%-45% -Gasohol Wear: 10% higher -Mineral oil: higher wear -Synthetic oil: Lower wear -Friction (unknown)
Bio-derived fuel blend dilution of Marine Engine oil and impact on Friction and Wear Behavior			
(Ajayi et al., 2016)	- Engine testing - Unidirectional sliding - Reciprocating sliding - Four-ball wear test - Gasoline, Ethanol Isobutanol - Engine oil: 10W-30	- Load:15N - Velocity: 0.1cm/s - 20.0cm/s - Speed: 10-300rpm, -Frequency: 0.1-5Hz -Four-ball load: 15kg - Speed: 1200rpm, - Temp: 70°C - Time:1h	- Dilution: 3.7%-6% - Viscosity drop: E0: 30%-43% E10: 25%-42% i-B16: 28-46% - No effect on Friction - Slightly affect wear and reduce load-carrying capacity
Tribometer investigation of the frictional response of piston rings when lubricated with the separated phased of lubricant contamination with ethanol and water			
(P. De Silva et al., 2011a)	- Plint TE77 -Lubricant: Shell Helix HX7, SAE 5W-30, no friction modifier - Ethanol 95% purity, Water	- Duration: 2h - Liner Temp: 70°C - 110°C, Test Temp: 25-40°C - Speed: 2000rpm -Load: 150N(4 MPa) - Stroke length: 5mm -Cold-start/warm up/ short-journey	-Friction reduction (Separated phase of lubricant-ethanol-water) -Viscosity decreased -Implication: Fuel economy in a fired gasoline engine
Tribological response of fresh and used engine oils: The effect of surface texturing, roughness and fuel type			
(Cousseau et al., 2015)	- Tribotest (ball on discs) - Ball: AISI 52100 - Discs: AISI H13 - Engine oil: 5W30 - E22, E100 7%water	- Duration: 20min - Test sample: 3ml - Temp: 40°C - Load: 35 N -Stroke length: 5mm - Frequency: 10 Hz - Max speed: 0.159m/s	-No effect on friction significantly -Slight effect on wear E22 is more oxidized -May cause oxidative wear

2.8.1 Effect on lubricant properties

2.8.1.1 Viscosity

The viscosity is greatly affected when it is contaminated by bioethanol. It was shown in a previous study that a low concentration of bioethanol decreases the viscosity of the engine oil (Spikes & Costa, 2016). Another study was conducted to investigate the effects of ethanol contamination on the properties of engine oils, in which 2% and 5% hydrate and anhydrous ethanol were added into the base and formulated oils. The results showed that the addition of a low concentration of ethanol into the oil decreases the viscosity of the base and formulated oils, particularly for anhydrous ethanol (Costa & Spikes, 2015). Veselá et al., (2009) conducted a study to compare the effect of BA95 fossil fuel and E85 on the quality and cleanliness of the engine oil at different temperatures. The tests were carried out on Saab 95 and 93 car engines lubricated with pure Mobil 1 0W-40 engine oil, and the properties were measured at 40°C and 100°C. The measurements were taken after a mileage of 7000 km, and the results showed that the viscosity of the engine oil decreases up to 20% for the Saab 95 car engine fueled with E85, whereas the viscosity of the engine oil decreases more than 20% for the Saab 93 car engine. The viscosity measured at 40°C is 69.379 mm^2/s and 69.263mm^2/s, respectively, whereas the viscosity of pure engine oil is 75.127mm^2/s. It shall be noted that the viscosity of the engine oil for both car engines fueled with E85 could not be measured at 100°C. In contrast, the viscosity of engine oil was measurable at both temperatures when fossil fuel BA95 (octane value: 95) was used to fuel the engine, and the results showed that the viscosity of the engine oil for both car engines fueled with this BA95 fossil fuel do not differ significantly from the viscosity of pure engine oil at 40°C and 100°C. The results indicated that there is a significant reduction in the viscosity of the engine oil for the Saab 95 and 93 car engines fueled with E85, which leads to a decrease in the lubricity of the oil.

2.8.1.2 Total base number and total acid number

The total base number (TBN) is a measure of the lubricant’s alkalinity and it reflects the ability of the lubricant to counteract corrosion. The TBN plays an important role to neutralize the total acid number (TAN) which is an indicator of the lubricant’s tendency toward oxidation. When the engine is in operation, acidic products are produced from the combustion of fuel and oxidation of the lubricant, which decrease the TBN and increase the TAN of the lubricant. Some researchers have studied the effect of bioethanol dilution on the TBN and TAN of the lubricant. Jakóbiec and Mazanek (2009) examined the changes in the TBN and TAN of SL/CF SAE 5W-30 engine oil. The experiments were carried out using a Motor vehicle engine fueled with two types of fuel: (1) gasoline 95 and (2) gasoline with 5 vol.% ethanol. The testing mileage was within a range of 5000–30000 km. The results showed that there is a significant decrease in the TBN of the engine oil for engine fueled with gasoline blended with 5% ethanol additive, with a value of approximately 52% in winter driving conditions. In contrast, the TBN of the engine oil decreases by 41% for the engine fueled with gasoline 95. Hence, it is evident that the decrease in the TBN is more pronounced for the engine fueled with the bioethanol blend. The results also showed that the TAN of the engine oil is higher for the engine fueled with gasoline blended with 5% ethanol additive. The increase in the TAN of the engine oil results in serious deterioration of the engine components due to oil oxidation as well as corrosion. Other researchers have also discovered that the oxidation level is higher for ethanol fuel, which increases the TAN of the engine oil (Friedl & Stimming, 2013; Yusoff et al., 2015).

2.8.2 Effect on lubricant performance

2.8.2.1 Friction

The friction characteristics of automotive lubricants contaminated with ethanol and water have also been investigated in previous studies. P. R. De Silva (2012) investigated the effect of ethanol and water contamination on the friction characteristics of the lubricant for both piston rings and cylinder liner in cold-start, warm-up, and short-trip conditions. Interestingly, the tribometer measurements showed that there is a significant reduction in friction when the contact surface between the piston rings and cylinder liner is lubricated with the lubricant contaminated with ethanol and water compared to the formulated oil. Likewise, Priest (2012) also observed a reduction in friction of the piston rings when the lubricant is contaminated with ethanol and water. Four types of engine oil samples were prepared: (1) engine oil mixed with 5 wt.% ethanol and 8 wt.% water, (2) engine oil mixed with 5 wt.% ethanol and 16 wt.% water, (3) engine oil mixed with 10 wt.% ethanol and 8 wt.% water and (4) engine oil mixed with 10 wt.% ethanol and 16 wt.% water. The tests were carried out at the following test conditions: (1) temperature: 20°C and 40°C, (2) engine speed: 1500rpm–2000rpm and (3) engine load: 100N and 200N. The results showed that there is a significant reduction in friction for the contact surfaces lubricated with lubricant–ethanol–water mixtures compared to pure engine oil. The addition of ethanol and water into the lubricant improves the ability of the lubricant to reduce friction.

2.8.2.2 Wear

Wear is the deformation of material on a surface, happening during the interaction between opposite sliding surfaces. A number of researchers have also investigated the effects of bioethanol dilution on the wear characteristics in engines. Ajayi et al. (2016) investigated the effect of fuel dilution rate of three lubricants exposed to E0, E10 and iB16 fuels on friction and wear behavior. The tests were carried out in the boundary lubrication regime. The results revealed that the dilution of these fuels has a significant effect on wear behavior. Chui and Baker (1980) studied the effect of bioethanol dilution on the wear and corrosion characteristics of engine oil during warm-up driving conditions. The tests were conducted in accordance with the ASTM Sequence V-D gasoline engine test within a temperature range of 27°C –49°C. The results showed that the concentration of bioethanol in the crankcase oil increases from 0% to 25%, whereas the concentration of iron in the crankcase oil increases from 200ppm to 2600ppm after 192 operating hours. Besser et al. (2012) developed a novel laboratory-based artificial aging method to investigate the effect of fuel dilution on oil degradation and formation of sludge and engine deposits. They formulated three types of engine oils: (1) engine oil mixed with bioethanol, (2) engine oil mixed with acetaldehyde and (3) engine oil mixed with acetic acid. The results showed that the addition of ethanol and acetaldehyde in the engine oil at low concentrations has a negligible effect on the progression of oil degradation. However, the results showed the presence of engine deposits at low concentrations of ethanol and the presence of some particles at high concentrations of ethanol. More importantly, the results showed the formation of heavy sludge for the engine oil mixed with acetic acid. It shall be highlighted that the formation of sludge and engine deposits is undesirable since these materials will clog valves and orifices. These materials also accelerate engine wear by trapping hard metal contaminants (Ancho, 2006).

2.9 Summary of fuel dilution and research gaps

2.9.1 Summary

- Bioethanol dilution is the condition in which unburned bioethanol accumulates in the crankcase through the cylinder walls, which in turn contaminates the lubricant. The mode of injection (pre-injection and post-injection) and the fuel properties are the causes of bioethanol dilution. Bioethanol dilution is higher compared to that for gasoline because of its higher heat of vaporization
- Bioethanol contains high oxygen content and has a hygroscopic nature which attracts the amount of water in lubricants. It is possible that the complex mixture of bioethanol, water, and lubricant as well as lubricant additives interact with each other over a period of time especially at high temperature, resulting in highly oxidative degradation of lubricants, corrosion, sludge formation and wear of engine components.
- The viscosity of the lubricant decreases when the lubricant is contaminated with bioethanol. The total base number decreases while the total acid number of the lubricant increases with an increase in the bioethanol dilution rate. The decrease in the total base number and the increase in the total acid number is detrimental to engine components since the lubricant loses its ability to protect these components from corrosion.

2.9.2 Research gaps

1. The discussion on tribological behavior of lubricant with various dilutions of bioethanol is very few and not clearly analyzed to provide a concrete understanding in this field.
2. Moreover, the addition of nanoparticle to bioethanol-diluted oil to improve friction and wear behaviors has not been documented yet
3. The study on the interaction of bioethanol with coated steel contact has not been clearly investigated.

CHAPTER 3: METHODOLOGY

3.1 Introduction

Chapter 3 describes the methodology for achieving the set objectives as shown in figure 3.1. Four-ball tester provides tribological evaluation of bioethanol-diluted lubricants and GP/WS_2 dispersed oils, while HFRR tester provides the friction and wear evaluation of GP/WS_2 dispersed oils tested with uncoated and ta-C coated surfaces. After testing, the worn surfaces were collected for surface analysis.

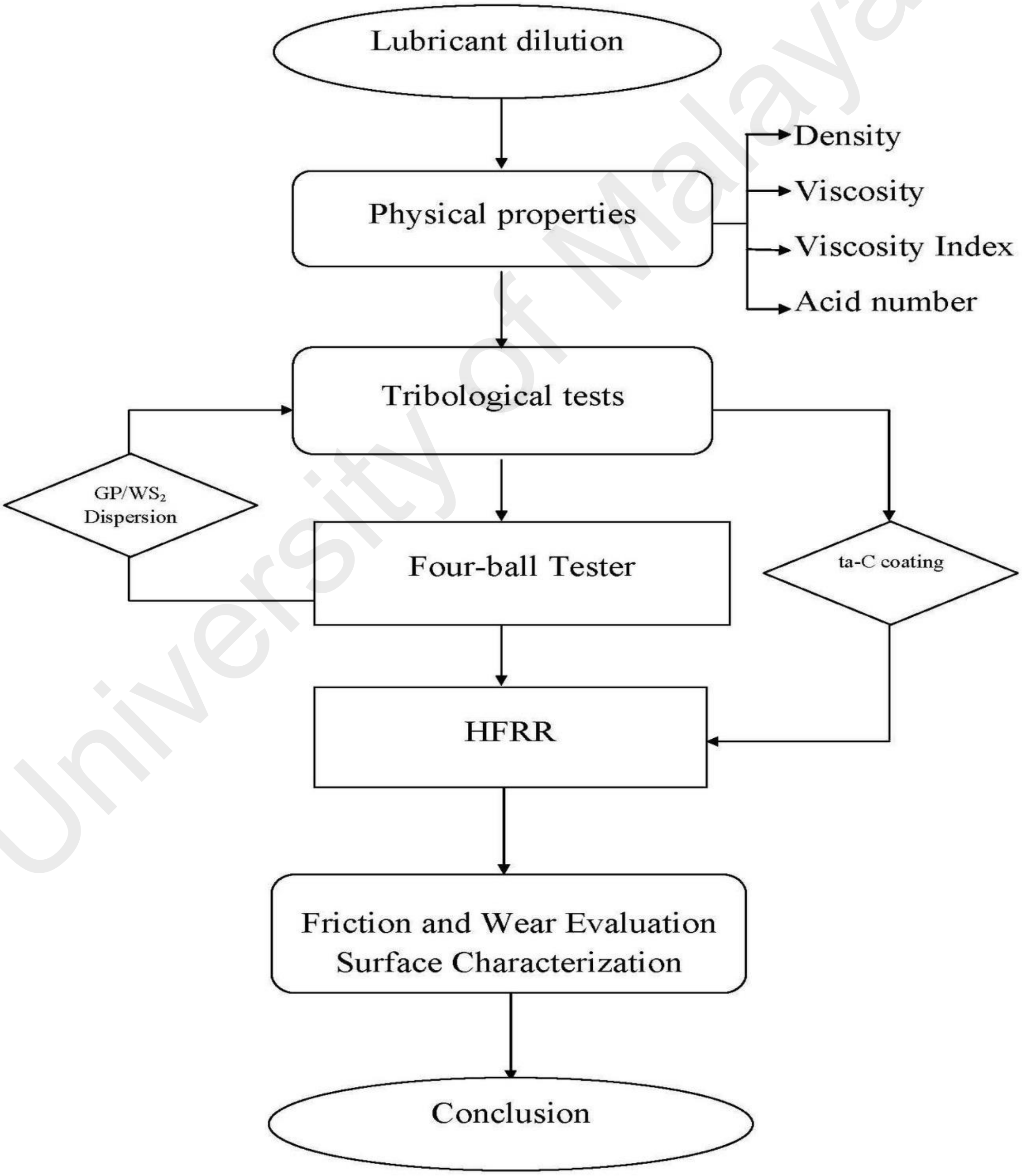

Figure 3. 1: Flow chart of research methodology

3.2 Material preparation

3.2.1 Material used

Commercial synthetic oil (SO, SAE 5W-40) collected from Malaysian market (Petronas, Malaysia) was employed in the four-ball wear test. SO denotes synthetic oil in the whole article. This lubricating oil is used in all types of passenger cars and high-performance vehicles equipped with fuel injection, turbocharger, or supercharger operating under the extreme conditions. Table 3.1 presents the physicochemical properties of the synthetic oil. Gasoline with research octane number (RON) 95 and bioethanol (purity 99.8%), which were obtained from Chemical Industries (Malaya) Sdn. Bhd., were used to add to the lubricant. Table 3.2 shows the properties of gasoline and bioethanol. The ball used for four-ball wear test was AISI alloy steel. For HFRR wear test, the alloy steel roller (AISI 52100) and plate (AISI 52100) are purchased from the foreign market. Table 3.3 describes the physical properties of the steel ball, roller and plate for four ball and HFRR wear test.

Table 3. 1: Physicochemical properties of synthetic oil

Synthetic oil	**Density (kg/l) 15℃**	**Viscosity ($\mathrm{mm^2/s}$)**		**Viscosity Index**	**Sulphated Ash (%wt)**	**TBN (mgKOH/g)**	**TAN (mgKOH/g)**
		40℃	**100 ℃**				
5W-40	0.854	82.03	13.20	171.00	0.82	9.10	1.40

Table 3. 2: Properties of gasoline and bioethanol

Properties	**Gasoline (RON 95)**	**Bioethanol**
Density ($\mathrm{g/cm^3}$) at 15℃	0.750	0.799
Kinematic viscosity at 15℃ ($\mathrm{mm^2/s}$)	0.542	1.713
Boiling point (℃)	35.00	78.00
Heat of vaporization (kJ/kg)	349.00	923.00

Table 3. 3: Specification of steel ball, steel roller, and steel plate

Physical properties	**Testing ball**	**Counter surface (roller)**	**Substrate (steel plate)**
Material	AISI 52100	AISI 52100	AISI 52100
Diameter	12.7 mm	6.35mm	-
Dimension	-	-	15mmx15mm
Hardness	64-66 Rc	64-66 Rc	60 Rc
Surface roughness	0.1 (C.L.A)	0.1 (C.L.A)	0.045 µm (Ra)
Poisson's ratio	-	0.26	0.30
Elasticity modulus	-	200 GPa	200 GPa
Composition	10.20% C, 0.45% Si, 0.12% P, 0.07% S, 1.46% Cr, 0.42% Mn, 0.06% Ni, 2.15% Zn and rest 85.06% Fe	10.20% C, 0.45% Si, 0.12% P, 0.07% S, 1.46% Cr, 0.42% Mn, 87.30% Fe	10.20% C, 0.45% Si, 0.12% P, 0.07% S, 1.46% Cr, 0.42% Mn, 87.30% Fe

3.2.2 Specimen cutting and polishing

The plate is cut into 15mmx15mm pieces to be used with high frequency reciprocating ring, using the metal cutting machine. After cutting, the plate samples were polished using the polishing machine in order to achieve specific roughness between 0.03µm (Ra) and 0.04µm (Ra) smooth surfaces. The substrates (plate) are polished by 600-, 800-, 1000-, 1500- and 2000-grade sand papers. Then, 3µm and 1µm diamond suspension with silicon paper are used for further polishing. Finally, the plates are polished with silicon carbide particles (0.01µm in size), and the polished plates were then coated with ta-C.

3.2.3 Specimen coating techniques

To coat the surface, Magnetron sputtering is used to deposit ta-C on the final polished surface in Ar/methane atmosphere. The machine is equipped with integrated arc and magnetron sputtering technology for greater flexibility. Therefore, this method is called hybrid magnetron sputtering. The reason for choosing ta-C coating is because it is known that this coating deposition is cost-effective and its friction and wear resistance is also better than other coatings such as a-C: H and ta-C:H. ta-C has much higher elastic modulus and hardness than hydrogen containing DLC’s. Moreover, ta-C coating has been deposited to tappet of the engine (Mutafov et al., 2014). The deposition of ta-C coating is performed via four main stages as shown in Table 3.4. Evacuating and preheating is the first stage to evacuate the vacuum chamber and ensure that all of the moisture absorbed by the material has been outgassed prior to deposition. The second stage is argon cleaning, through which the ions scrub or clean the surface or remove micro oxides so that the adhesion of coating substrate is improved. Next stage is the coating phase. In this stage, the high energy sputtering process deposits a dense well-adhered smooth underlayer to reach a proper thickness and then transit to deposit a dense smooth ta-C coating onto the final surface layer. After final deposition, the substrate is cooled down for 30 min before taken out from the chamber.

Table 3. 4: Process of ta-C coating deposition

Coating process	Time	Current (A)	Voltage (V)	Gas pressure (mbar)
Evacuating and preheat up to 150℃	30 min	-	-	-
Argon cleaning	30 min	-	75	2.5 (argon)
Chromium deposition	10 min	60	40	-
ta-C deposition	90 min	20	160	0.5 (acetylene)
Cooling	30 min	-	-	-

3.3 Sample preparation

3.3.1 Lubricant and fuel blending

In this study, five bioethanol-gasoline blends such as gasoline (E0), gasoline-10 vol.% bioethanol (E10), gasoline-20 vol.% bioethanol (E20), gasoline-30 vol.% bioethanol (E30) and gasoline-85 vol.% bioethanol (E85) were formulated. Each fuel blend was mixed at an appropriate volume of 100 ml. Table 3.5 describes the combination of gasoline and bioethanol sample. The KS 260 basic orbital shaker was running for 30 min, at room temperature and at speed of 400 rpm. After blending bioethanol with gasoline, some physicochemical properties were measured in order to investigate the changes of properties of each fuel blend, compared to the base fuel. Table 3.6 shows the physicochemical properties of each gasoline-bioethanol blend. Then each fuel blend was added to SO at the rate of 6 vol.% in order to prepare fuel-oil samples for the test (i.e. 6%E10-SO representing 6 vol.% E10 with synthetic oil). 6 vol.% concentration is selected because ethanol has more tendency to reach oil sump due to its high heat of vaporization and the permissible dilution rate of fuel in engine oil is limited to 4% for gasoline engines. To receive homogenous test samples, the magnetic stirrer was used to mix blended fuels and lubricants at an appropriate volume of 100 ml. The stirrer was running for 20 min, at a constant speed of 400 rpm and at ambient temperature. Table 3.7 shows the combination of the blended fuel-oil samples.

Table 3. 5: Combination of gasoline-bioethanol fuel samples

Fuel sample	Descriptions
E0	0% bioethanol + 100% gasoline
E10	10% bioethanol + 90% gasoline
E20	20% bioethanol + 80% gasoline
E30	30% bioethanol + 70% gasoline
E85	15% bioethanol + 85% gasoline

Table 3. 6: Physicochemical properties of bioethanol-gasoline blended fuels

Properties	Unit	E10	E20	E30	E85
Density at 15℃	kg/m^3	0.754	0.758	0.763	0.788
Kinematic viscosity at 15℃	mm^2/s	0.576	0.647	0.748	1.411
Kinematic viscosity at 20℃	mm^2/s	0.546	0.614	0.705	1.292

Table 3. 7: Combination of blended fuel-oil samples

Fuel-oil sample:	Descriptions
SO	Synthetic oil
6%E0-SO	6%E0 +97%synthetic oil
6%E10-SO	6%E10 +97% synthetic oil
6%E20-SO	6%E20 +97% synthetic oil
6%E30-SO	6%E30 +97% synthetic oil
6%E85-SO	6%E85 +97% synthetic oil

3.3.2 Synthesis of GP/WS_2 nanocomposite additive

GP and WS_2 were used as nanocomposite additive because GP/WS_2 is known to perform better lubrication than GP alone. It is suitable to be used with engine oil with dilution of bioethanol because it helps to reduce corrosion from bioethanol dilution. GP and exf-WS_2 were dispersed in distilled water with a mass ratio of 1: 9; the mixture was then sonicated and stirred at room temperature for 1 hour each using a KQ-700E ultrasonic system and a magnetic stirrer. To generate active functional sites, we dropped two drops of concentrated hydrochloric acid into the reaction mixture. We then stirred the mixture and sealed it in a 50-ml autoclave, which was maintained at 240℃ for 24 hours. Finally, the resulting product, GP/WS_2, was filtered using a TG-16 high-speed centrifuge and repeatedly washed with distilled water and bioethanol before being freeze-dried for further use. Figure 3.2 shows the TEM image of GP and WS_2 nanocomposite.

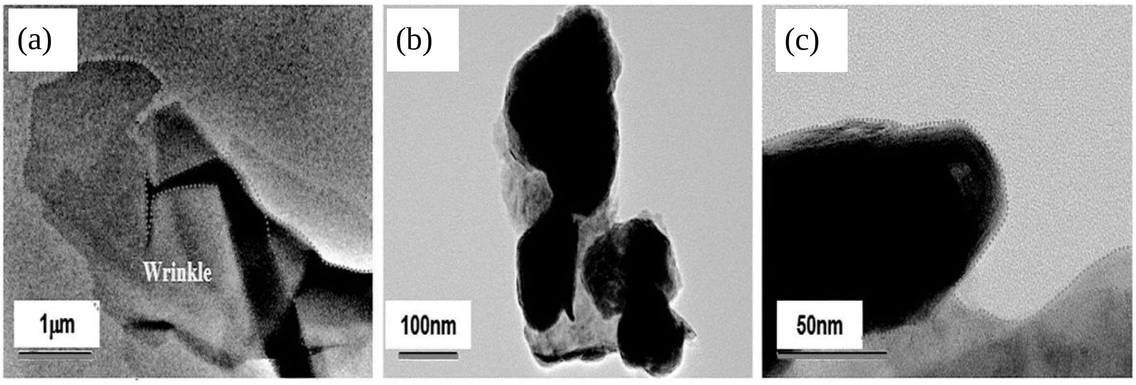

Figure 3. 2: shows TEM image of (a) GP, (b) WS_2, and (c) GP/WS_2

3.3.3 Lubricant and GP/WS_2 nanocomposite dispersion

The nanocomposite of tungsten disulfide and graphene (GP/WS_2) additive was added as an engine oil additive to the bioethanol-oil mixtures at five different concentrations of 0.01wt%, 0.02wt%, and 0.04wt%, 0.06wt%, and 0.1wt%, in order to reduce wear losses of various bioethanol-diluted engine oils. It shall be notified that various concentrations of nanocomposite were selected to find out the optimum concentrations. The concentration of nanocomposite should be as low as possible to be added into lubricant and high enough to reduce the influence of high amount of bioethanol dilution. These concentrations were selected in previous studies (Zheng et al., 2017). Table 3.8 shows the detail of the physical properties of the nanocomposite (GP/WS_2) additive. Inorganic nanoparticle additive is well-known for having poor dispersion stability in an organic liquid, so the same concentration of surfactant Span-80 ($C_{24}H_{44}O_6$) was used as a dispersing agent. Fluid mixture was stirred for 10 min and sonicated for 30 min, resulting in a stable dispersion of GP/WS_2 oil. Figure 3.3 shows the image of bioethanol-diluted lubricant with and without dispersion of GP/WS_2 at the concentration of 0.04wt% after 1 week and after 4 weeks. After 1 week, all dispersed oils are still dark and turbid. This shows that the Span-80can enhance the dispersion stability. However, the agglomeration phenomenon was also noted through careful observation. After 3 to 4 weeks, an amount of precipitate was observed in each dispersed solution. Table 3.9 shows the combination of dispersed oil.

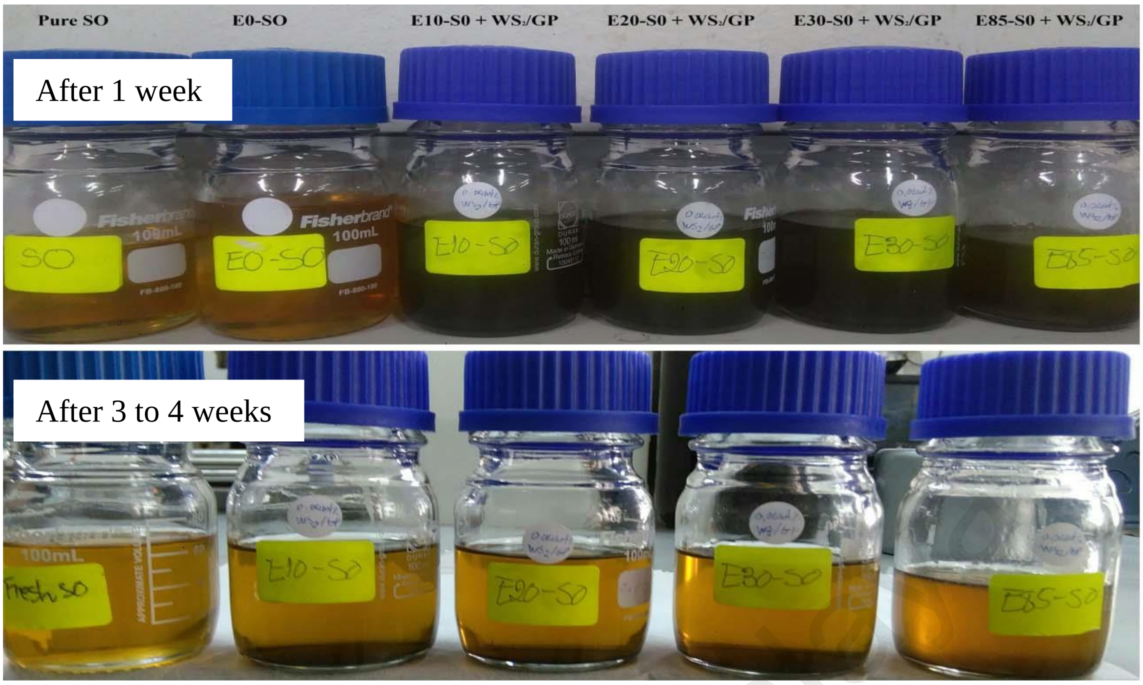

Figure 3. 3: Image of bioethanol-diluted oils with dispersion of GP/WS$_2$

Table 3. 8: Detail of the nanocomposite

Properties	**Description: nanocomposite (GP/WS$_2$)**
Chemical name	Graphene (GP) and Tungsten Disulfide (WS$_2$)
Molecular weight	-/248 g/mol
Purity	99.9% /99.9%
Average Particle Size	~20nm/ 40-80nm
Chemical stability	Inert, non-toxic/ inert, non-toxic

Table 3. 9: Preparation of the fuel-lubricant-additive blending

Oil samples	**Combination**
E10-SO $_{GP/WS2}$	E10+SO+GP/WS$_2$(0.01wt%; 0.02wt %; 0.04wt %; 0.06wt%; 0.1wt%)
E20-SO $_{GP/WS2}$	E10+SO+GP/WS$_2$(0.01wt%; 0.02wt %; 0.04wt %; 0.06wt%; 0.1wt%)
E30-SO $_{GP/WS2}$	E10+SO+GP/WS$_2$(0.01wt%; 0.02wt %; 0.04wt %; 0.06wt%; 0.1wt%)
E85-SO $_{GP/WS2}$	E10+SO+GP/WS$_2$(0.01wt%; 0.02wt %; 0.04wt %; 0.06wt%; 0.1wt%)

3.4 Physicochemical properties

In order to observe oil degradation by fuel dilution, the physicochemical properties of fuel diluted lubricant such as density, viscosity, viscosity index (VI), acid number were measured by using instruments mentioned in Table 3.10. All properties measurements were measured according to ASTM standard methods. Table 3.11 indicates the properties of synthetic oil diluted with 6 vol.% of gasoline-bioethanol blends. Stabinger viscometer was used to measure viscosity index, density at 15°C and kinematic viscosity at 40°C and 100°C. The acid number were measured using TAN analyzers.

Table 3. 10: List of equipment used for properties test

Property	Equipment/Model	Manufacturer	Test method	Accuracy
Density	Stabinger Viscometer, SVM 3000	Anton Paar, UK	ASTM D445	±0.1 kg/m^3
Kinematic viscosity	Stabinger Viscometer, SVM 3000	Anton Paar, UK	ASTM D445	±0.1 mm^2/s
Viscosity Index	Stabinger Viscometer, SVM 3000	Anton Paar, UK	ASTM D445	±0.1
TAN	TAN Analyzer,	Metrohm, Switzerland	ASTM D664	±0.001 mgKOH/g

Table 3. 11: Physicochemical properties of each fuel-oil blend

Test sample	Viscosity (mm^2/s)		Viscosity Index	Density (g/cm^3) 15 °C	Acid number (mgKOH/g)
	40 °C	100°C			
Pure SO	82.03	13.2	171	0.854	1.4
E0-SO	58.52	10.99	183	0.851	2.11
E10-SO	56.63	10.86	182	0.851	2.17
E20-SO	57.14	N.M.	N.M.	0.851	2.28
E30-SO	57.69	N.M.	N.M.	0.852	2.36
E85-SO	62.45	N.M.	N.M.	0.852	2.89

N.M. = Not measurable (Due to the evaporation of ethanol at 100°C)

3.5 Tribological testing

3.5.1 Four-ball tester

Four-ball machine (TR-30H) was used in order to investigate the effect of different bioethanol-gasoline blended fuel dilutions of lubricating oil on friction and wear characteristics under boundary condition. Figure 3.4 illustrates the schematic diagram of the four-ball wear tester. The balls used were alloy steel balls. To set up each test, the steel balls and the oil cup were thoroughly cleaned by using toluene and wiped by using a neat tissue to make them completely dry before introducing the lubricant. Three stationary balls were placed into oil cup and locked tightly together by using locking ring and nut while another rotatory ball was put into the upper rotating ball chuck. Each fuel-oil sample of 10 ml (i.e. 6%E10-SO) was slowly injected into the oil cup to avoid air bubbles until it fully covered the three stationary balls, and then placed the prepared ball chuck and oil cup to their position in the test machine. To investigate the friction and wear behaviors, the four-ball machine was performed for 60 ± 1 min, at a temperature of 75 ± 2℃, under normal loads of 40 ± 0.2 kg and 80 ± 0.2 kg and at a constant rotational speed of 1200 ± 60 rpm. After having completed the test, frictional data, and the stationary balls were collected for evaluating coefficient of friction (COF) and wear scar diameter (WSD) values, respectively, as well as for performing SEM/EDS analysis to observe the worn surface characteristic.

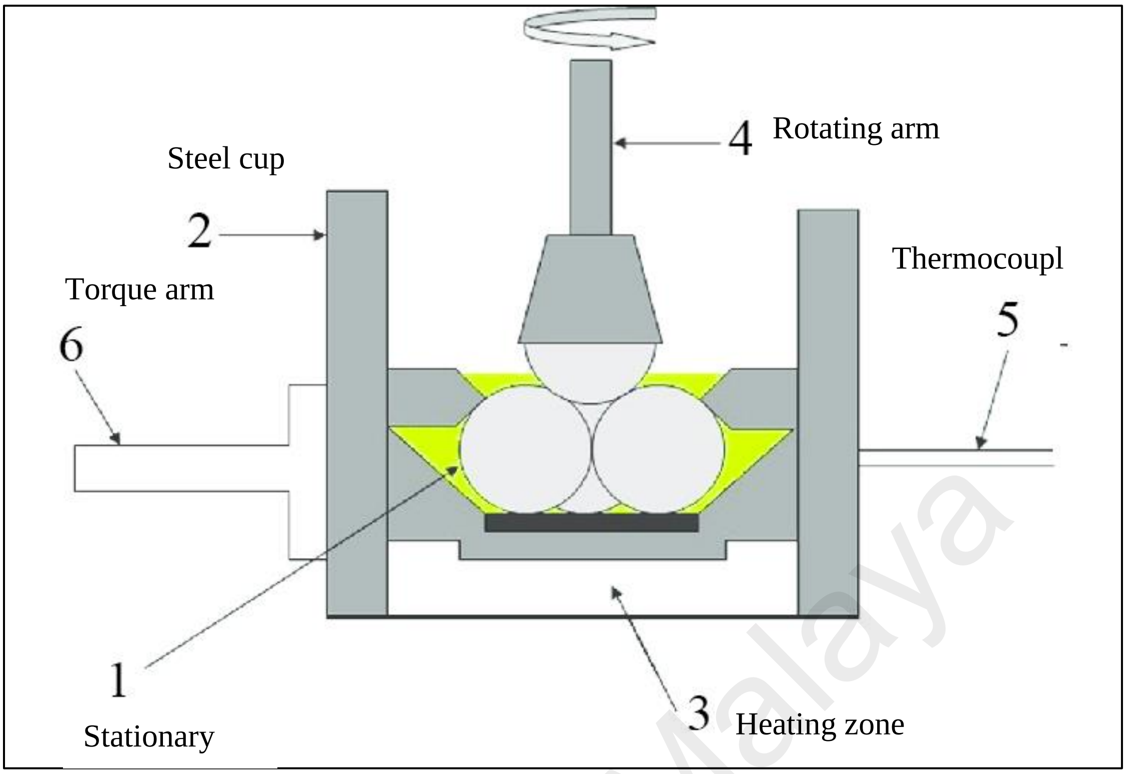

Figure 3. 4: Schematic diagram of the four-ball machine

3.5.2 HFRR wear tester

In this study, the tribological behaviors were examined using a high frequency reciprocating ring (HFRR). The schematic diagram is illustrated in Figure 3.5. It determined the friction and wear characteristics of the fresh engine oils and bioethanol-diluted engine oil. The roller specimens used in this test were made of polished and hardened AISI 52100 steel with a diameter of 6.35mm and the final polished uncoated plate specimen was made of gray cast iron. The detail description of the steel roller and plate is shown in the table above. Prior to testing, equipment and specimens must be clean and dry using toluene and tissue. The roller was inserted into the holder attached to the friction transducer, and the polished plate was put into the oil bath. Table 3.12 shows the operating conditions of HFRR. These conditions do not exactly resemble the engine application; however, they are closely related to the situation of piston-ring assembly conditions. The normal temperature of engine oil during start-and-stop driving condition is from 25°C to 80°C. To reduce the evaporation of bioethanol, the test was performed at

75°C. Upon completion of each test, plate specimens were collected for surface analyses by SEM/EDS, and profilometry.

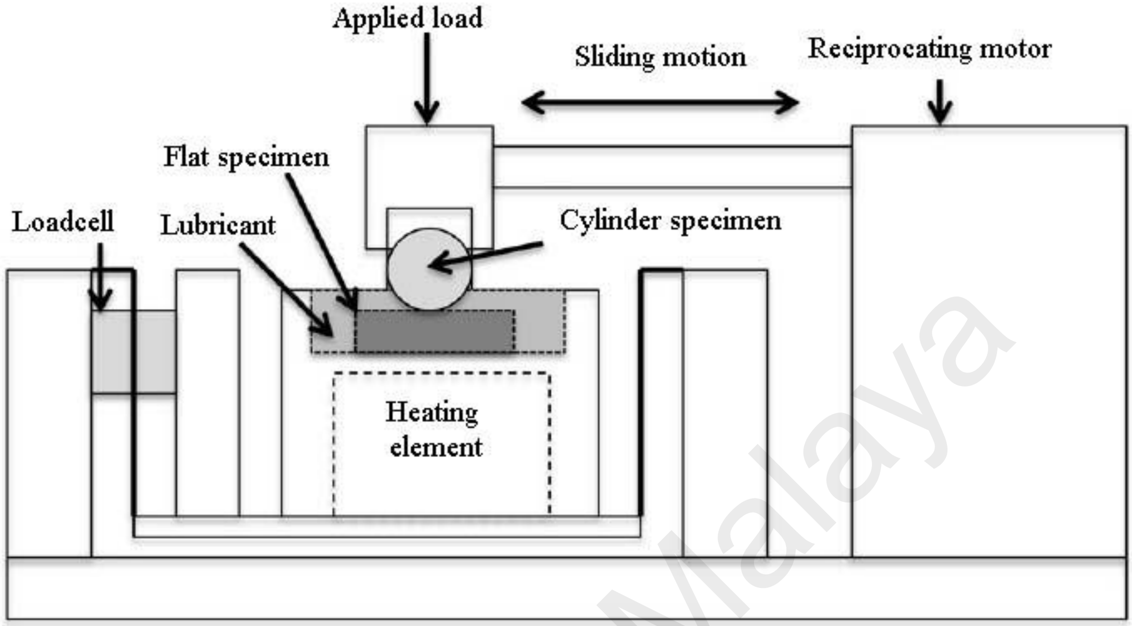

Figure 3. 5: Schematic diagram of high frequency reciprocating ring (HFRR)

Table 3. 12: Operating conditions of high frequency reciprocating ring

Parameters	**Conditions**
Operating time	1h
Frequency	10Hz
Applied load	100N
Stroke length	2mm
Test temperature	75°C

3.6 Tribological analyses

3.6.1 Friction coefficient

a. Four-ball machine

Four-ball wear test, the coefficient of friction was calculated by mean of frictional torque and spring constant. The value of frictional torque was determined by a load cell. The lower balls created the maximum amount of torque. The expression used to evaluate the coefficient of friction is shown in equation 1 (M. H. Mosarof et al., 2016).

$$\text{Friction Coefficient } (\mu) = \frac{\text{Friction Torque}(kg \times mm) \times \sqrt{6}}{3 \times \text{Applied Load}(kg) \times \text{distance}(mm)} = \frac{T \times \sqrt{6}}{3 \times W \times r} \tag{1}$$

Where *T, W,* and *r* express friction torque (kg.mm), applied load (kg) and distance (mm), respectively; the distance (*r*) measured from the center of the lower ball contact surface to the axis of rotation was 3.67 mm.

b. High Frequency Reciprocating Ring test

High frequency reciprocating ring test, the coefficient of friction was calculated by mean of frictional force and applied load. The expression used to evaluate the coefficient of friction is shown in equation 2 (Ahmed Arslan et al., 2016).

$$\text{Friction Coefficient } (\mu) = \frac{\text{Actual Friction Force (N)}}{\text{Applied Load}(N)} = \frac{F(N)}{W(N)} \tag{2}$$

Where *F* and W express actual friction force (N), applied load (N), respectively

3.6.2 Wear scar diameter

a. Four-ball machine

Optical microscope model C2000 (IKA, UK) was used to measure wear scar diameter produced on the three tested balls to an accuracy of 0.01 mm. To measure the scar area of each ball, the used oil was poured from the oil cup without loosening the ball holder, because it is more efficient to measure the scars without removing the three balls from the holder. Tissue was used to wipe the scar area on each ball in the oil cup, and the oil cup was then placed on the special base of the microscope. After measuring the wear scar diameter of those three balls, the arithmetic average result was calculated.

b. High Frequency Reciprocating Ring

After testing, the specimens were rinsed with n-heptane before wear track characterization. An average of three measurements on the wear track was performed to calculate the wear volume. Finally, the wear coefficient was calculated by Archard equation ($V_i = k_i \times F \times s$) (A. Arslan et al., 2015), where V_i is the wear volume, k_i is the specific wear rate coefficient, F is the normal load, and s is the total distance traveled.

3.6.3 Flash temperature parameter

Flash temperature parameter (FTP) refers to the possibility of lubricant to break down (Masjuki & Maleque, 1997). The higher the FTP is, the less possibility of lubricant film breakdowns. This FTP can be measured by the thermocouple and expressed by a solitary number of FTP. In four-ball experimental conditions, the FTP was calculated using *equation 3* below (Ing et al., 2012):

$$FTP = \frac{Applied\ load\,(kg)}{Wear\ scar\ diameter\,(mm)} = \frac{W}{d^{1.4}} \tag{3}$$

Where, W expresses applied load (kg), and d expresses wear scar diameter (mm).

3.7 Surface analysis technique

After the tribological test, the morphology of wear tracks was investigated by scanning electron microscope (SEM) and film element composition was performed by EDS Analyzer, which is the most known instrument for the surface analytical techniques. High-resolution images of surface topography, with excellent depth of field, were taken using a highly focused scanning electron beam. Three areas of wear scar surfaces were captured and discussed respectively to prove friction and wear behaviors of each fuel diluted oil. EDS was attached to SEM to determine the aromatic percentage of the worn surfaces. It provided the quantitative analysis of elemental distribution in a surface.

3.8 Error analysis

During the experiment, there might be errors arising from instrument selection, testing condition, environmental condition, observation, calibration and reading and collecting data (Mofijur et al., 2014); therefore, error analysis is necessary. The test was repeated three times, and the collected data was averaged. The accuracy for WSD and COF are ± 0.01mm and ± 0.05, respectively. The acceptable uncertainty is less than or equal to 5%. *Appendix (A)* shows the error analysis associated with each measurement. The overall uncertainty of this study was calculated by using *equation 4*.

$$\text{Overall uncertainty} = \text{Square root of } [(\text{uncertainty of COF})^{2} + (\text{uncertainty of WSD})^{2}] \qquad (4)$$

$$OU = \sqrt{UFC_{L40}^{2} + UFC_{L80}^{2} + UWSD_{L40}^{2} + UWSD_{L80}^{2}}$$

$$= \sqrt{2.501^{2} + 1.773^{2} + 2.556^{2} + 2.6569^{2}} = 4.80\%$$

Where OU = overall uncertainty; UCOF = COF uncertainty; UWSD = WSD uncertainty

CHAPTER 4: RESULTS AND DISCUSSION

4.1 Introduction

This chapter describes the results of properties, friction and wear characteristics of engine oil diluted with gasoline-bioethanol blends. It consists of four main sections, which explain those results and findings based on test conditions and test samples. Section 4.1 is the introduction. Section 4.2 describes the effect of bioethanol dilution on tribological characteristics of synthetic oil at fixed temperature of 75°C and under two different loads of 40kg and 80kg, using four-ball wear tester while section 4.3 describes the improvement study on the tribological characteristics of synthetic oil with the dispersion of GP/WS_2, using the same wear test machine. Section 4.4 concerns the results of the combined effect of GP/WS_2 nanocomposite and ta-C coating on friction and wear of bioethanol-diluted synthetic oil tested with high frequency reciprocating ring (HFRR).

4.2 Effect of various bioethanol blends on fully synthetic oil

4.2.1 Viscosity

Viscosity is an essential property of automotive engine oil, which should be high enough to resist the internal flow and low enough to prevent substantial energy loss (Ljubas et al., 2010). Viscosity is high when used oil has been deteriorated by oxidation or by solid contaminants while it is low when used oil is diluted with lower viscosity oil or by fuel. Change in the engine oil viscosity due to fuel dilution is undesirable in the lubrication system of an engine as it influences the lubricating efficiency and oil film thickness. Inadequate oil viscosity affects lubricating film and load bearing capacity leading to excessive wear of bearings, journals and other moving components, low oil pressure and poor oil economy (Agarwal & Gupta, 2014).

Figure 4.1 shows the degradation of the viscosity of synthetic oil (SO) diluted with different types of fuel blends, measured at 40℃. It is investigated that the viscosity decreased significantly when synthetic oil was diluted with bioethanol blends. This is due to the lower viscosity of the diluted fuels. The variations in the viscosity of each diluted oil sample were almost identical. Synthetic oil diluted with E85 fuel had higher viscosity compared to other fuel diluted oil samples. The viscosity of E85-SO dropped to 62.45mm^2/s from the base oil value of 82.03mm^2/s, which meant that E85-SO might have lower lubricating performance, thus increasing the friction, especially during full hydrodynamic lubrication where viscosity plays a very important role in reducing friction. The drop of viscosity indicates that the amount of fuel deteriorated the lubricating efficiency of the oil. E0-S0 had the viscosity of 58.52mm^2/s which was slightly higher than the viscosities of E10-SO, E20-SO, and E30-SO. This indicates that oil contaminated with gasoline, which is the hydrocarbon compound, has lower lubricity, and undergoes more severe degradation compared to oil contaminated with a small amount of bioethanol. It can be stated that fuel dilution has a significant effect on the oil viscosity. It can result in two opposing effects: one beneficial effect and one detrimental effect. A decrease in viscosity is expected to lower the viscous losses of the lubricating oil, which reduce the overall engine friction and increase the efficiency of the engine. However, in boundary lubrication, the difference in viscosity has no significant effect on friction characteristic. The reduction in lubricating oil viscosity also reduces engine oil's film thickness. As a result, it will push the contact surface more into the boundary lubrication regime (Ajayi et al., 2016). This will result in high friction and wear after a long use

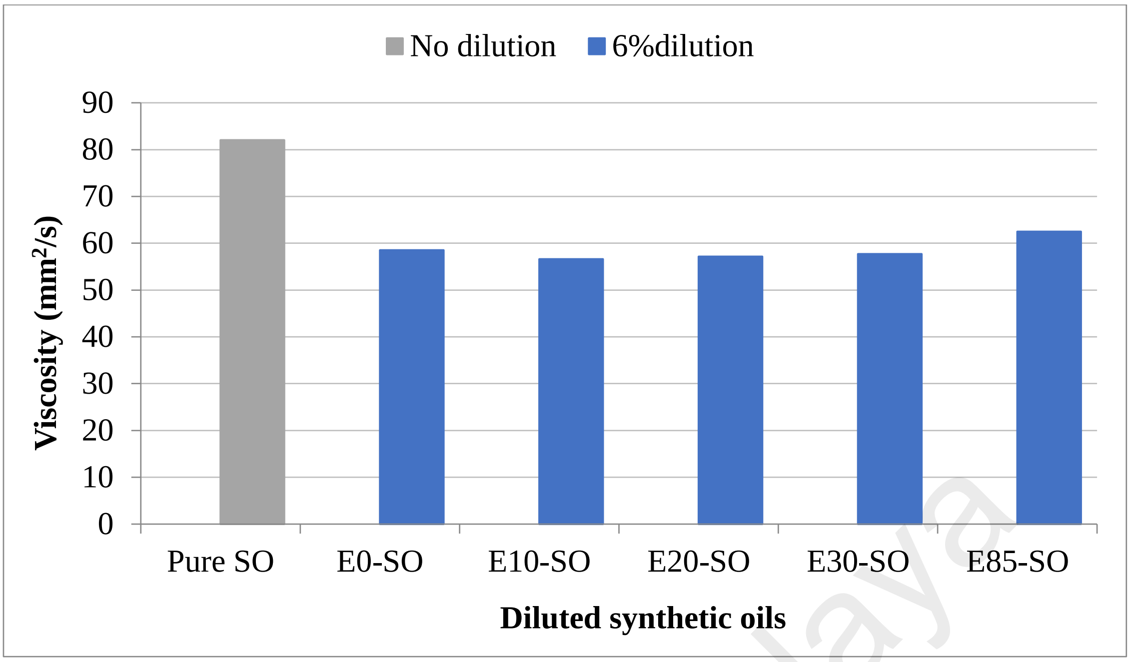

Figure 4. 1: Viscosity of each diluted synthetic oil measured at 40°C

4.2.2 Acid number

Acid number is the quantity of acid-like derivatives in the lubricant (Arumugam & Sriram, 2012). At higher temperature, fuel molecules and other organic acids inside lubricant may decompose during operation and hence, increase the acidity. The acid number values are shown in figure 4.2. Since bioethanol is highly evaporative at high temperature, the change in the acid number of each fuel-oil sample was determined before conducting four-ball wear tests. Generally, the acid value of the new oil is not necessarily nil since oil additives can be acidic in nature. An increase in acid number indicates that lubricant is contaminated with bioethanol and when acid number increase, it makes the metal surface more susceptible to corrosion (Arumugam & Sriram, 2012). It can be seen that synthetic oil samples diluted with 6% of bioethanol-gasoline fuels show higher acid number, compared to fresh SO. This, in turn, may provoke undesirable corrosive wear on engine components (Besser et al., 2012; Jakóbiec & Mazanek, 2009). Bioethanol is more chemically reactive than gasoline due to the presence of oxygen. This possibly interacts with lubricant base fluid and dissolved additives such as detergent and dispersants, leading to oil degradation. The degradation of ethanol in the lubricant creates ethanoic (acetic) acid, which attacks soft metals and increases oxidation of the oil (Howard, 2014). As a consequence, it is possible that 6% dilution rate may cause serious effects such as oxidation and corrosion of engine oil, especially synthetic oil diluted with fuel containing 85 vol.% of bioethanol (E85-SO). Lubricant diluted with bioethanol-gasoline mixtures become degraded and produce higher wear compared to fresh engine oil.

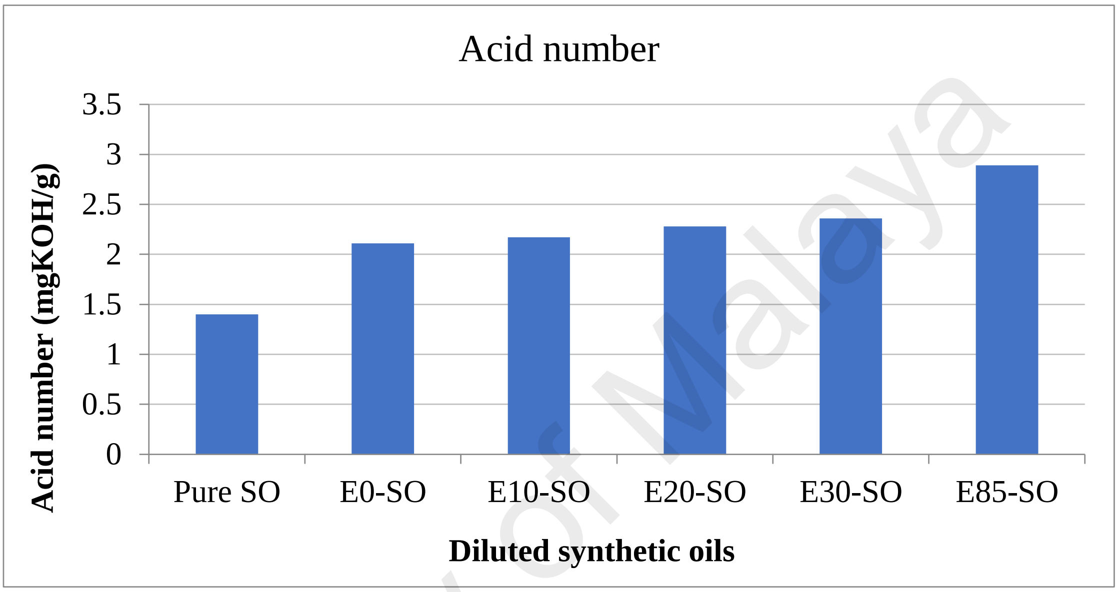

Figure 4. 2: Acid value of each diluted synthetic oil

4.2.3 Flash temperature parameter

Flash temperature parameter (FTP) refers to the possibility of lubricant to break down (Masjuki & Maleque, 1997). Generally, a greater FTP number indicates a better lubricating efficiency of the lubricant while a smaller FTP number indicates the reduction in lubricating film thickness (M. H. Mosarof et al., 2016). As seen in *equation 3*, load, and wear scar diameter predicts FTP number. Figure 4.3 presents the variations of the FTP of fresh synthetic oil and diluted synthetic oils tested at both conditions. At the load of 40kg, it can be seen that fresh synthetic oil (SO) had the highest FTP (178) indicating that fresh SO provided better lubricating performance and had less possibility of lubricating film breakdown, while all fuel diluted synthetic oils showed lower FTP number. The FTP values of E0-SO, E10-SO, E20-SO, E30-SO, and E85-SO were 155, 156, 157, 153, and 145, which meant their lubrication performance is worse compared non-diluted oil. The least FTP yielded from E85-SO, which contained a higher amount of bioethanol inside the synthetic oil while E10-SO showed lower FTP value compared to other fuel diluted synthetic oils. The FTP number dropped significantly when the load was increased to 80kg, which can be explained that at higher load and temperature the degradation of tested lubricating oil may occur and thus push the rubbing surface close to each other, which eventually increase the friction (Shahabuddin et al., 2013). The FTP values of lubricating oils were slightly different. Pure SO, E0-SO, E10-SO, E20-SO, E30-SO, and E85-SO had FTP values of 34, 33, 29, 32, 31, and 28, respectively. The fresh synthetic oil still had higher FTP compared to the fuel-diluted oils, which means that it may have the possibility to generate lubricating film during high load. However, fuel contaminant particularly bioethanol fuel inside synthetic oil deteriorated lubricating properties and may cause lubricating film breakdown at high load.

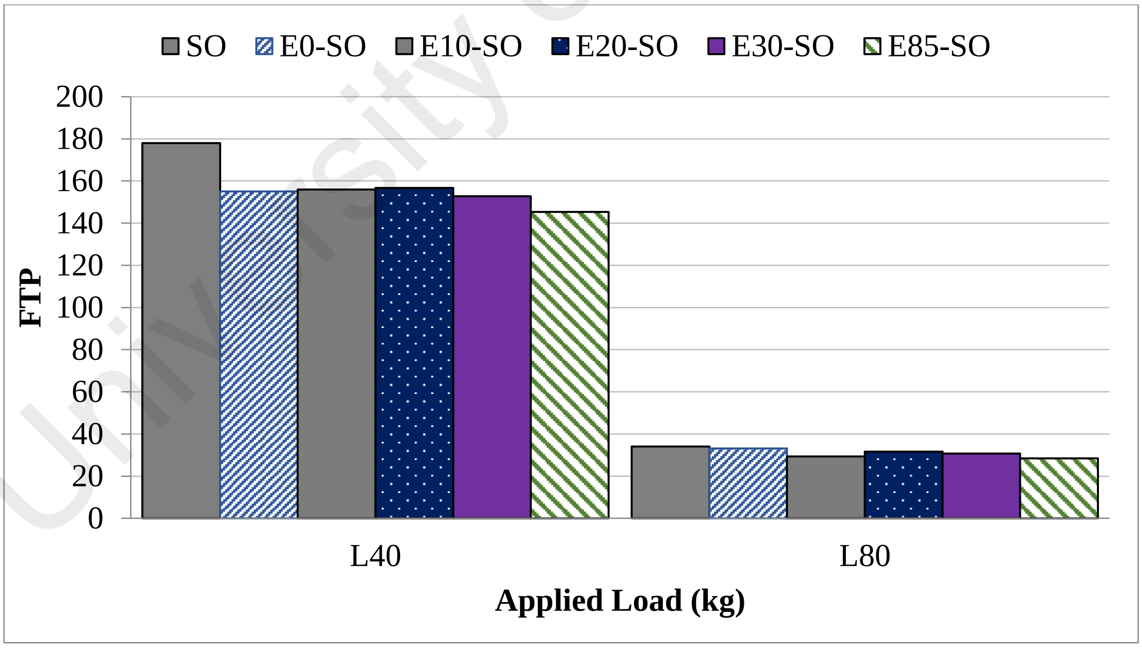

Figure 4. 3: Flash temperature parameter of diluted synthetic oil at both loads 40kg and 80kg

4.2.4 Effect on friction of bioethanol-diluted oil at 40 kg and 80 kg

Figure 4.4 describes the variation of COF of synthetic oil (SO) contaminated with bioethanol blended fuels at the load of 40kg. The average COF values of fresh oil and fuel-diluted oils tested at 40kg and 80kg are shown in figure 4.5. At 40kg, the friction coefficients yielded from diluted synthetic oils were slightly higher than that yielded from the fresh synthetic oil. Based on the data averaged from the three tests, it is shown that E0-SO, E10-SO, E20-SO, E30-SO, and E85-SO had COF values of 0.111, 0.108, 0.106, 0.109 and 0.112, respectively. It can be seen that the average COF of SO was not the lowest value (0.108) while E20-SO had the lowest COF value (0.106). However, synthetic oil had the lowest frictional behavior as shown in figure 4.4. At first 30 min, SO performed higher friction, compared to E10-SO, E20-SO, and E30-SO while its friction decreased to the minimum value during the remaining time. It might be due to the fact that oil additive has been activated to create lubricating film after half an hour. All fuel diluted oils had increasing or stable frictional characteristics, compared to fresh synthetic oil. It is observed that all bioethanol-diluted oils yielded lower friction at first 30 min, which was probably because of the presence of oxygen and polarity of bioethanol that could enhance the lubricity of the oils (Agudelo et al., 2011). Moreover, there might be a stronger physical adsorption on surfaces of the rotating balls and a local hydrodynamic effect which reduce interference between asperities and increase contact resistance, thus stabilizing the friction behavior in the lubricant wear test (Lin et al., 2013). However, the synthetic oil contains base fluid and oil additive concentrations which possibly react with bioethanol under the presence of oxygen, causing oil degradation and oxidation, thus increasing friction. The more fuel dilutes into the lubricant, the more interactive effects on lubricant additive occurs after a particular operating time; as a result, no lubricating film may generate. E85-SO yielded lower friction compared to SO, but after 15min it yielded the highest friction value due to the higher amount of bioethanol. It shall be notified that gasoline would result in higher friction compared to intermediate-level bioethanol fuels because gasoline (the mixture of hydrocarbon) has less lubricity than a polar molecule such as bioethanol (Agudelo et al., 2011). The variation of COF of diluted synthetic oils tested under the load of 80kg is shown in figure 4.6. At this high load, it can be seen that all fuel-diluted oils showed higher COF with an increase in bioethanol amount except for E20-SO when compared to fresh synthetic oil. The average COF values of E0-SO, E10-SO, E20-SO, E30-SO, and E85-SO were 0.129, 0.113, 0.132, 0.115 and 0.118, respectively while SO had COF value of 0.111 which was slightly lower (figure 4.5). Synthetic oil performed the lowest frictional characteristics and had the minimum value during the whole testing time. As mention earlier, when synthetic oil was not diluted by a mixture of gasoline and bioethanol, it has better lubricating efficiency compared to fuel-diluted oils because the oil additive plays a role in reducing friction by creating the lubricating film. It can be seen that E0-SO and E20-SO had significantly higher COF values, respectively. This might be related to the potential drop across the contact surface during high load; as a result, the contact resistance decreased and lead to more severe metal-to-metal contact between the contact surface of the balls (Agudelo et al., 2011). Moreover, it might be due to the fact that the physical adsorption and local hydrodynamic effects became very weak, resulting from the thermal vibration of these fuel-oil molecules and causing a decrease in the viscosity of these tested oils mixtures. As a result, the high contact stress on surfaces caused plastic deformation of the contact surface, thus increasing the contact area and reducing the stress in the contact region (Lin et al., 2013). Overall, it can be stated that a small amount of bioethanol in lubricant may help increase the lubricity of the lubricant temporarily, but increase friction when it interacts with lubricant and oil additives. There might be also oxidation between bioethanol and oil additives, which can destroy the lubricating performance.

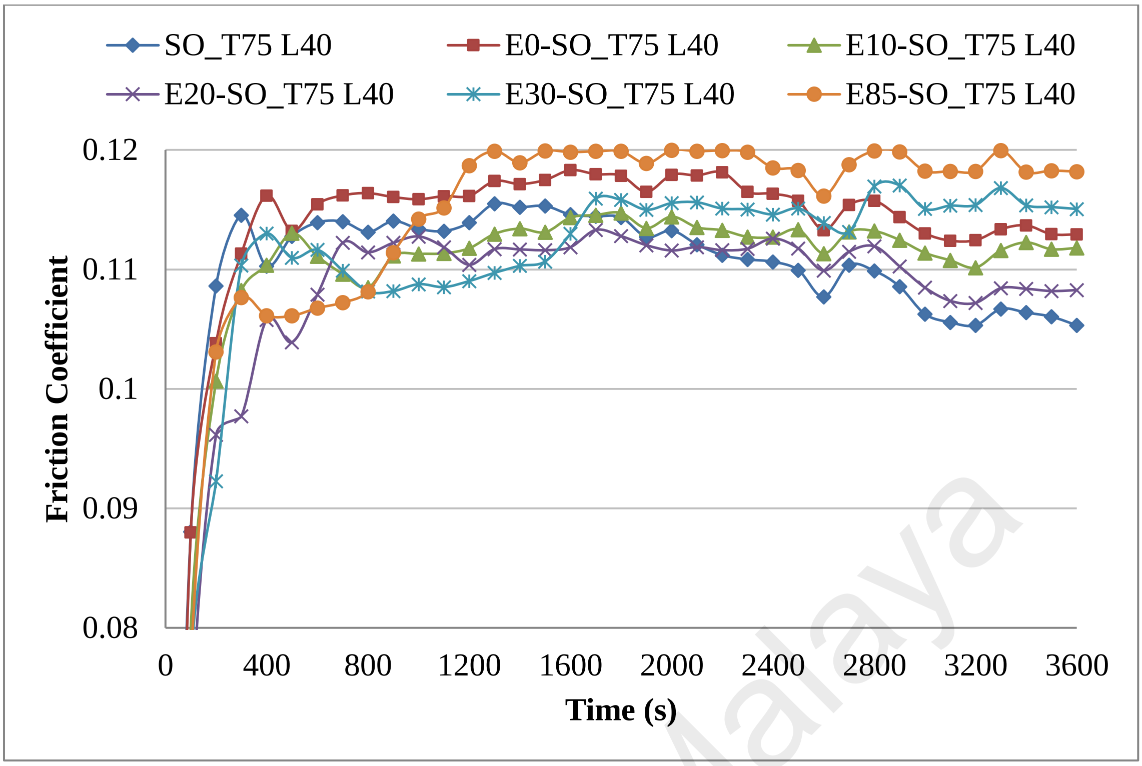

Figure 4. 4: Friction of bioethanol-diluted synthetic oil at load 40kg

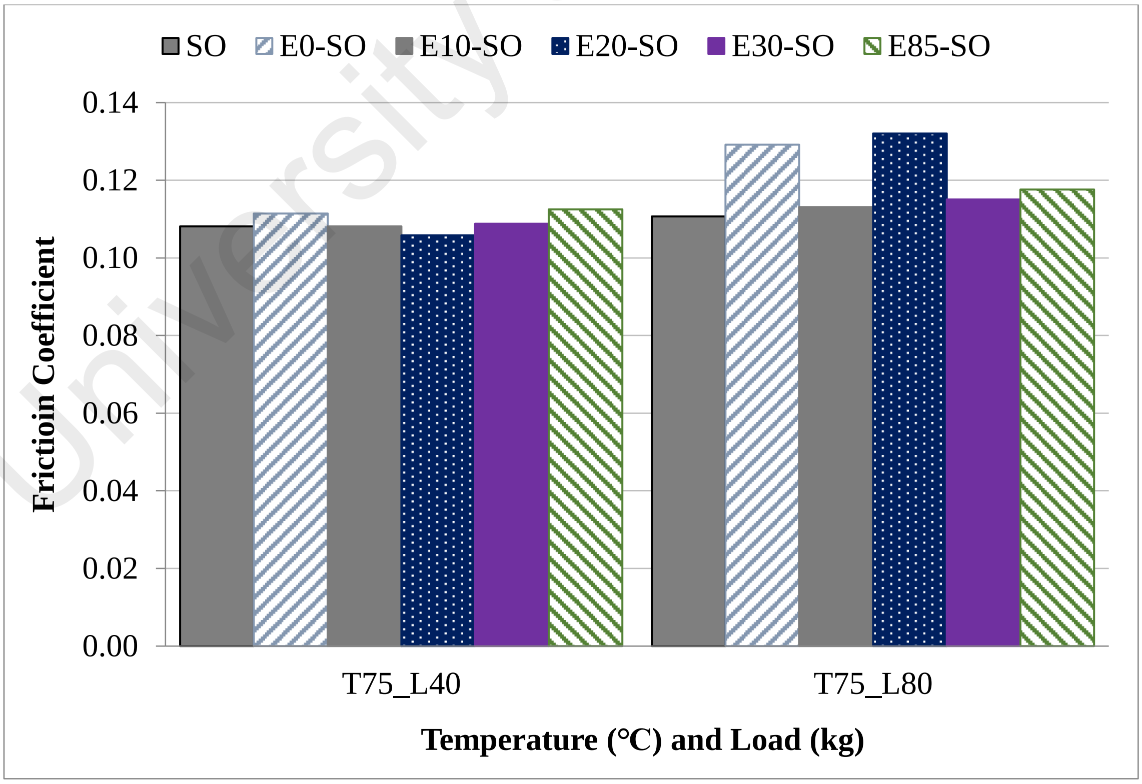

Figure 4. 5: Average COF of bioethanol-diluted synthetic oils at 75°C at both loads 40kg and 80kg

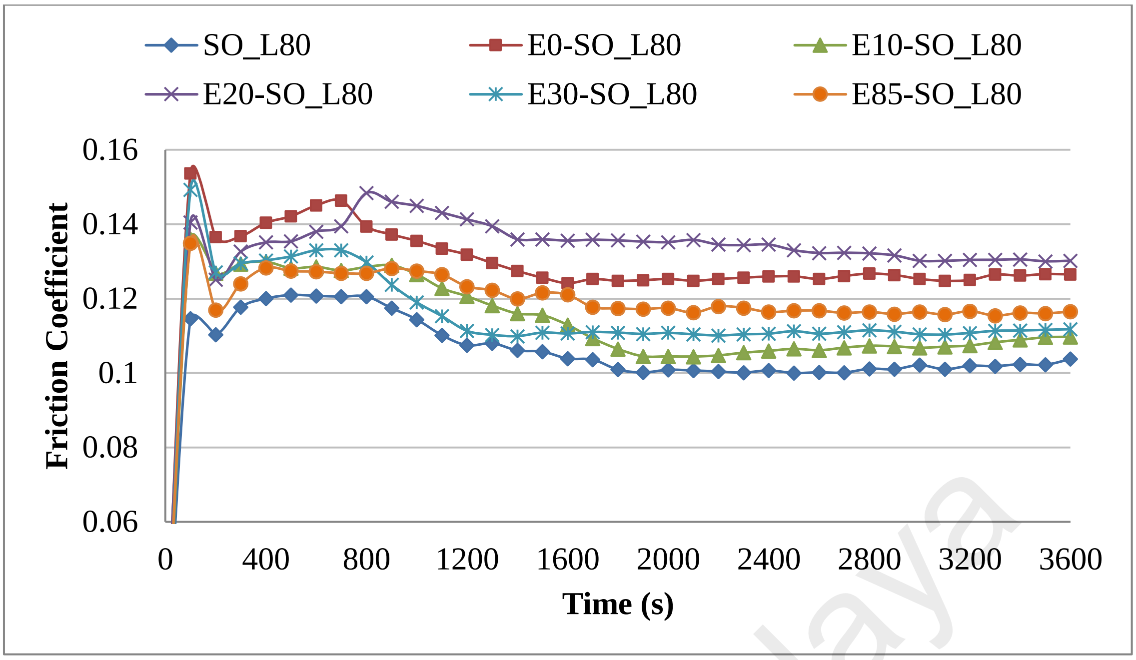

Figure 4. 6: Friction of bioethanol-diluted synthetic oils at load 80kg

4.2.5 Effect on wear scar diameter

Figure 4.7 illustrates the variation of wear scar diameter (WSD) of the ball tested with synthetic oil diluted with various gasoline-bioethanol fuels at 40kg and 80kg. Although gasoline-bioethanol fuel dilution has little effect on frictional behavior, it is observed that the WSD seems to increase significantly with an increase in bioethanol amount inside synthetic oil. The WSD of the three stationary balls were measured and averaged for graph plotting. Generally, when the scar is large, it indicates a severe deterioration of material on the contact surfaces. At 40kg load, it can be seen that all fuel diluted synthetic oils had higher wear scar diameter, compared to their fresh oil. The WSD of E0-SO, E10-SO, E20-SO, E30-SO, and E85-SO were 0.380 mm, 0.379 mm, 0.377 mm, 0.384 mm and 0.398 mm, respectively while synthetic oil yielded WSD of 0.344 mm. The increase in the values of WSD for fuel diluted oils is due to the fact that the contact pressure of metal surface of the ball increase and causes deterioration from the oxidation of oxygenated bioethanol, especially in the case when SO is contaminated with higher percentages of gasoline-bioethanol mixtures. The addition of bioethanol is known to reduce the film thickness of the lubricating oil (Costa & Spikes, 2015). Fresh synthetic oil which was not contaminated with fuel mixture had a better lubricating performance due to its oil additive concentration which can generate the lubricating film. However, in the case of fuel dilution of engine oil, it affected lubricating properties (weakening the lubricant detergency, forming acid and corrosion, and disruption of the oil film strength causing metal asperities to contact each other promoting engine wear), thus increasing in friction and wear. Moreover, fuel dilution reduces oil viscosity, and the concentration of engine oil additives, potentially compromising lubricant's performance (Agarwal et al., 2014). Inadequate oil viscosity affects oil film formation and load-bearing capacity. This can potentially lead to excessive wear of bearing, journals and other moving components (Agarwal et al., 2014). The effect of load on wear scar is very significant. The large amount of WSD could cause more wear. At 80kg load, the contact area is very big; as a result, the WSD of each test lubricant is extremely large, compared to the ball tested at 40kg. All fuel-diluted oil samples namely E0-SO, E10-SO, E20-SO, E30-SO, and E85-SO had WSD of 1.879 mm, 2.045 mm, 1.943 mm, 1.980 mm, and 2.095 mm respectively while the WSD of SO was 1.844 mm. Upon increasing of operation time, the oil additive will be depleted gradually and bioethanol may react with base fuel and lubricant additive under the presence of oxygen, and causes oil oxidation of some of the lubricant constituents and subsequent formation of carboxylic acid and eventually destroys lubricating performance (Rahimi et al., 2012). E10-SO and E85-SO had higher WSD compared to other oils. This high increase in WSD of these tested oils was due to the drop in physical adsorption and hydrodynamic effect, which reduces the contact resistance, thus increasing wear scar diameter. It might be also due to the chemical attack on the surface of the ball by bioethanol presented in these oils (Lin et al., 2013). It shall be notified that the less effect on WSD is due to a large evaporated amount of bioethanol from the lubricant. It is believed that the WSD is more severe and pronounced when 6% of bioethanol fuel dilutes into the oil sump of the vehicle engine, where fuel always dilutes during engine operation. It is better for old vehicle engines, which may have more dilution up to more than 5% of fuel inside lubricant to use superior engine oil in order to avoid serious friction and wear from bioethanol, which can lead to engine catastrophic failure.

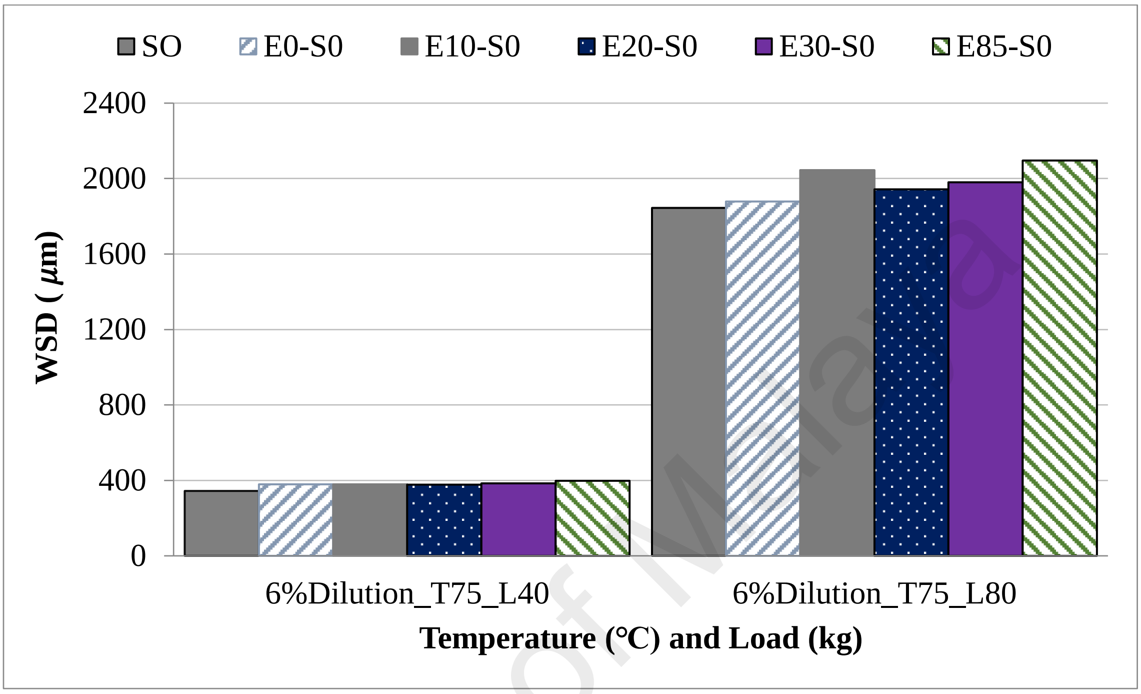

Figure 4. 7: Wear scar diameter of bioethanol-diluted oil samples at 75°C and at both loads 40kg and 80kg

4.2.6 Worn surface analyses

4.2.6.1 SEM analysis

Figure 4.8 shows the worn surface morphologies of stationary balls tested in SO, E0-SO, E10-SO, E20-SO, E30-SO, and E85-SO at 40kg. For fresh synthetic oil, the ball surface indicated mild abrasive wear. The micro grooves along the sliding direction were presented on the worn surface (figure 4.8a). It shall be notified that the adhesive wear is indicated on the worn surface when it is greater than 20μm (Lu et al., 2005). In figure 4.8b-4.8e, more severe surface deteriorations were found on the balls tested with lubricant diluted with gasoline-bioethanol mixtures. The ball surface of bioethanol oils looked smoother, compared to that of gasoline oil because bioethanol is a polar molecule, which has a better lubricity compared to gasoline (the mixture of hydrocarbon). However, the worn surface of the balls tested with bioethanol-diluted synthetic oil (E10-SO, E20-SO, E30-SO, and E85-SO) seems to undergo chemical reaction between lubricant (base fluid and oil additives) and bioethanol which may cause chemical wears such as oxidative and corrosive wear, thus affecting oil lubricity. This is due to the higher oxygen content of bioethanol inside the oil, which enhances the oxidation of fuel-oil mixture (figure 4.8b-4.8e). This wear caused material removal by oxidative chemical reaction of the metal surface under the presence of oxygen in the bioethanol-oil mixture. It is observed that there were presences of the corrosive product of black color because oxidization and corrosion occurred and corrosive acids enhanced corrosive wear (Briscoe et al., 1992; Zulkifli et al, 2013). Moreover, during the test at elevated temperature, the oxidation of fuel-oil mixture may generate peroxide in the presence of oxygen, and this peroxide will undergo further reaction to form carboxylic acid, ketones, aldehydes, and alcohols; as a result, it may increase the acidity of the lubricant as seen in figure 4.8c-4.8e (Rizvi, 2009; Y. Wu et al., 2013). From this SEM, it can be deduced that bioethanol blend inside synthetic oil resulting from fuel dilution is possible to destroy lubricating performance and also affect the friction and wear losses of lubricant.

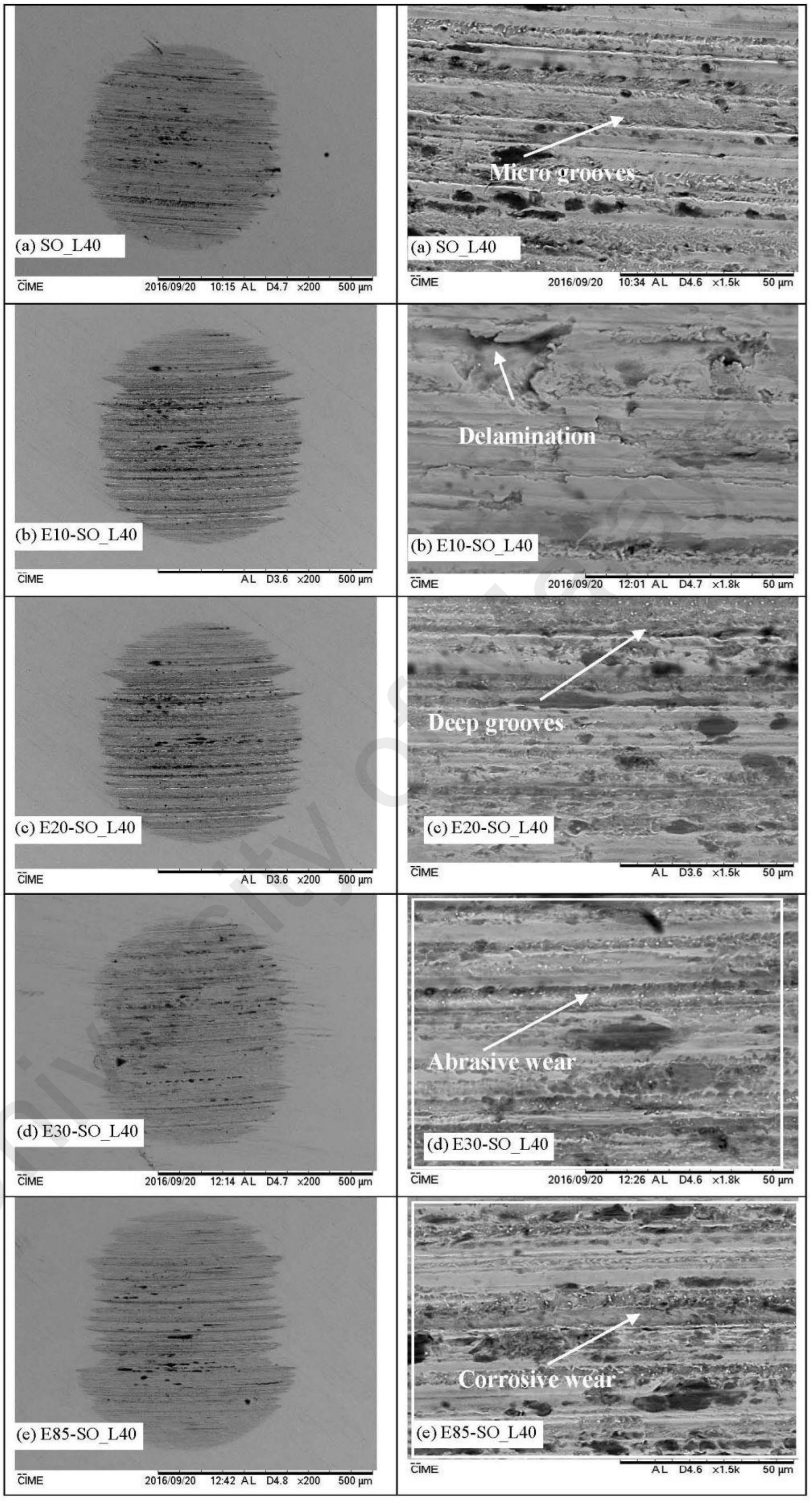

Figure 4. 8: Worn surface of steel balls tested with fresh and diluted synthetic oils (Test condition: Load=40kg; Speed=1200rpm; Duration=1h; Temperature=75°C)

4.2.6.2 EDS analysis

The atomic percentage of the ball surface tested with fuel-diluted synthetic oil at 40kg is shown in Table 4.1. Iron (Fe), Carbon (C) and Chromium (Cr) indicate their origin in the steel balls. The elemental compositions such as Sulfur (S), Calcium (Ca) and Phosphor (P) are likely the result of deposition from the oil and its anti-wear additives (Besser et al., 2012; Besser et al., 2014; Uy et al., 2011). The presence of Sodium (Na) and Oxygen (O) are typically the results from fuel contaminants (Cousseau et al., 2015). Figure4.9 indicates higher levels of calcium, sulfur, phosphorous and oxygen, which play an important role to generate lubricating film in the rubbing surface. These elemental compositions are typically found on samples tested in oils with detergent and antiwear/anti-oxidation additives (Uy et al., 2007). Calcium is also the important ingredient in detergent which plays a role to indicate the total base number (TBN) in the oil, compared to other elements (Pawlak, 2003). However, oil additives are diminished by the amount of bioethanol-gasoline mixture inside the synthetic oil (Uy et al., 2011). It can be seen that the increase in Sodium (Na) in fuel diluted oil samples indicates that there is fuel contamination of engine oil. Thus, engine oil contains high acid products which may promote oxidative wear (Cousseau et al., 2015) and the small amount of bioethanol interferes with the decomposition of oil anti-wear additive (i.e. ZDDP) which is essential for tribofilm generation and wear mechanism (Costa & Spikes, 2016). Moreover, the decrease in levels of sulfur, calcium, and phosphorus is likely due to the interaction between the wear surface and antiwear/anti-oxidative in the oil. Kovalchenko et al., (2002) reported that reduction of sulfur in oil will degrade the wear and scuffing protection of the lubricants, resulting in reliability and durability problems for various oil-lubricated engine components.

Table 4. 1: EDS analysis of balls tested with fresh SO and bioethanol-diluted synthetic oils at load 40kg

Samples		Element (at.%)						
	Fe	C	Cr	P	S	Ca	O	Na
SO	51.86	27.45	1.11	2.77	4.96	1.34	10.50	-
E10-SO	47.69	29.19	0.85	1.18	4.45	0.62	7.81	8.13
E20-SO	43.71	35.80	0.94	1.21	3.63	0.76	6.57	7.39
E30-SO	61.52	20.96	1.18	1.69	6.14	0.64	7.86	6.14
E85-SO	60.41	22.70	1.13	1.66	2.45	0.70	4.16	6.79

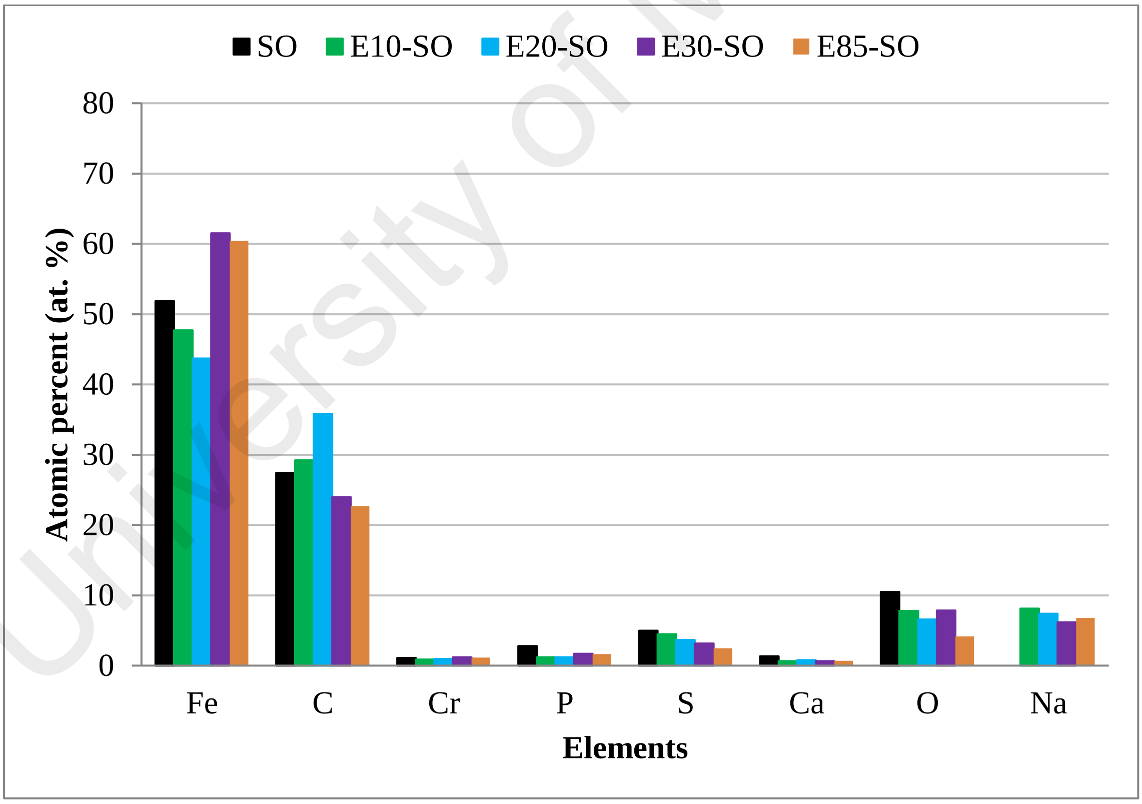

Figure 4. 9: Aromatic percent of worn surface tested with each bioethanol-diluted synthetic oil at load 40kg

4.3 Effect of GP/WS2 nanocomposite on engine oil performance

4.3.1 Effect on friction and wear of pure engine oil

Figure 4.10 shows a plot of average COF and WSD of SO dispersed with various concentrations of GP/WS$_2$. The friction coefficient was effectively reduced after adding GP/WS$_2$ due to the its synergistic lubrication and antiwear potential. However, the concentrations resulted in different friction-reducing efficiencies. The frictional trend shows the concavity in proportion with the concentration of GP/WS$_2$, and the friction reduction reached a maximum at 0.04wt%, which was considered as the optimal concentration. 0.01wt%-0.04wt% GP/WS$_2$ showed decreasing trend and then was selected for further investigation with bioethanol-diluted engine oil. It is seen that further increase in the concentration increased friction, probably due to the inhomogeneous dispersion (M. f. Guo et al., 2015). Similarly, it can also be seen that the average WSD of the dispersed SO reduced with an increase in GP/WS$_2$ concentration. Further increase in GP/WS$_2$ concentration from 0.06wt%-0.1wt% yielded an increase in WSD, probably due to the agglomeration of the nanoparticle during the lubricating process (Dan Li et al., 2008). The GP/WS$_2$-dispersed oils exhibited the lowest friction and WSD at 0.04wt%.

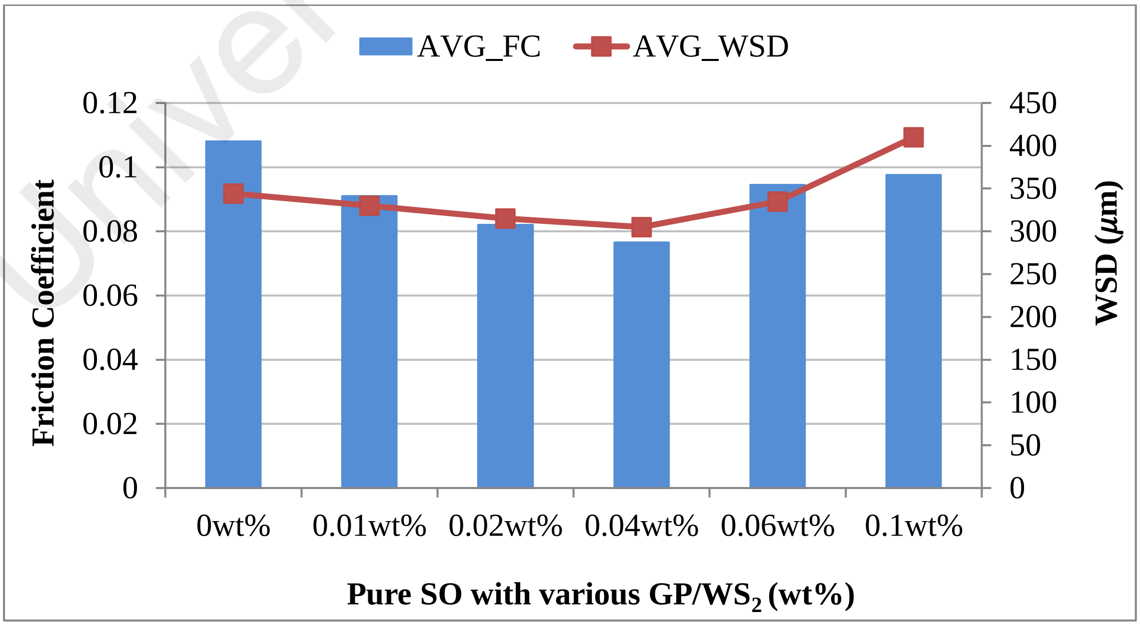

Figure 4. 10: Average COF and WSD of SO dispersed with GP/WS$_2$ at load 40kg

4.3.2 Effect on friction and wear of bioethanol-diluted synthetic oils

This section explains the influence of GP/WS$_2$ nanocomposite at various concentrations when lubricated with bioethanol-diluted engine oil. Figure 4.11 shows (a) friction coefficient and (b) average COF and WSD for fresh oil and their blends with GP/WS$_2$ at 0.01wt%. The addition of GP/WS$_2$ can reduce the effect of bioethanol on engine oil in term of tribological behavior. Although not all GP/WS$_2$ dispersed oil samples yield lower friction than pure engine oil (SO), it can be observed that all GP/WS$_2$ dispersed oil sample show decreasing trends of friction coefficient, and decrease smoothly with the operating time (figure 4.11a). The average friction of the bioethanol-diluted oil samples dispersed with GP/WS$_2$ such as E10-SO$_{GP/WS2}$, E20-SO$_{GP/WS2}$, E30-SO$_{GP/WS2}$, and E85-SO$_{GP/WS2}$ are 0.105, 0.110, 0.116, and 0.102, respectively, while the friction value of SO is 0.109. The variation of friction is relatively small when compared with bioethanol-diluted engine oils with the addition of GP/WS$_2$, and the frictional trend of each dispersed oil sample decreased, which indicates that the added GP/WS$_2$ plays its role in reducing friction and compensates the undesirable tribological effect from bioethanol. Wear losses is reduced when 0.01wt% GP/WS$_2$ is dispersed to the oil (figure 4.11b). The WSD of E10-SO$_{GP/WS2}$, E20-SO$_{GP/WS2}$, E30-SO$_{GP/WS2}$, and E85-SO$_{GP/WS2}$ are 0.322mm, 0.340mm, 0.347mm, 0.356mm, respectively while the WSD of pure SO is 344mm. E10-SO$_{GP/WS2}$ and E20-SO$_{GP/WS2}$ have smaller WSD, compared to pure SO, whereas E30-SO$_{GP/WS2}$, and E85-SO$_{GP/WS2}$ still yield higher WSD than pure SO due to their higher amount of bioethanol which cannot be compensated with 0.01wt% GP/WS$_2$. GP/WS$_2$ has synergistic lubricating behavior and the tiny grain size covers the metal surface to creat lubricating film which can reudce friction and wear (Zheng et al., 2017). Therefore, it can be stated that this wear protection is attributed to increased tendency to form a protective film with GP/WS$_2$.

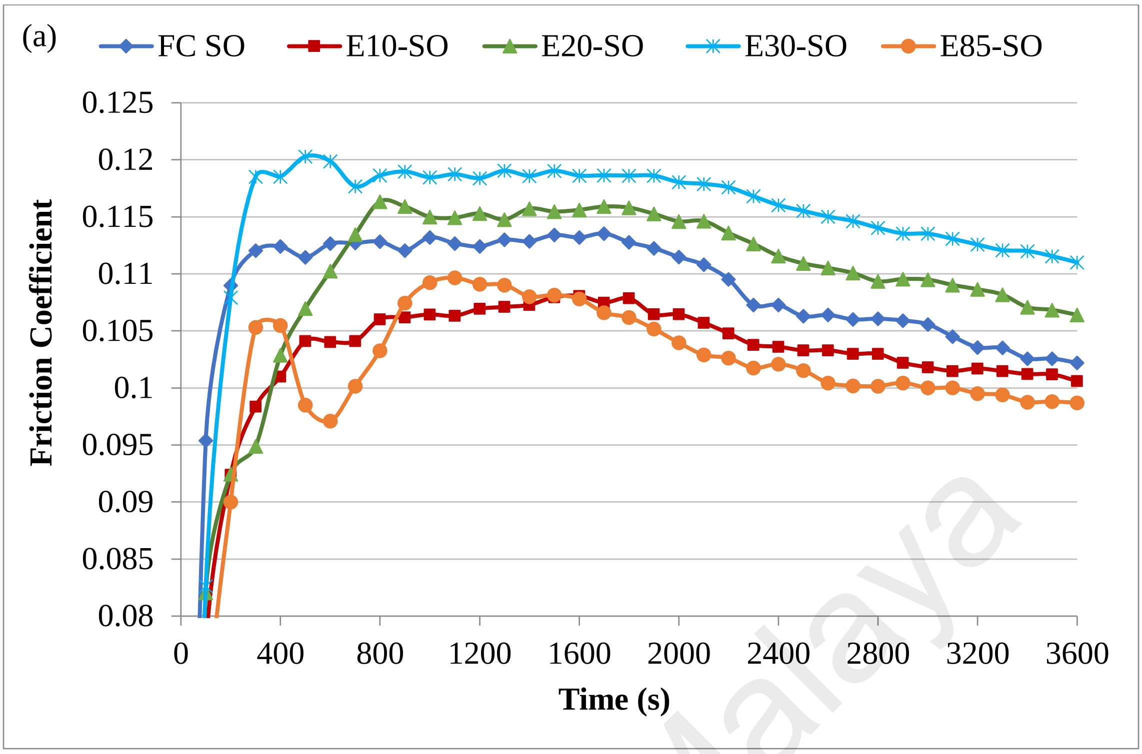

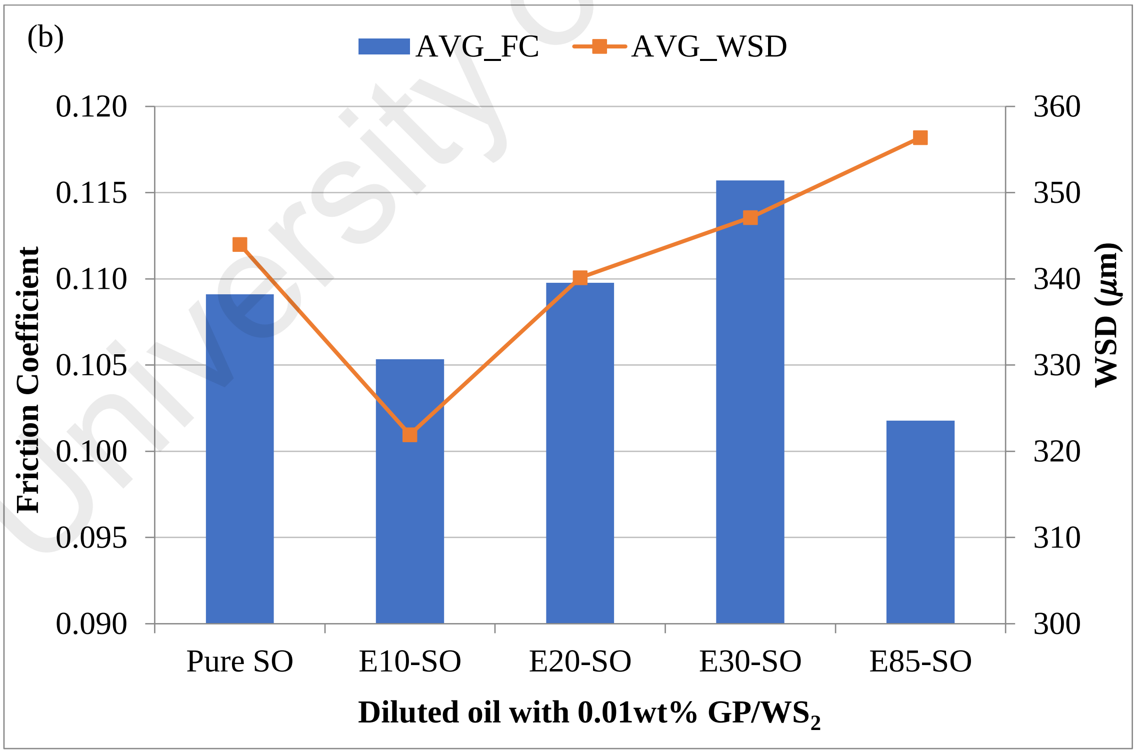

Figure 4. 11: (a) Friction coefficient and (b) Average COF and WSD for fresh oil and their blends with GP/WS_2 at 0.01wt% tested at 40kg

It is observed that GP/WS_2 has more ability to improve the undesirable friction and wear of bioethanol-diluted engine oil when the concentration of GP/WS_2 increases to 0.02wt%. Figure 4.12a shows the friction coefficient of bioethanol-diluted lubricants as a function of the operating time after the dispersion of nanocomposite (GP/WS_2). The dispersed oil samples display similar frictional trend to the pure SO but the highest friction coefficient is reduced when compared to bioethanol-diluted oil samples. The average COF and WSD of these oil samples are shown in figure 4. 12b. Based on the data averaged from the three tests, it is shown that E10-$SO_{GP/WS2}$, E20-$SO_{GP/WS2}$, E30-$SO_{GP/WS2}$, and E85-$SO_{GP/WS2}$ have COF value of 0.089, 0.102, 0.109 and 0.105, respectively and WSD value of 0.279mm, 0.342mm, 0.341mm,and 0.332mm while friction and WSD of pure SO are 0.109 and 0.344mm. It can also be seen that the COF and WSDs decrease upon adding 0.02wt% concentration of this additive. In section 4.2.4 and section 4.2.5, it shows that all bioethanol-diluted oils had increasing frictional characteristics and wear scar, compared to fresh synthetic oil. However, when dispersing GP/WS_2 nanocomposite, it has positive influence to reduce friction and wear losses of bioethanol-diluted oil, and all GP/WS_2 dispersed oil samples show slightly lower friction and WSDs compared to pure oil. The E30-$SO_{GP/WS2}$ shows slightly higher friction coefficient. This is probably due to the fact that the GP/WS_2 addition of this oil sample is not well-dispersed. The result of friction and wear loss improvement originates from the synergistic lubricating behavior of the combined nanocomposite additive (Cai et al., 2016; Zheng et al., 2017). The smaller grain size and uniform dispersion of this nanocomposite may favor the release of the friction-reducing and antiwear potential during sliding operation (Y. B. Guo & Zhang, 2016). Therefore, to eliminate the undesirable effect of bioethanol dilution of engine oil, this finding suggests that 0.02wt% should be added to the engine oil to resist the effect bioethanol dilution in the crankcase during engine operation.

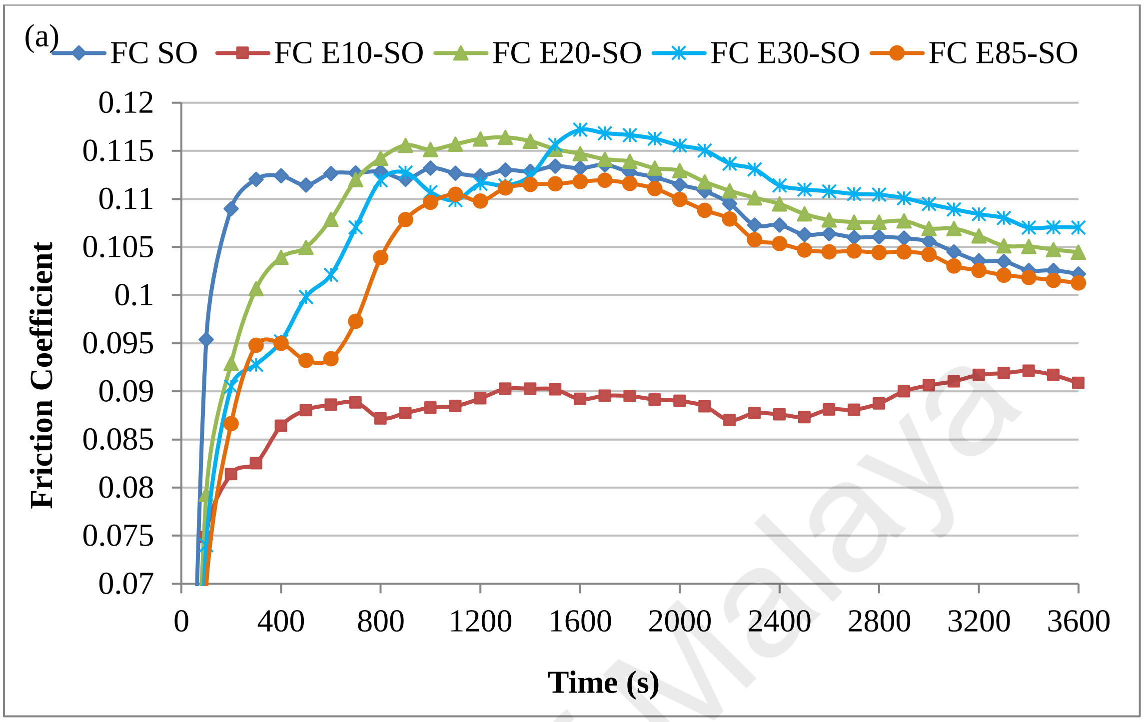

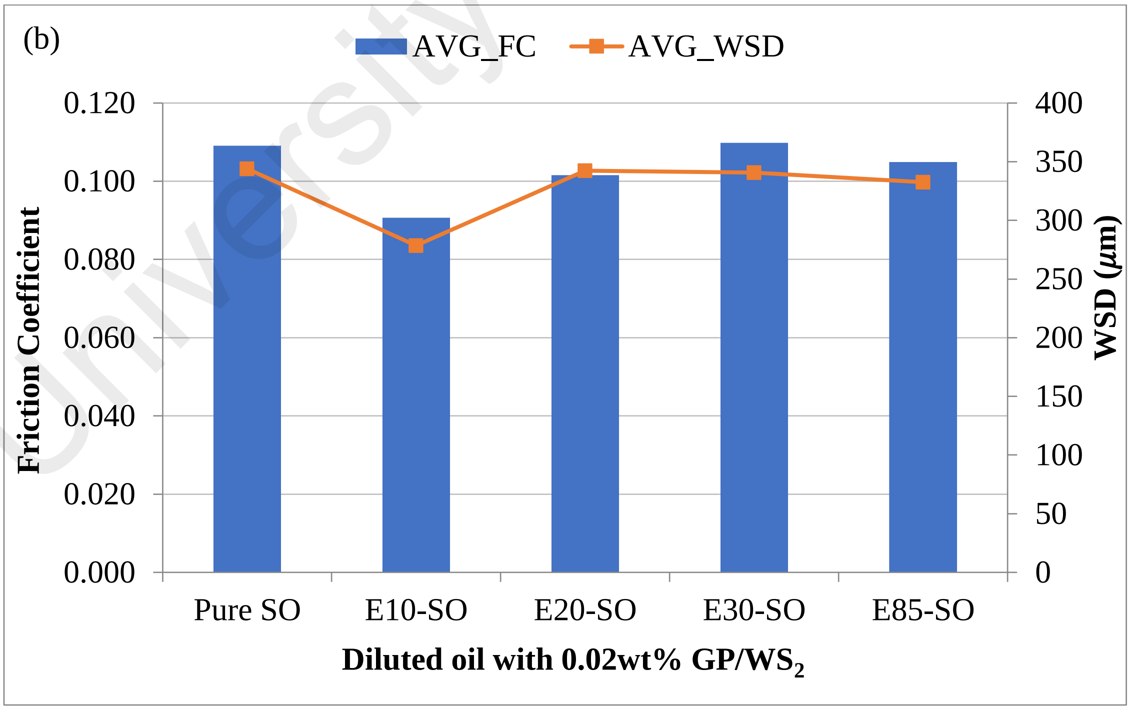

Figure 4. 12: (a) Friction coefficient and (b) Average COF and WSD for fresh oil and their blends with GP/WS$_2$ at 0.02wt% tested at 40kg

Figure 4.13 presents (a) friction coefficient and (b) average COF and WSD for fresh oil and their blends with GP/WS_2 at 0.04wt%. It can be seen that 0.04wt% GP/WS_2 shows significant performance to enhance tribological behavior in all bioethanol-diluted oil samples. In figure 4.13a, all oil samples dispersed with 0.04wt% GP/WS_2 yield slightly lower friction coefficient, compared to the pure SO during the first 30 min, and also have lower friction values than all bioethanol-diluted oil samples. However, during the remaining sliding time, E30-$SO_{G/WS2P}$, and E85-$SO_{GP/WS2}$ showed slightly higher friction than pure SO. The average COF and WSD of these dispersed oil samples are shown in figure 4. 13b. The friction values of E10-$SO_{GP/WS2}$, E20-$SO_{GP/WS2}$, E30-$SO_{GP/WS2}$, and E85-$SO_{GP/WS2}$ are 0.107, 0.106, 0.108 and 0.108, respectively and WSDs values of 0.327mm, 0.332mm, 0.327mm,and 0.323mm while friction and WSD of pure SO are 0.109 and 0.344mm. Based on this result, it is observed that further increase in GP/WS_2 concentration to 0.04wt% remains almost identical friction but continues to reduce more wear, especially for higher bioethanol-diluted oil samples. Average friction values of all dispersed oils are lower than that of pure SO. The WSD decreased significantly upon the addition of 0.04wt% concentration of GP/WS_2. It is notified that the COF and WSD of E30-$SO_{GP/WS2}$, and E85-$SO_{GP/WS2}$ reduce remarkably when adding 0.04wt%, while E10-$SO_{GP/WS2}$, E20-$SO_{GP/WS2}$ can yield lower COF and WSD when only 0.02wt% GP/WS_2 is needed. The reduction friction and wear losses is attributed to the synergistic lubricating behavior of the combined nanocomposite (Zheng et al., 2017), which may favor the release of the friction-reducing and antiwear potential during sliding operation due to tiny grain size and uniform dispersion (Y. B. Guo & Zhang, 2016); as a result, the undesirable effect of bioethanol dilution of engine oil can be properly compensated on the basis of nanocomposite addition. This finding suggests that 0.04wt% should be added to the engine oil used with higher bioethanol-fueled engine in order to resist the effect bioethanol dilution in the crankcase during engine operation.

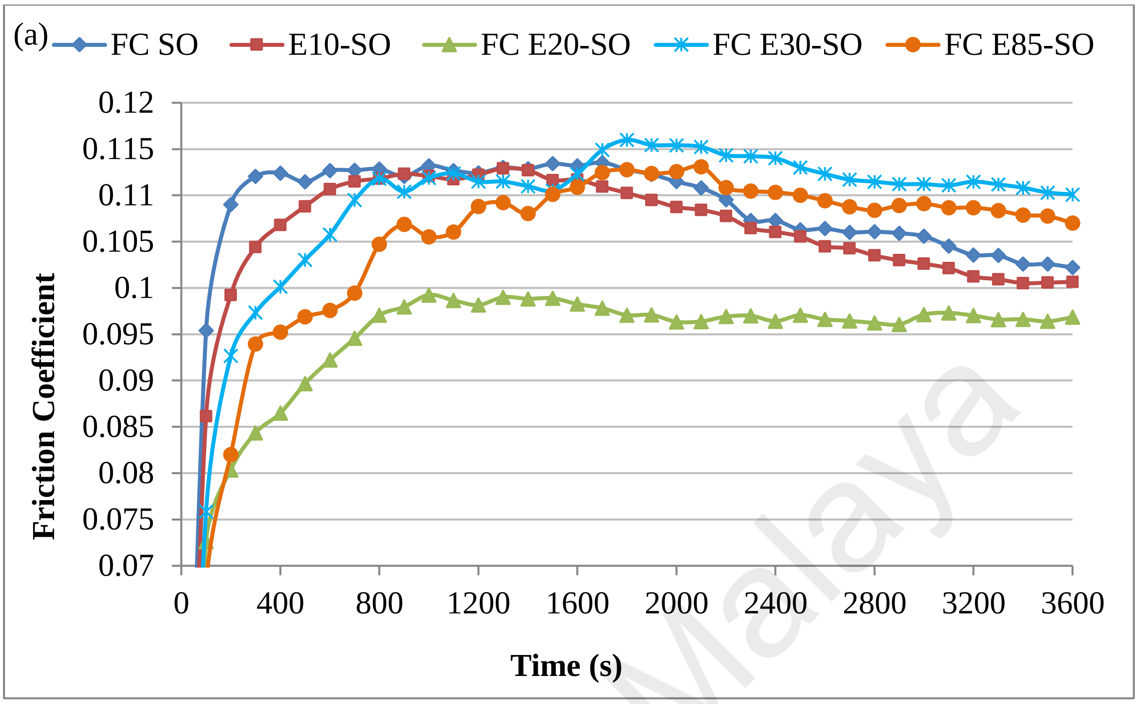

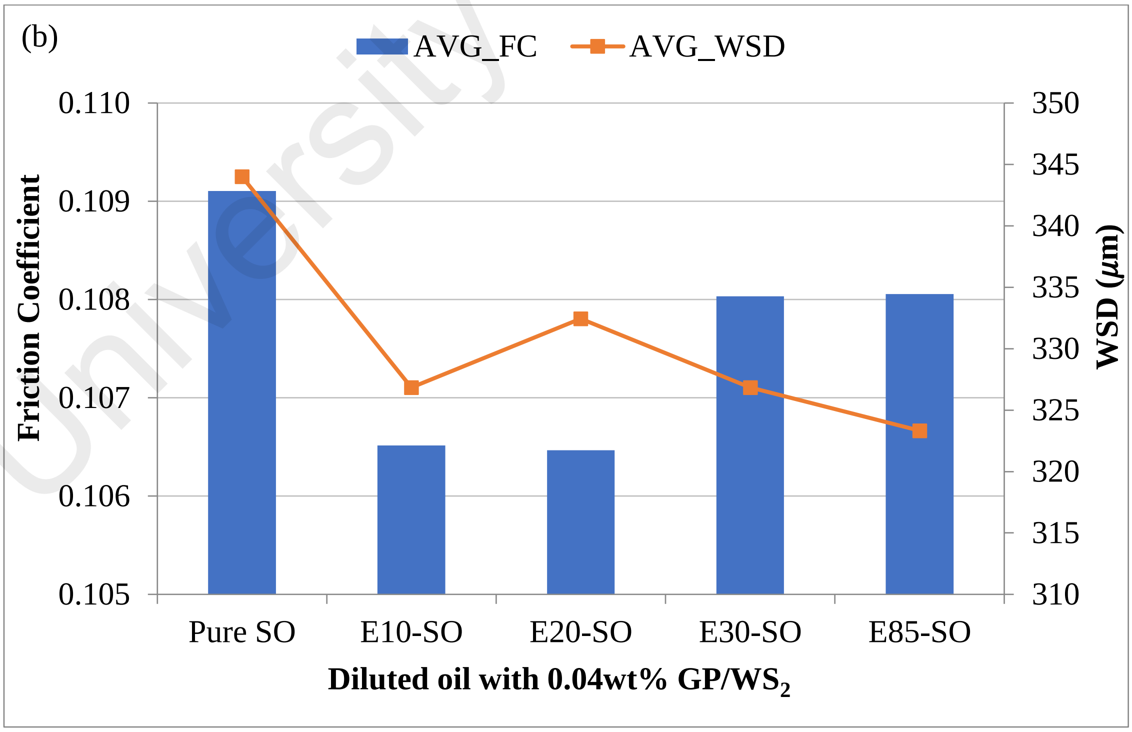

Figure 4. 13: (a) Friction coefficient and (b) Average COF and WSD for fresh oil and their blends with GP/WS$_2$ at 0.04wt% tested at 40kg

4.3.3 Effect of load on friction and wear of GP/WS_2-bioethanol-oil

This study also carried out to investigate the effect of loads on friction and wear behaviors of bioethanol-diluted oils dispersed with GP/WS_2, and the result is then compared to the friction and wear values of pure SO tested at the same various loads. As E10-SO dispersed with GP/WS_2 showed great reduction in friction and wear, E10-$SO_{GP/WS2}$ at 0.02wt% is selected for load testing. Figure 4.14 presents (a) and (b) friction coefficient of SO and E10-$SO_{GP/WS2}$, and (c) average COF and WSD of SO and E10-$SO_{GP/WS2}$ at 0.02wt%. As the load increases, the friction coefficient and wear scar diameter increase. It can be seen that the friction coefficient of pure SO increases with the increase of load except at load 80 kg, at which the friction value yields slightly lower than at load 40kg after about 25min (figure 4.14a). The friction coefficient of pure SO at various loads shows slightly decreasing trend and remains stable throughout the remaining time. This may be due to the presence of a friction-reducing additive which already contains in this commercial automotive engine oil. Even very small amounts of sulfur impurities (order of 100 ppm) can have a significant impact on the wear behavior of the lubricant (Kovalchenko et al., 2002). However, as discussed in section 4.2.4, the bioethanol dilution destroys the ability of the existing additive to reduce friction and wear behaviors as well as load-carrying capacity of engine oil. COF of bioethanol-diluted oil samples yielded higher friction and wear, compared to pure SO. Therefore, to investigate the enhancement of load carrying capacity of bioethanol-diluted oil samples, the GP/WS_2 dispersed oil samples were also tested at the same various loads. It is observed that E10-$SO_{GP/WS2}$ tested at load 40kg-100kg shows remarkably decreasing trend of friction coefficient during the whole testing period, and all friction values are lower as compared to those of pure SO (figure 4.14b). Average COF and WSD of SO and E10-$SO_{GP/WS2}$ are presented in figure 4.14c. The average COF and WSD of SO at different loads are 0.109, 0.121, 0.114 and 0.125, respectively, and 0.348mm, 0.574mm, 1.844mm and 2.566mm, respectively, while E10-SO$_{GP/WS2}$ has COF at different loads of 0.103, 0.110, 0.1137 and 0.121 respectively, and WSD at different loads of 0.305mm, 0.514mm, 1.727mm and 2.452mm, respectively. It can be seen that E10-SO$_{GP/WS2}$ has lower friction and wear at all different loads compared to pure SO, meaning that GP/WS$_2$ nanoparticle has synergistic lubricating behavior (Zheng et al., 2017), anti-wear and friction-reducing capacity (Y. B. Guo & Zhang, 2016) as well as improving load-carrying capacity of the bioethanol-diluted engine oil (Eswaraiah et al., 2011). The result shows higher load resistance, probably due to the fact that when load increases, elastic deformation of the GP/WS$_2$ takes place and then it will reduce the buffering friction. This nanoparticle is nanoscale (1-2nm), which can form nano-bearing between sliding surfaces, and then this added additive can play a role as a mechanical reinforcing element during friction. Therefore, it can strengthen load resistance in this GP/WS$_2$ dispersed oil.

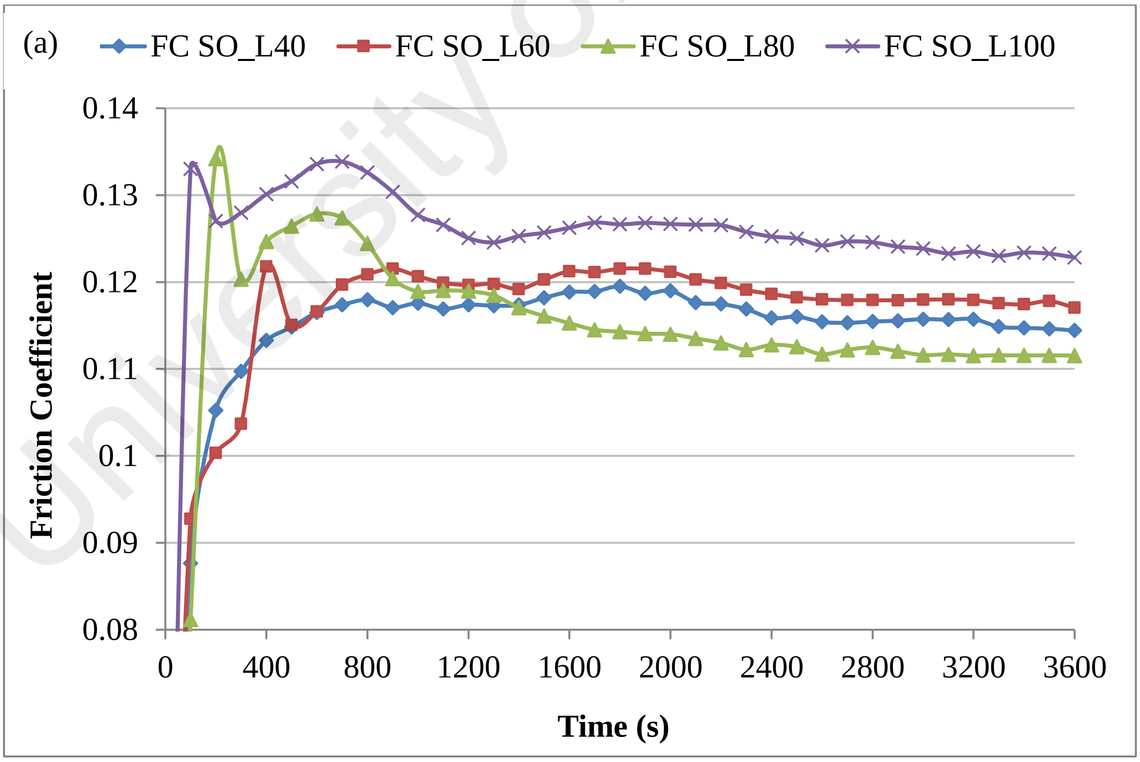

Figure 4. 14: Friction coefficient of (a) fresh SO, (b) E10-SO$_{GP/WS2}$, and (c) Average COF and WSD of SO and E10-SO$_{GP/WS2}$ at 0.02wt% at various loads

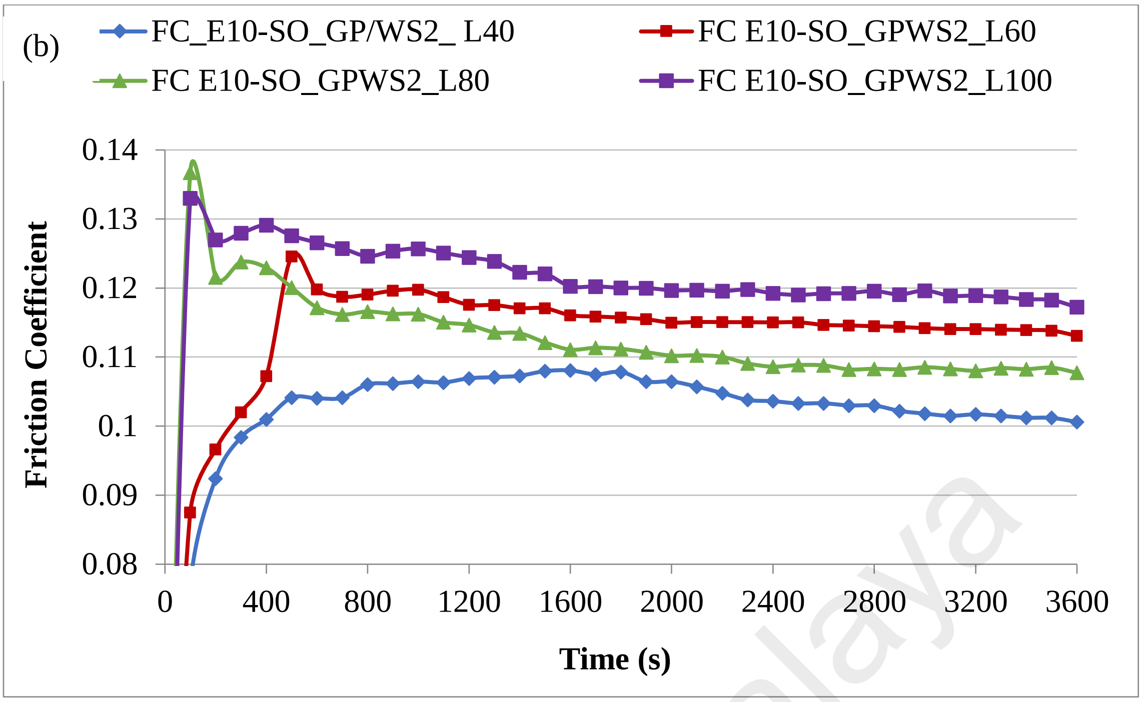

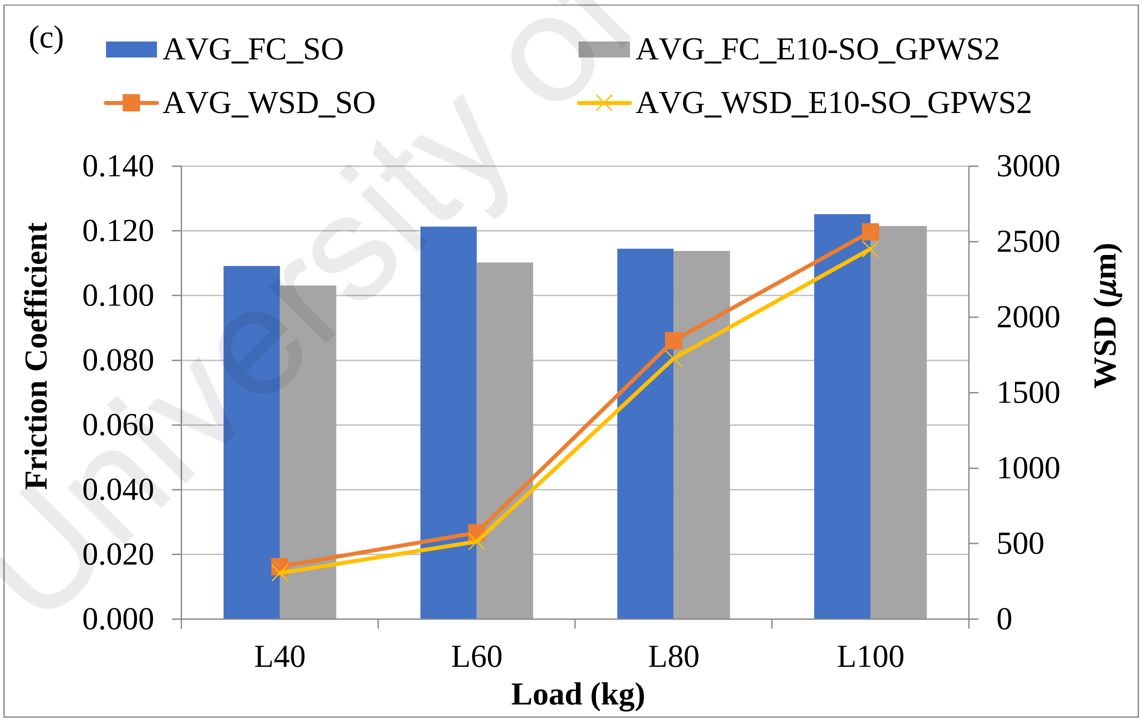

Figure 4.14: Friction coefficient of (a) fresh SO, (b) E10-SO$_{GP/WS2}$, and (c) Average COF and WSD of SO and E10-SO$_{GP/WS2}$ at 0.02wt% at various loads (continued)

4.3.4 Worn surface analyses

4.3.4.1 SEM analysis

The worn surface was examined in order to observe the performance of GP/WS_2 in protecting sliding surfaces from wear losses. Typically, there are several types of wear mechanisms in a tribological system such as abrasive, adhesive, pitting, corrosive, oxidative wear. The type of wear mechanism is dependent on the test fluid, test conditions (particularly speed and temperature) and lubrication regime since all of these influence wear behavior (M. Mosarof et al., 2016).

The previous section already discussed the wear characteristic of pure SO, it can be seen that there is minimal small groove at the ball surface. This is indeed expected since pure SO has superior anti-wear performance compared to bioethanol-diluted oil samples. In figure 4.15, the comparison of the worn surface morphologies of stationary balls tested with bioethanol-diluted oils (A) without dispersion of GP/WS_2, and (B) with dispersion of GP/WS_2 at 0.02 wt% is presented. The addition of bioethanol as fuel dilution shows the increase in wear losses as the WSDs of bioethanol-diluted oil samples are higher, compared to pure SO. In figure 4.15a_1- 4.15d_1, more severe surface deteriorations, roughness, and material spallation were found on the balls tested with bioethanol-diluted oil samples. The grooves along the surface were slightly big. The worn surface of the balls tested with bioethanol-diluted oils also indicated more surface deterioration from abrasive wear and chemical wear. It seems that there is a black, corrosive product on the worn surface of the balls tested in these bioethanol-diluted oil samples. This may be due to oxidation and therefore, the presence of corrosive acids enhances corrosive wear, as shown in figure 4.15a_1-4.15d_1 (Briscoe et al., 1992; Zulkifli et al., 2013). This oxidation may be the consequence of chemical reactions between the fuel-oil blends in presence of oxygen (O), which degrades the lubricity of the lubricant. This is due to the presence of acids from the bioethanol which promotes oxidative wear on the rubbing surfaces of the balls (Cousseau et al., 2015). As wear progresses over time, the surface topographical features will change and their contributions to friction will also change. This leads to more variation in the friction coefficient (Kovalchenko et al., 2002).

However, the addition of GP/WS_2 nanocomposite to bioethanol oil blends reduces WSD due to the enhancement of the lubricating efficiency (figure 4.15a_2-4.15d_2.) The wear surface becomes much brighter and smoother and it seems to be covered by the deposited GP/WS_2 film as shown in figure 4.15a_2-4.15d_2. Although WSD reduced when using GP/WS_2 additive compared to pure SO, the worn surface also indicates some groove (figure 4.15c_2-4.15d_2). This surface morphology indicates that GP/WS_2 can improve the lubricating ability of the engine oil with a dilution of bioethanol. During the real process, the nanoscale additive GP/WS_2 filled the contact surfaces and then can serve as spacers, preventing some real contact (Y. B. Guo & Zhang, 2016). Base on previous studies, it was documented that graphene and nanoparticle as engine oil additives can deposit on the friction interface and form a protective film (Zheng et al., 2017). Therefore, in this study, it is also believed that the combination of graphene and tungsten disulfide (GP/WS_2) deposited on the contacted surface of the balls during sliding process. Then, it generated the synergistic lubrication and form a protective film induced by the friction heat that can smooth surfaces and reduce the rubbing between the balls (Meng et al., 2016a; Zheng et al., 2017). The tribofilms could not only bear the load of the steel ball, but also prevent the direct contact of two mating metal surfaces (Song & Li, 2011). It is notified that the presence of GP/WS_2 can eliminate the presence of black corrosive product on the sliding surfaces. This is probably due to the fact that the amount of GP/WS_2 in the bioethanol-diluted oil sample can prevent the occurrence of oxidation and corrosion, which may cause chemical wear during the sliding process (Berman et al., 2014).

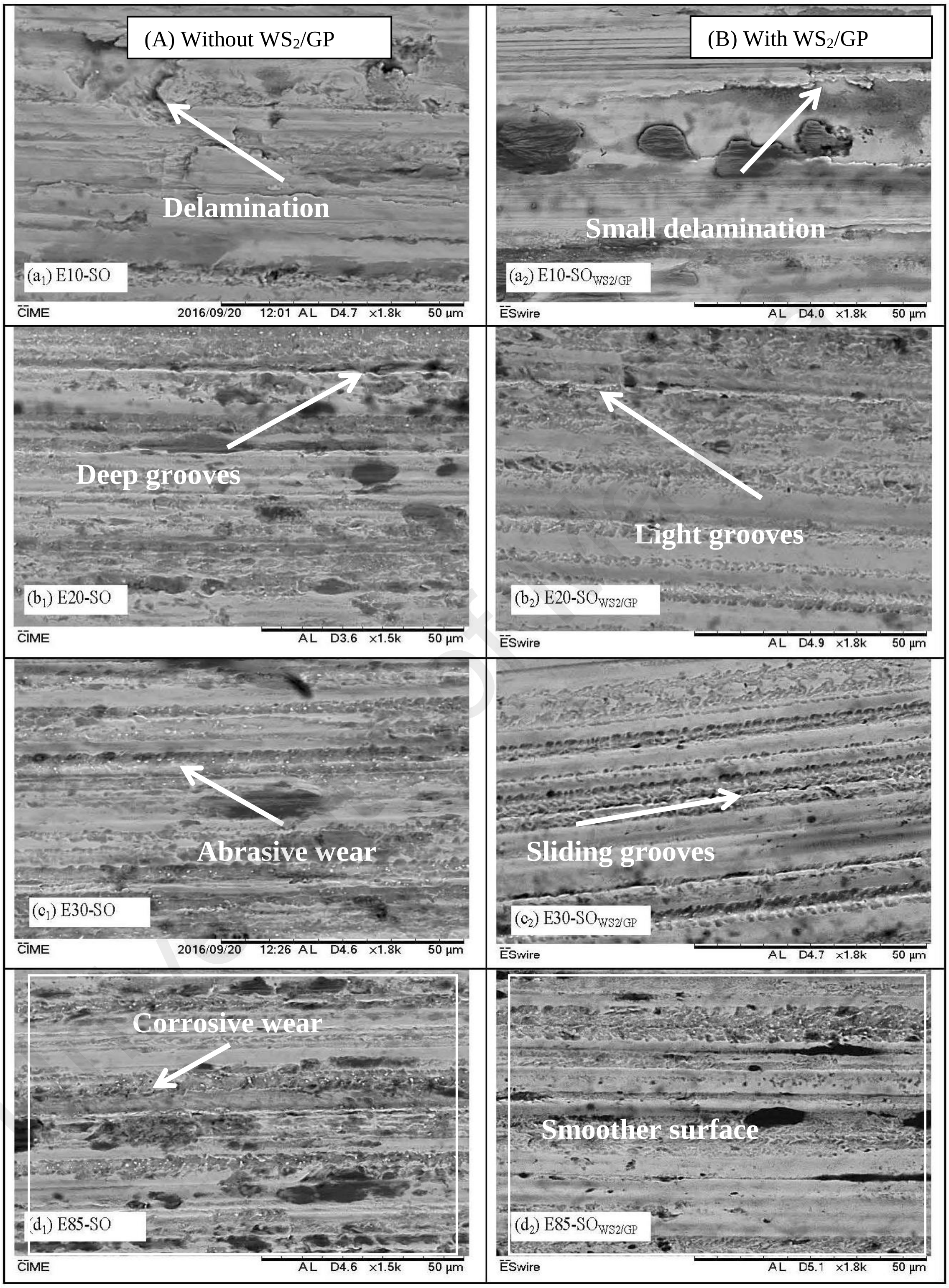

Figure 4. 15: Worn surface tested with bioethanol-diluted oils (A) without dispersion of GP/WS_2, and (B) with dispersion of GP/WS_2 (0.02 wt%)

4.3.4.2 EDS analysis

Figure 4.16 shows the EDS in the wear scar of the balls tested in SO, E10-SO, and E10-$SO_{GP/WS2}$. Figure 4.16a presents the EDS of the ball tested with pure SO. The peaks of Fe, C and Cr originate from the ball, and S and P are results of oil additives which can generate protective film and prevent the surface from sliding contact. This makes the surface smoother and has less deterioration. However, oil additives can be diminished by the fuel dilution (Uy et al., 2011). Figure 4.16b shows the presence of Na in the wear scar of the ball lubricated with E10-SO. The small amount of ethanol may interfere with the decomposition of the oil's anti-wear additive (*i.e.* ZDDP) which plays a critical role in tribofilm formation and wear mechanism (Costa & Spikes, 2016), and the high peak of O shows tribochemical oxidation since bioethanol-diluted oil contains higher acidity. The lower peaks of P and S indicate that bioethanol dilution destroyed oil additives, thus more surface roughness and deterioration due to lack of protective film. Kovalchenko et al. (2002) reported that the reduction of sulfur in the engine oil will degrade the scuffing protection of the lubricant. In figure 4.16c, it shows the EDS analysis of the wear scar of the ball lubricated with E10-$SO_{GP/WS2}$. After the addition of the combined GP/WS_2, peaks of W and S can be detected. Strong peaks of Fe and C were observed as graphene is made from carbon. The results of this EDS analysis further confirm that these two nano-additives GP/WS_2 adsorbed on the sliding contact and then generate the synergistic effect to reduce the friction and wear behaviors of pure commercial automotive lubricant, especially bioethanol-diluted engine oil (Zheng et al., 2017). The added GP/WS_2 can compensate the undesirable effect of bioethanol dilution in lubricant. It is also notified that the presence of GP/WS_2 is capable of reducing the occurrence tribo-oxidation from the dilution of bioethanol into engine oil (Zheng et al., 2017) as this can be observed by the lowest concentration of O.

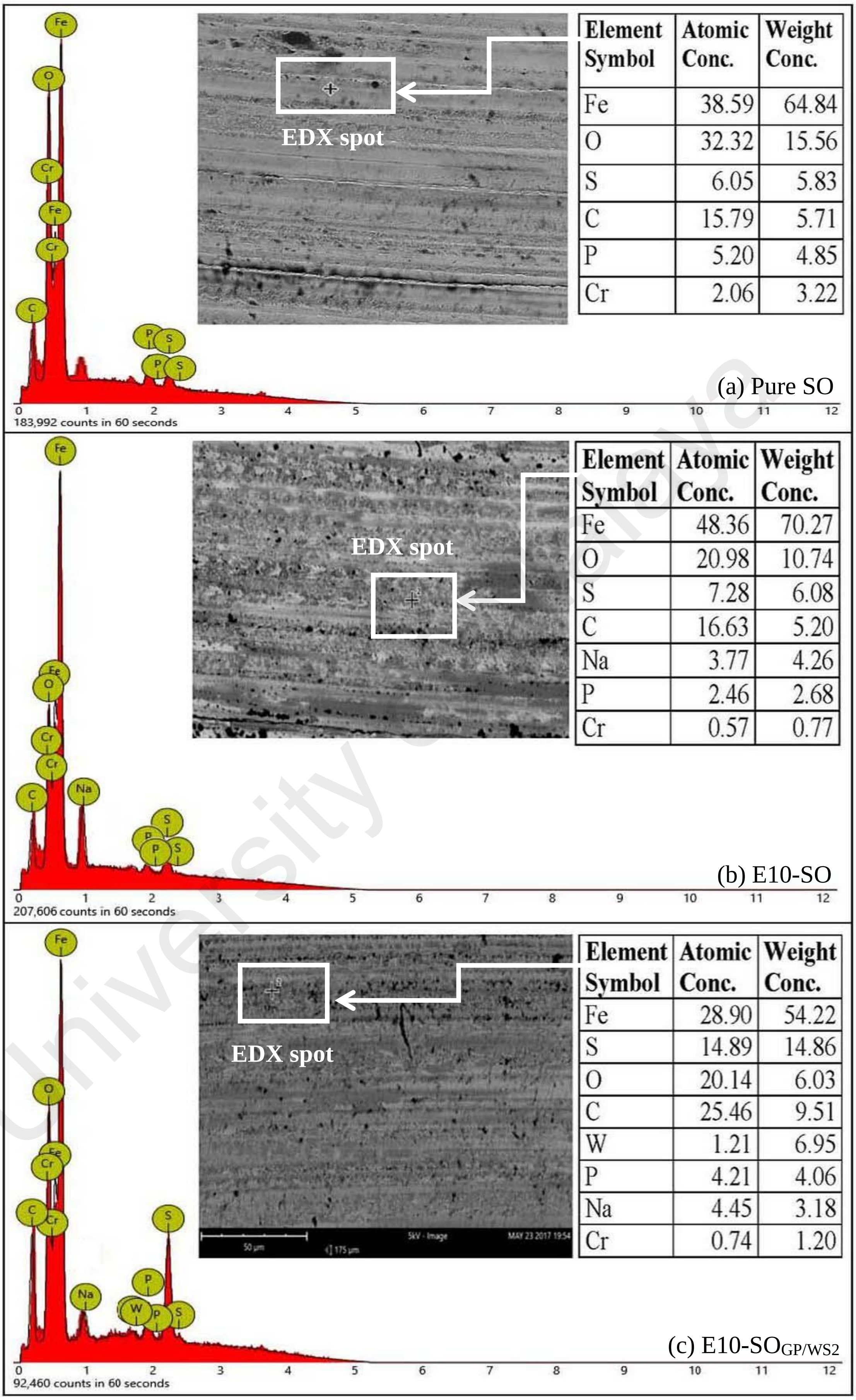

(a) Pure SO

Element Symbol	Atomic Conc.	Weight Conc.
Fe	38.59	64.84
O	32.32	15.56
S	6.05	5.83
C	15.79	5.71
P	5.20	4.85
Cr	2.06	3.22

(b) E10-SO

Element Symbol	Atomic Conc.	Weight Conc.
Fe	48.36	70.27
O	20.98	10.74
S	7.28	6.08
C	16.63	5.20
Na	3.77	4.26
P	2.46	2.68
Cr	0.57	0.77

(c) E10-SO$_{GP/WS2}$

Element Symbol	Atomic Conc.	Weight Conc.
Fe	28.90	54.22
S	14.89	14.86
O	20.14	6.03
C	25.46	9.51
W	1.21	6.95
P	4.21	4.06
Na	4.45	3.18
Cr	0.74	1.20

Figure 4. 16: EDS spectra of the wear scars of balls lubricated with (a) Fresh SO, (b) E10-SO, (c) E10-SO$_{GP/WS2}$ at 0.02wt%

4.4 Combined effect of GP/WS_2 nanocomposite and ta-C coating

4.4.1 Effect of GP/WS_2 and ta-C on friction

The combined effect of GP/WS_2 and ta-C coating was studied to understand the lubricating performance of bioethanol-diluted oil by using high HFRR. First, pure SO, E10-SO and E10-$SO_{GP/WS2}$ were tested with uncoated steel contacts, so that we can compare the results to the oil samples tested with ta-C coated steel contacts, and can understand the effect of nanocomposite and coating separately. Figure 4.17a presents the friction coefficients under the lubrication of pure SO, E10-SO and E10-$SO_{GP/WS2}$ with the uncoated surface. Pure SO shows low friction coefficient as it contains some main additives, so that it yields lower friction, while E10-SO yields slightly higher friction due to the presence of bioethanol inside the oil mixture, which degrades oil additive and then decreases lubricating performance. After the addition of 0.02 wt% GP/WS_2, E10-$SO_{GP/WS2}$ yields lower friction coefficient, compared to pure SO due to synergistic lubrication of GP/WS_2. However, the combined effect of GP/WS_2 and ta-C coating show a significant reduction in friction of all oil samples. Figure 4.17b presents the friction coefficients under the lubrication of pure SO, E10-SO and E10-$SO_{GP/WS2}$ with ta-C coated steel plate. It can be seen that the friction initially decreases and then gradually increases when all oil samples are tested with ta-C coated plate. Pure SO, E10-SO, and E10-$SO_{GP/WS2}$ yield low and almost identical coefficient of friction. This signifies that ta-C coating has high surface energy and high contact pressure at boundary lubrication condition which can reduce the contact area and protect sliding surface. ta-C provides low friction against steel with synthetic oil. It can be seen that the coating enhances running-in condition which can reduce the micropitting wear significantly. Therefore, the ta-C coating and GP/WS_2 play important role in improving lubricating performance, meaning that coating helps protect the surface from scuffing while GP/WS_2 penetrates into the metal-to-metal surface to generate lubricating film.

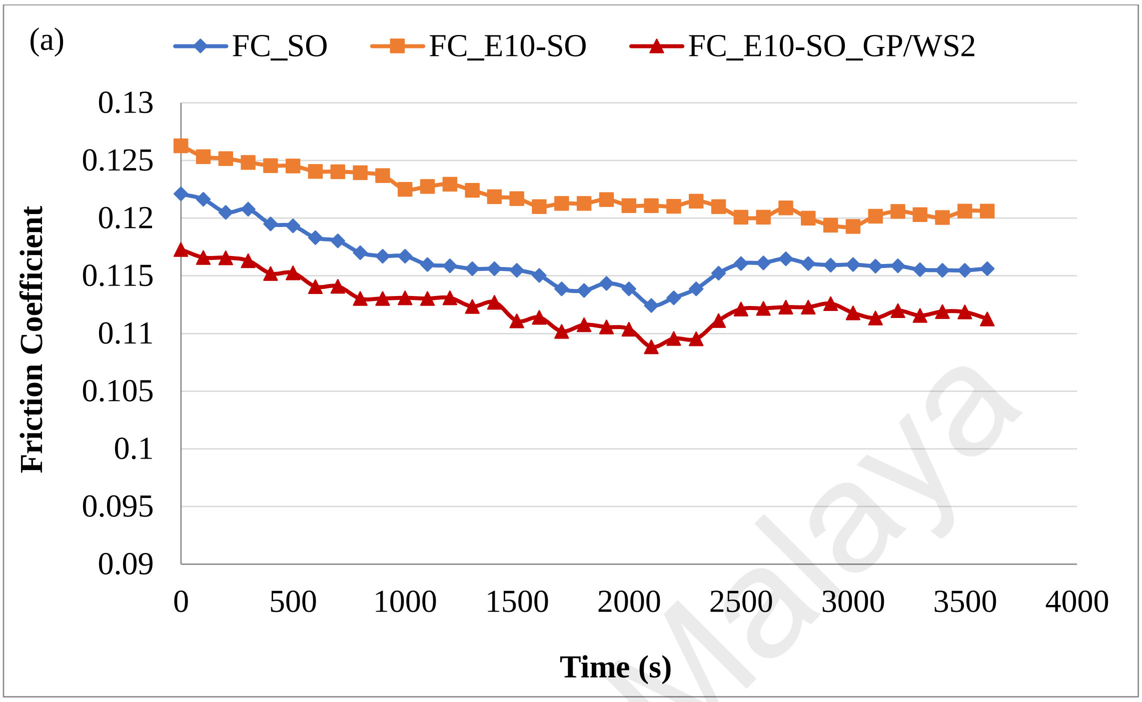

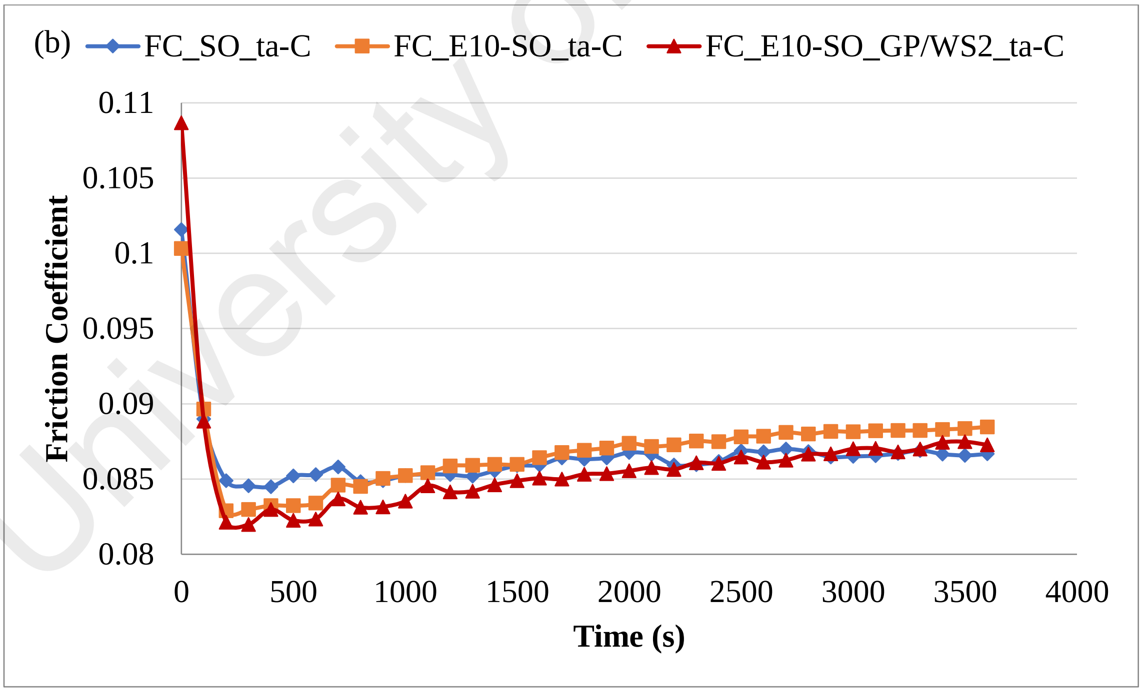

Figure 4. 17: Friction coefficient of SO, E10-SO and E10-SO$_{GP/WS2}$ at 0.02wt%, tested with (a) uncoated steel and (b) ta-C coated steels

4.4.2 Effect of GP/WS_2 and ta-C on Wear

Figure 4.18 shows the wear rates of SO, E10-SO, and E10-$SO_{GP/WS2}$ at 0.02wt% tested with (a) uncoated steels and (b) ta-C coated steels. First, pure SO, E10-SO and E10-$SO_{GP/WS2}$ were tested with uncoated steel contacts in order to compare wear behavior to the oil samples tested with ta-C coated steel contacts, as well as investigating individual wear protection of nanocomposite and coating. The wear coefficient of SO, E10-SO and E10-$SO_{GP/WS2}$ tested with uncoated contacts are presented in Figure 4.18a. Pure SO yield low wear coefficient as it contains some main additives, which can generate lubricating film between the rubbing contacts, while E10-SO (the bioethanol-diluted oil) yields slightly higher wear rate. The reason for this increase is probably due to the fact that oil additives are depleted by the presence of bioethanol dilution, which reduces protective film, thus increasing the contact region of the sliding surface. E10-$SO_{GP/WS2}$ yields the lowest wear losses after dispersing 0.02wt% GP/WS_2 because small grain size of GP/WS_2 penetrates into the sliding surface, and then creates space to avoid metal-to-metal contact. However, despite the dilution of bioethanol, further decrease in wear losses can be achieved when these oil samples are tested with ta-C coating. This indicates that the combined effect of GP/WS_2 and ta-C coating takes joint action in reducing wear losses. Figure 4.18b presents the wear coefficient of SO, E10-SO, and E10-$SO_{GP/WS2}$ tested with ta-C coated plate. Compared with the uncoated plate, SO further decreases wear losses when tested with ta-C coated steel contact. Moreover, E10-SO yields similar wear rate to pure SO, probably due to the significant effect of coating, which can protect steel surface lubricated with bioethanol-diluted oil. The ta-C coating also helps reduce the effect of bioethanol. ta-C coating has high surface energy that give good wettability for lubricant and it has high contact pressure at boundary lubrication condition which can reduce the contact area and protect sliding surface. ta-C has high hardness and excellent wear resistance to provides low friction against steel. E10-$SO_{GP/WS2}$ tested with ta-C steel contact has the lowest wear rate due to the fact the coating helps protect the surface from scuffing while GP/WS_2 penetrates into the metal-to-metal surface to generate lubricating film to keep space between sliding contacts and reduce wear losses.

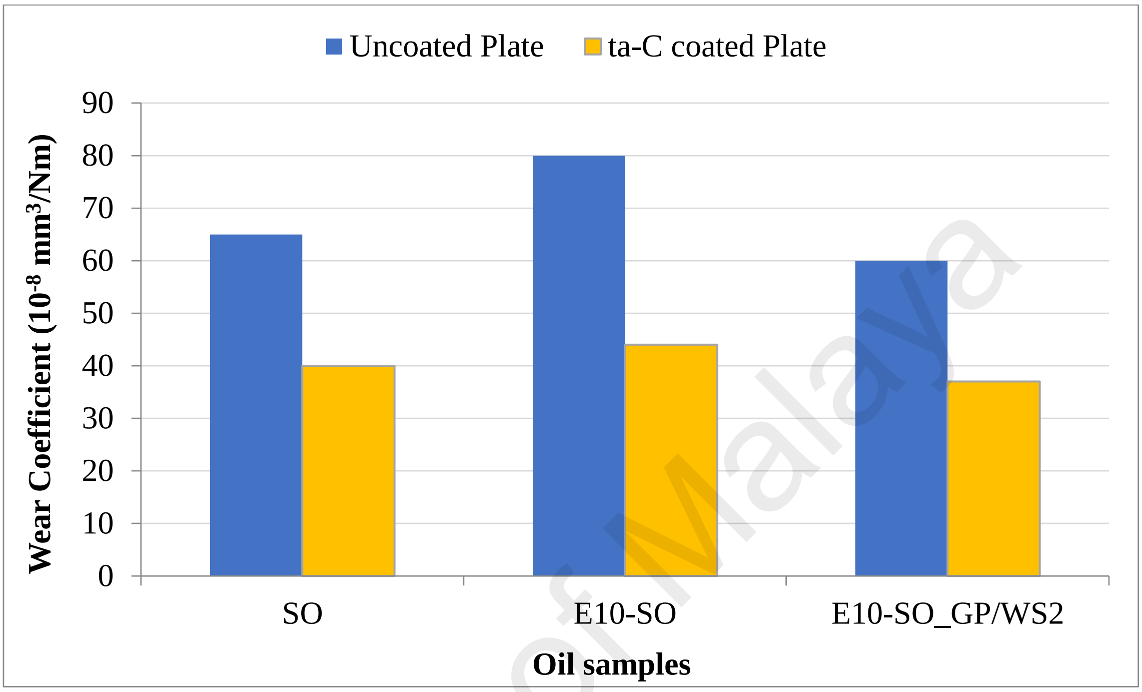

Figure 4. 18: Wear coefficient of SO, E10-SO, and E10-$SO_{GP/WS2}$ at 0.02wt%, tested with uncoated plate and ta-C coated plate

4.4.3 Worn surface analyses

4.4.3.1 SEM analysis

Figure 4.19 presents the SEM image of the uncoated surfaces and ta-C coated surfaces. The SEM of uncoated surface lubricated with SO shows a few small grooves as pure synthetic oil contains some main additives, which can prevent the surface from direct contact. For E10-SO, the worn surface shows more deterioration and displays deep grooves on the surface. This is because bioethanol dilution reduces the lubricating capacity of the engine oil. After adding GP/WS_2, E10-$SO_{GP/WS2}$ tested with uncoated plate shows a smoother surface with no obvious sliding grooves. The nanocomposite works to protect the sliding surfaces from direct contact. However, The SEM image of the ta-C coated plate under the lubrication of SO, E10-SO, and E10-$SO_{GP/WS2}$ shows no obvious of surface deterioration. Pure SO shows coating structure on the worn surface with no machining marks, while E10-SO shows almost identical surface defect to pure SO despite the present of bioethanol dilution, but it shows a small coating structure delamination. With combined effect of GP/WS_2 and ta-C, E10-$SO_{GP/WS2}$ presents the same smoother surface without obvious defects. All oil samples show almost identical surface pattern. ta-C coating has high surface energy that give good wettability for lubricant and it has high contact pressure at boundary lubrication condition which can reduce the contact area and protect sliding surface. ta-C has high hardness and excellent wear resistance to provides low friction against steel with synthetic oil. The roughness shown in the image indicates the bum structure of ta-C coating. It can be stated that the GP/WS_2 nanocomposite and ta-C coating can help eliminate the undesired effect of bioethanol dilution on engine oil lubrication.

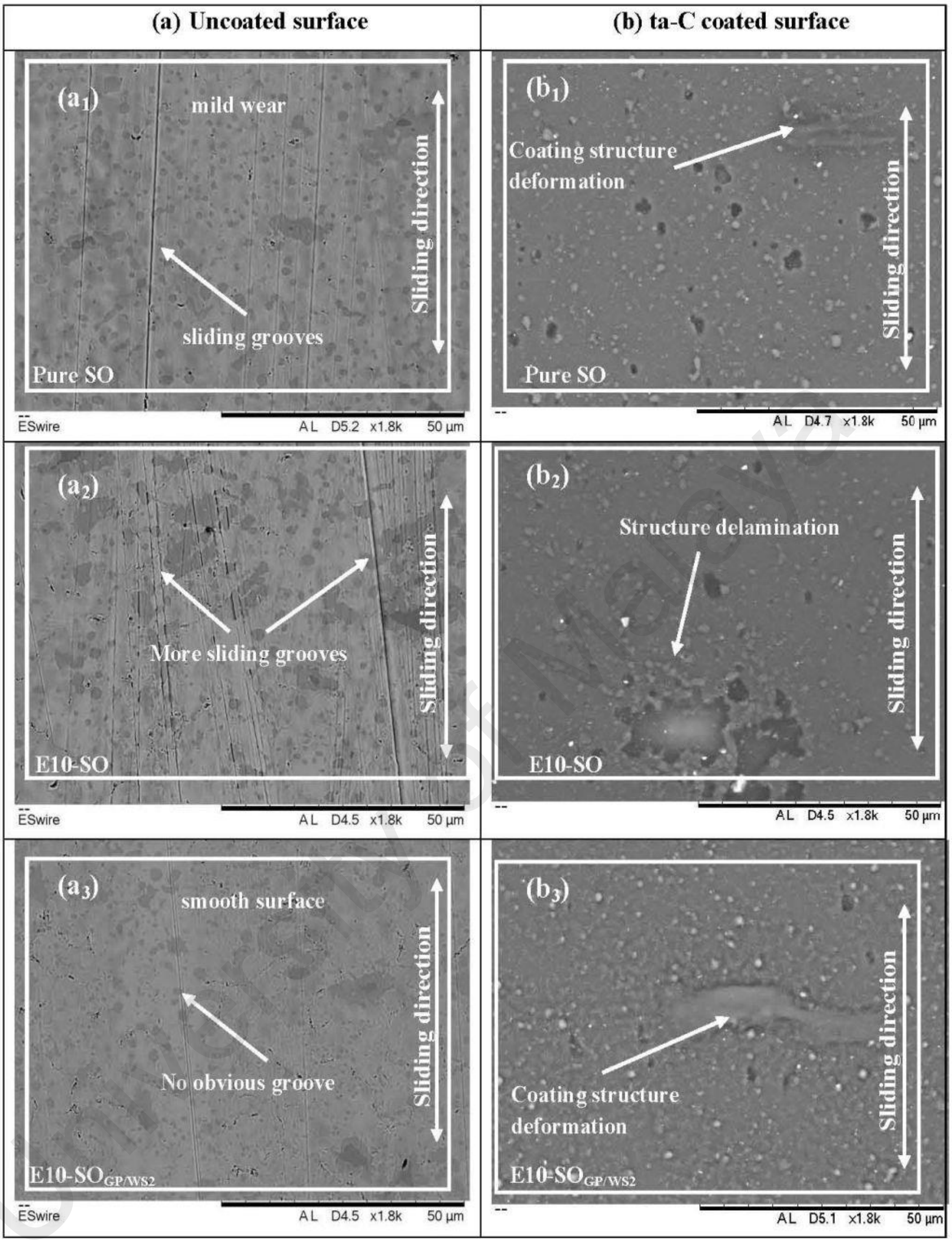

Figure 4. 19: SEM image of (a) uncoated plates and (b) ta-C coated plates lubricated with SO, E10-SO, and E10-$SO_{GP/WS2}$ at 0.02wt%

4.4.3.2 EDS analysis

This EDS analysis was performed to observe the elemental distribution of GP/WS_2 and ta-C. Figure 4.20 presents the elements in the wear scar of tested with ta-C coated plates under lubrication with SO, E10-SO, and E10-$SO_{GP/WS2}$. Figure 4.20a presents EDS of SO lubricated with ta-C coated plate. It shows very high percentage of carbon (C) followed by oxygen (O) and other elements such as ferrous (Fe) and chromium (Cr). These elements are originated from the ta-C coating. Similarly, E10-SO shows almost identical elemental distribution to SO. It can be observed from the EDS (figure 4.20b) that concentrations of sulfur (S) did not significantly change. It did not also show the presence of Sodium (Na) which indicates bioethanol dilution. Based on this EDS, it is shown that coating plays a major role in preventing the surface from deterioration. In figure 4.20c, it shows the EDS analysis of the ta-C coated plate lubricated with E10-$SO_{GP/WS2}$. The EDS is richer in Carbon compared to other oil samples. Moreover, the small peaks of W and S can be detected as nanocomposite is made from graphene and tungsten disulfide (GP/WS_2). The lower percentage of oxygen (O) reveals that GP/WS_2 and ta-C can significantly reduce the tribochemical oxidation of bioethanol-diluted engine oil. The results of this EDS analysis further confirm that GP/WS_2 deposited on ta-C coated surface, and jointly help reduce friction and wear of engine oil.

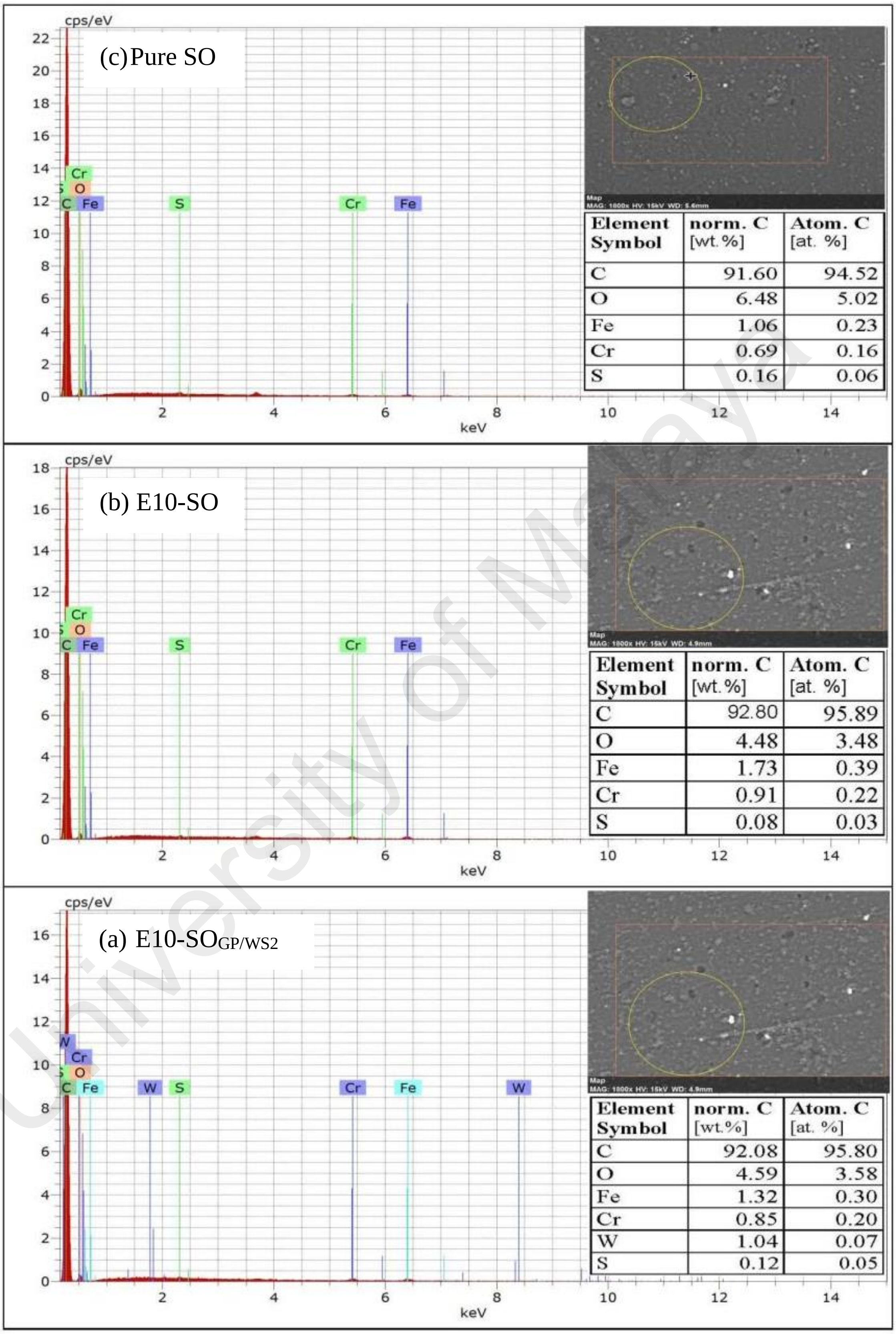

(c) Pure SO

Element Symbol	norm. C [wt.%]	Atom. C [at. %]
C	91.60	94.52
O	6.48	5.02
Fe	1.06	0.23
Cr	0.69	0.16
S	0.16	0.06

(b) E10-SO

Element Symbol	norm. C [wt.%]	Atom. C [at. %]
C	92.80	95.89
O	4.48	3.48
Fe	1.73	0.39
Cr	0.91	0.22
S	0.08	0.03

(a) E10-SO$_{GP/WS2}$

Element Symbol	norm. C [wt.%]	Atom. C [at. %]
C	92.08	95.80
O	4.59	3.58
Fe	1.32	0.30
Cr	0.85	0.20
W	1.04	0.07
S	0.12	0.05

Figure 4. 20: EDS spectra of the wear scars of ta-C coated plates lubricated with (a) Fresh SO, (b) E10-SO, and (c) E10-SO$_{WS2/GP}$ at 0.02wt%

CHAPTER 5: CONCLUSIONS AND RECOMMENDATIONS

5.1 Conclusions

This experimental study was conducted to assess the impact of bioethanol-gasoline blends on the tribological performance of engine oil and the influences of nanocomposite (GP/WS_2) and ta-C coating. The conclusions can be drawn as follows:

- The addition of all bioethanol-gasoline blends to the fresh oil decreases the viscosity of the fresh oil significantly to about 30%, and it increases the acid number marginally. The addition of bioethanol-gasoline fuels to synthetic oil slightly increases the friction compared to fresh oil at both loads, and it remarkably increases wear losses from 10% to 16%, accordingly. From the SEM result, the worn surface of the ball tested with fuel-oil samples has more surface deterioration than that tested with fresh oil.

- The friction coefficient was reduced slightly and wear scar diameter were reduced from 5% to 20%, accordingly, with the increase of WS_2/GP composite concentrations (0.01wt%-0.04wt %), as compared to those of bioethanol-diluted oil samples.

- The Present of WS2/GP nanocomposite and ta-C coating can exhibit excellent lubrication behavior. It can reduce not only the undesirable effect of bioethanol on engine oil but also friction and wear losses to about 25% and 39%, respectively.

The GP/WS_2 nanocomposite alone or the combination of WS2/GP and ta-C plays a major role to reduce friction and wear losses of sliding contact. From this study, it is suggested that 0.01%-0.02wt%.WS2/GP should be added to engine oil used with the bioethanol-fueled engine to improve the lubricating efficiency of the engine and to hamper the effect of bioethanol dilution on engine oil.

5.2 Recommendations

This research work has been carried out to understand the friction and wear characteristics of bioethanol-diluted engine oil as well as improving the tribological performance by using nanocomposite of graphene and tungsten disulfide (GP/WS_2). This study also provided the understanding of combined effect of GP/WS_2 and ta-C coating on engine oil with dilution of bioethanol. In this regard, the following recommendation for the future work can be suggested.

1. This research work carried out to test for friction and wear using four ball machine and high frequency reciprocating ring. It is recommended to focus on engine durability test using the bioethanol-fueled engine so that the study of friction and wear losses, fuel dilution, and oil degradation can be achieved.

2. In this research work, only 6% dilution by volume was selected for testing. It is recommended to use higher percentage dilution as fuel dilution of engine oil can be found up to 25% in the crankcase of the engine.

3. Moreover, this study focuses only on bioethanol fuel. It is also recommended that other alcohol fuel blends or other biodiesel fuel blends should be further investigated.

4. From this experimental study, it is suggested that the study on bioethanol-resistant engine oil production for higher bioethanol-fueled engine should be carried out.

REFERENCES

AFDC. (2016). Global Ethanol Production-Alternative Fuel Data Center. Retrieved from http://www.afdc.energy.gov/data/10331

Agarwal, A. K., & Gupta, J. G. (2014). Effect of Biodiesel Utilization on Tribological Properties of Lubricating Oil in a Compression Ignition Engine *Novel Combustion Concepts for Sustainable Energy Development* (pp. 75-87): Springer.

Agarwal, A. K., Pandey, A., Gupta, A. K., Aggarwal, S. K., & Kushari, A. (2014). *Novel combustion concepts for sustainable energy development*: Springer.

Agudelo, J., Delgado, Á., & Benjumea, P. (2011). The lubricity of ethanol-gasoline fuel blends. *Revista Facultad de Ingeniería Universidad de Antioquia*(58), 9-16.

Ajav, E., & Akingbehin, O. (2002). A study of some fuel properties of local ethanol blended with diesel fuel. *the CIGR Journal of Scientific Research and Development, 4*.

Ajayi, O. O., Lorenzo-Martin, C., Fenske, G., Corlett, J., Murphy, C., & Przesmitzki, S. (2016). Bioderived Fuel Blend Dilution of Marine Engine Oil and Impact on Friction and Wear Behavior. *Journal of Tribology, 138*(2), 021603.

Akponah E, A. O., Ubogu M. (2013). Bio-ethanol production from cassava effluent using Zymomonas mobilis and Saccharomyces cerevisiae isolated from rafia palm (Elaesis guineesi) SAP. *European Journal of Experimental Biology, 3*(4), 247-253.

Al Mahmud, K., Varman, M., Kalam, M., Masjuki, H., Mobarak, H., & Zulkifli, N. (2014). Tribological characteristics of amorphous hydrogenated (aC: H) and tetrahedral (ta-C) diamond-like carbon coating at different test temperatures in the presence of commercial lubricating oil. *Surface and Coatings Technology, 245*, 133-147.

Allmaier, H., Knauder, C., Salhofer, S., Reich, F., Schalk, E., Ofner, H., & Wagner, A. (2015). An experimental study of the load and heat influence from combustion on engine friction. *International Journal of Engine Research*, 1468087415579784.

Alptekin, E., & Canakci, M. (2009). Characterization of the key fuel properties of methyl ester–diesel fuel blends. *Fuel, 88*(1), 75-80.

Ancho, L. C. (2006). Oxidation in lubricant base oils.

Arslan, A., Masjuki, H., Kalam, M., Varman, M., Mufti, R., Mosarof, M., . . . Quazi, M. (2016). Surface Texture Manufacturing Techniques and Tribological Effect of Surface Texturing on Cutting Tool Performance: A Review. *Critical Reviews in Solid State and Materials Sciences,* 1-35.

Arslan, A., Masjuki, H., Varman, M., Kalam, M., Quazi, M., Al Mahmud, K., . . . Habibullah, M. (2015). Effects of texture diameter and depth on the tribological performance of DLC coating under lubricated sliding condition. *Applied Surface Science, 356*, 1135-1149.

Arslan, A., Masjuki, H. H., Varman, M., Kalam, M. A., Quazi, M. M., Al Mahmud, K. A. H., . . . Habibullah, M. (2015). Effects of texture diameter and depth on the tribological performance of DLC coating under lubricated sliding condition. *Applied Surface Science, 356*(Supplement C), 1135-1149. doi:https://doi.org/10.1016/j.apsusc.2015.08.194

Arslan, A., Masjuki, H. H., Varman, M., Kalam, M. A., Quazi, M. M., & Mosarof, M. H. (2016). Effect of change in temperature on the tribological performance of micro surface textured DLC coating. *Journal of Materials Research*, 1-11.

Arumugam, S., & Sriram, G. (2012). Comparative study of engine oil tribology, wear and combustion characteristics of direct injection compression ignition engine fuelled with castor oil biodiesel and diesel fuel. *Australian Journal of Mechanical Engineering, 10*(2), 119-128.

Australia, B. A. o. (2017). Ethanol use around the world. Retrieved from http://biofuelsassociation.com.au/biofuels/ethanol/ethanol-use-around-the-world/

Avinash, A., & Sasikumar, P. (2015). A comprehensive study on the emission characteristics of E-diesel dual-fuel engine. *Alexandria Engineering Journal*.

Baena, L., Gómez, M., & Calderón, J. (2012). Aggressiveness of a 20% bioethanol–80% gasoline mixture on autoparts: I behavior of metallic materials and evaluation of their electrochemical properties. *Fuel, 95*, 320-328.

Balat, M. (2011). Production of bioethanol from lignocellulosic materials via the biochemical pathway: A review. *Energy Conversion and Management, 52*(2), 858-875. doi:http://dx.doi.org/10.1016/j.enconman.2010.08.013

Balat, M., & Balat, H. (2009). Recent trends in global production and utilization of bio-ethanol fuel. *Applied Energy, 86*(11), 2273-2282.

Banerji, A., Lukitsch, M., & Alpas, A. (2016). Friction reduction mechanisms in cast iron sliding against DLC: Effect of biofuel (E85) diluted engine oil. *Wear, 368*, 196-209.

Battez, A. H., González, R., Viesca, J., Fernández, J., Fernández, J. D., Machado, A., . . . Riba, J. (2008). CuO, ZrO 2 and ZnO nanoparticles as antiwear additive in oil lubricants. *Wear, 265*(3), 422-428.

Becker, E. P. (2004). Trends in tribological materials and engine technology. *Tribology International, 37*(7), 569-575.

Berman, D., Erdemir, A., & Sumant, A. V. (2014). Graphene: a new emerging lubricant. *Materials Today, 17*(1), 31-42.

Besser, C., Schneidhofer, C., Dörr, N., Novotny-Farkas, F., & Allmaier, G. (2012). Investigation of long-term engine oil performance using lab-based artificial ageing illustrated by the impact of ethanol as fuel component. *Tribology International, 46*(1), 174-182.

Besser, C., Steinschütz, K., Dörr, N., Novotny-Farkas, F., & Allmaier, G. (2014). Impact of engine oil degradation on wear and corrosion caused by acetic acid evaluated by chassis dynamometer bench tests. *Wear, 317*(1–2), 64-76.

Bewilogua, K., & Hofmann, D. (2014). History of diamond-like carbon films—from first experiments to worldwide applications. *Surface and Coatings Technology, 242*, 214-225.

Boons, M., Van den Bulk, R., & King, T. (2008). *The impact of E85 use on lubricant performance* (0148-7191). Retrieved from

Briscoe, B., Thomas, P., & Williams, D. (1992). Microscopic origins of the interface friction of organic films: the potential of vibrational spectroscopy. *Wear, 153*(1), 263-275.

Cai, Z.-b., Zhao, L., Zhang, X., Yue, W., & Zhu, M.-h. (2016). Combined Effect of Textured Patterns and Graphene Flake Additives on Tribological Behavior under Boundary Lubrication. *PloS one, 11*(4), e0152143.

Cerny, J., & Vaclavickova, I. (2006). Shear stability of motor oils. *Goriva i maziva, 45*(5), 323-330.

Chen, G., Shen, Y., Zhang, Q., Yao, M., Zheng, Z., & Liu, H. (2013). Experimental study on combustion and emission characteristics of a diesel engine fueled with 2, 5-dimethylfuran–diesel, n-butanol–diesel and gasoline–diesel blends. *Energy, 54*, 333-342.

Cho, D.-H., & Lee, Y.-Z. (2009). Evaluation of ring surfaces with several coatings for friction, wear and scuffing life. *Transactions of Nonferrous Metals Society of China, 19*(4), 992-996.

Chui, G., & Baker, R. (1980). *Lubrication behavior in ethanol-fueled engines*. Paper presented at the Proceedings of the IV International Symposium on Alcohol Fuels Technology, Guaruja-SP-Brasil, 5-8 Oct. 1980.

Chui, G., & Millard, D. (1981). *Development and testing of crankcase lubricants for alcohol fueled engines* (0148-7191). Retrieved from

Costa, H. L., & Spikes, H. (2015). Effects of Ethanol Contamination on Friction and Elastohydrodynamic Film Thickness of Engine Oils. *Tribology Transactions, 58*(1), 158-168.

Costa, H. L., & Spikes, H. A. (2016). Impact of ethanol on the formation of antiwear tribofilms from engine lubricants. *Tribology International, 93*, 364-376.

Cousseau, T., Acero, J. S. R., & Sinatora, A. (2015). Tribological response of fresh and used engine oils: The effect of surface texturing, roughness and fuel type. *Tribology International*.

De Silva, P., Priest, M., Lee, P., Coy, R., & Taylor, R. (2011a). Tribometer investigation of the frictional response of piston rings when lubricated with the separated phases of lubricant contaminated with the gasoline engine biofuel ethanol and water. *Tribology Letters, 43*(2), 107-120.

De Silva, P., Priest, M., Lee, P., Coy, R., & Taylor, R. (2011b). Tribometer investigation of the frictional response of piston rings with lubricant contaminated with the gasoline engine biofuel ethanol and water. *Proceedings of the Institution of Mechanical Engineers, Part J: Journal of Engineering Tribology, 225*(6), 347-358.

De Silva, P. R. (2012). *The impact of biofuel ethanol on lubrication and friction in the piston assembly of a gasoline engine.* University of Leeds.

Demirbas, A. (2007). Producing and using bioethanol as an automotive fuel. *Energy Sources, Part B, 2*(4), 391-401.

Deng, X., Kousaka, H., Tokoroyama, T., & Umehara, N. (2014). Tribological behavior of tetrahedral amorphous carbon (ta-C) coatings at elevated temperatures. *Tribology International, 75*, 98-103.

Dhar, A., & Agarwal, A. K. (2014). Experimental investigations of effect of Karanja biodiesel on tribological properties of lubricating oil in a compression ignition engine. *Fuel, 130*, 112-119.

Enomoto, Y., & Yamamoto, T. (1998). New materials in automotive tribology. *Tribology Letters, 5*(1), 13-24.

Equey, S., Roos, S., Mueller, U., Hauert, R., Spencer, N. D., & Crockett, R. (2008). Tribofilm formation from ZnDTP on diamond-like carbon. *Wear, 264*(3), 316-321.

Erdemir, A. (2005). Review of engineered tribological interfaces for improved boundary lubrication. *Tribology International, 38*(3), 249-256. doi:10.1016/j.triboint.2004.08.008

Eswaraiah, V., Sankaranarayanan, V., & Ramaprabhu, S. (2011). Graphene-based engine oil nanofluids for tribological applications. *ACS applied materials & interfaces, 3*(11), 4221-4227.

Eyre, T., & Crawley, B. (1980). Camshaft and cam follower materials. *Tribology International, 13*(4), 147-152.

Ferrarese, A., Marques, G., Tomanik, E., Bruno, R., & Vatavuk, J. (2010a). Piston ring tribological challenges on the next generation of flex-fuel engines. *SAE International Journal of Engines, 3*(2), 85-91.

Ferrarese, A., Marques, G., Tomanik, E., Bruno, R., & Vatavuk, J. (2010b). Piston ring tribological challenges on the next generation of flex-fuel engines. *SAE International Journal of Engines, 3*(2010-01-1529), 85-91.

Friedl, J., & Stimming, U. (2013). Model catalyst studies on hydrogen and ethanol oxidation for fuel cells. *Electrochimica Acta, 101*, 41-58.

Gili, F., Igartua, A., Luther, R., & Woydt, M. (2011). The impact of biofuels on engine oil performance. *Lubrication Science, 23*(7), 313-330.

Gu, G. X. (2014). *Development and application of a lubricant composition model to study effects of oil transport, vaporization, fuel dilution, and soot contamination on lubricant rheology and engine friction.* Massachusetts Institute of Technology.

Guo, M. f., Cai, Z.-b., Zhang, Z.-c., & Zhu, M.-h. (2015). Characterization and lubrication performance of diesel soot nanoparticles as oil lubricant additives. *RSC Advances, 5*(123), 101965-101974.

Guo, Y. B., & Zhang, S.-W. (2016). The Tribological Properties of Multi-Layered Graphene as Additives of PAO2 Oil in Steel–Steel Contacts. *Lubricants, 4*(3), 30.

Gur'yanov, Y. A. (2007). Criteria for limiting contamination of motor oil by fuel. *Chemistry and Technology of Fuels and Oils, 43*(1), 30-36.

Gusain, R., Mungse, H. P., Kumar, N., Ravindran, T., Pandian, R., Sugimura, H., & Khatri, O. P. (2016). Covalently attached graphene–ionic liquid hybrid nanomaterials: synthesis, characterization and tribological application. *Journal of Materials Chemistry A, 4*(3), 926-937.

Gwidon, W. S., & Andrew, W. B. (1993). 13 Corrosive and Oxidative Wear. In G. W. Stachowiak & A. W. Batchelor (Eds.), *Tribology Series* (Vol. Volume 24, pp. 637-656): Elsevier.

Hazar, H., & Temizer, İ. (2012). The engine performance of a diesel engine and the research of the effect of fuel additives on engine oil and engine parts. *Scientific Bulletin of the Petru Maior University of Targu Mures, 9*(2).

Heywood, J. B. (1988). *Internal combustion engine fundamentals* (Vol. 930): Mcgraw-hill New York.

Howard, k. (2014). Advanced engine oils to improve the performance of modern intermal combustion engines. In R. Folkson (Ed.), *Alternative Fuels and Advanced Vehicle Technologies for Improved Environmental Performance: Towards Zero Carbon Transportation*. UK: Elsevier.

Hu, T., Teng, H., Luo, X., & Chen, B. (2015a). Impact of Fuel Injection on Dilution of Engine Crankcase Oil for Turbocharged Gasoline Direct-Injection Engines. *SAE International Journal of Engines, 8*(3), 1107-1116.

Hu, T., Teng, H., Luo, X., & Chen, B. (2015b). Impact of Fuel Injection on Dilution of Engine Crankcase Oil for Turbocharged Gasoline Direct-Injection Engines. *SAE International Journal of Engines, 8*(2015-01-0967), 1107-1116.

Hu, T., Teng, H., Luo, X., & Chen, B. (2015c). Impact of Fuel Injection on Dilution of Engine Crankcase Oil for Turbocharged Gasoline Direct-Injection Engines. *SAE International Journal of Engines*, *8*(2015-01-0967).

Ing, T. C., Mohammed Rafiq, A., Azli, Y., & Syahrullail, S. (2012). The effect of temperature on the tribological behavior of RBD palm stearin. *Tribology Transactions, 55*(5), 539-548.

Jafari, H., Idris, M., Ourdjini, A., Rahimi, H., & Ghobadian, B. (2010). Effect of ethanol as gasoline additive on vehicle fuel delivery system corrosion. *Materials and corrosion, 61*(5), 432-440.

Jakóbiec, J., & Mazanek, A. (2009). Comparative assessment of SL/CF SAE 5W/30 lubricating oil service in engines fuelled by 95 hydrocarbon gasoline and gasoline with 5%(V/V) ethanol additive. *Teka Komisji Motoryzacji i Energetyki Rolnictwa, 9*.

Johnston, S., & Hainsworth, S. V. (2013). Effect of DLC coatings on wear in automotive applications. *Surface engineering*.

Kalin, M., Velkavrh, I., Vižintin, J., & Ožbolt, L. (2008). Review of boundary lubrication mechanisms of DLC coatings used in mechanical applications. *Meccanica, 43*(6), 623-637.

Kano, M., & Tanimoto, I. (1991). Wear mechanism of high wear-resistant materials for automotive valve trains. *Wear, 151*(2), 229-243.

Kevin Fisher, R. M. (2006). Illinois State Geological Survey Evaluation of CO2 Capture Options from Ethanol Plants. *Trimeric Corporation*.

Kim, S., & Dale, B. E. (2004). Global potential bioethanol production from wasted crops and crop residues. *Biomass and Bioenergy, 26*(4), 361-375.

Kim, Y., Park, H., An, J. U., Kan, T.-S., & Park, J. (2011). Development of nano diamond polymer coating on piston skirt for fuel efficiency. *SAE International Journal of Engines, 4*(2011-01-1401), 2080-2086.

Koçar, G., & Civaş, N. (2013). An overview of biofuels from energy crops: Current status and future prospects. *Renewable and Sustainable Energy Reviews, 28*, 900-916.

Koji Kato, & Adachi, K. (2000). Wear mechanisms. In B. Bhushan (Ed.), *Modern tribology handbook* (Vol. 1, pp. 273-299). New York: CRC press.

Kovalchenko, A., Ajayi, O. O., Erdemir, A., & Fenske, G. R. (2002). *Friction and wear performance of low-friction carbon coatings under oil lubrication* (0148-7191). Retrieved from

Kržan, B., Novotny-Farkas, F., & Vižintin, J. (2009). Tribological behavior of tungsten-doped DLC coating under oil lubrication. *Tribology International, 42*(2), 229-235.

Kwanchareon, P., Luengnaruemitchai, A., & Jai-In, S. (2007). Solubility of a diesel–biodiesel–ethanol blend, its fuel properties, and its emission characteristics from diesel engine. *Fuel, 86*(7), 1053-1061.

Lapuerta, M. n., García-Contreras, R., Campos-Fernández, J., & Dorado, M. P. (2010). Stability, lubricity, viscosity, and cold-flow properties of alcohol− diesel blends. *Energy & fuels, 24*(8), 4497-4502.

Li, D., Müller, M. B., Gilje, S., Kaner, R. B., & Wallace, G. G. (2008). Processable aqueous dispersions of graphene nanosheets. *Nature nanotechnology, 3*(2), 101-105.

Li, D., Zhen, H., Xingcai, L., Wu-gao, Z., & Jian-Guang, Y. (2005). Physico-chemical properties of ethanol–diesel blend fuel and its effect on performance and emissions of diesel engines. *Renewable energy, 30*(6), 967-976.

Lide, D. R. (2000). *CRC handbook of chemistry and physics* (81 st ed.). Maryland: CRC Press.

Lin, Y.-C., Kan, T.-H., Chen, J.-N., Tsai, J.-C., Ku, Y.-Y., & Lin, K.-W. (2013). Tribological performance of engine oil blended with various diesel fuels. *Tribology Transactions, 56*(6), 997-1010.

Ljubas, D., Krpan, H., & Matanović, I. (2010). Influence of engine oils dilution by fuels on their viscosity, flash point and fire point. *Nafta, 61*(2), 73-79.

Lu, X., Cotter, J., & Eadie, D. (2005). Laboratory study of the tribological properties of friction modifier thin films for friction control at the wheel/rail interface. *Wear, 259*(7), 1262-1269.

Martyr, A. J., & Plint, M. A. (2012). Tribology, Fuel, and LubricantEngine Testing *Engine testing: The design, building, modification and use of powertrain test facilities*: Elsevier.

Masjuki, H., & Maleque, M. (1997). Investigation of the anti-wear characteristics of palm oil methyl ester using a four-ball tribometer test. *Wear, 206*(1), 179-186.

Matuszewska, A., Odziemkowska, M., & Czarnocka, J. (2013). Properties of bioethanol-diesel oil mixtures.

Meng, Y., Su, F., & Chen, Y. (2016a). Supercritical Fluid Synthesis and Tribological Applications of Silver Nanoparticle-decorated Graphene in Engine Oil Nanofluid. *Scientific reports, 6*.

Meng, Y., Su, F., & Chen, Y. (2016b). Supercritical Fluid Synthesis and Tribological Applications of Silver Nanoparticle-decorated Graphene in Engine Oil Nanofluid. *Scientific Reports, 6,* 31246.

Mistry, K. K., Morina, A., & Neville, A. (2011). A tribochemical evaluation of a WC–DLC coating in EP lubrication conditions. *Wear, 271*(9), 1739-1744.

Mofijur, M., Masjuki, H., Kalam, M., Atabani, A., Fattah, I. R., & Mobarak, H. (2014). Comparative evaluation of performance and emission characteristics of Moringa oleifera and Palm oil based biodiesel in a diesel engine. *Industrial Crops and Products, 53,* 78-84.

Mosarof, M., Kalam, M., Masjuki, H., Arslan, A., Monirul, I., Ruhul, A., . . . Khuong, L. (2016). Analysis of thermal stability and lubrication characteristics of Millettia pinnata oil. *RSC Advances, 6*(84), 81414-81425.

Mosarof, M., Kalam, M. A., Masjuki, H., Arslan, A., ISLAM, M. M., Ruhul, A. M., . . . Leang, S. K. (2016). Analysis of thermal stability and lubrication characteristics of Millettia pinnata oil. *RSC Advances*.

Mosarof, M. H., Kalam, M. A., Masjuki, H. H., Alabdulkarem, A., Ashraful, A. M., Arslan, A., . . . Monirul, I. M. (2016). Optimization of performance, emission, friction and wear characteristics of palm and Calophyllum inophyllum biodiesel blends. *Energy Conversion and Management, 118*(Supplement C), 119-134. doi:https://doi.org/10.1016/j.enconman.2016.03.081

Mosarof, M. H., Kalam, M. A., Masjuki, H. H., Alabdulkarem, A., Habibullah, M., Arslan, A., & Monirul, I. M. (2016). Assessment of friction and wear characteristics of Calophyllum inophyllum and palm biodiesel. *Industrial Crops and Products, 83*, 470-483.

Mutafov, P., Lanigan, J., Neville, A., Cavaleiro, A., & Polcar, T. (2014). DLC-W coatings tested in combustion engine—Frictional and wear analysis. *Surface and Coatings Technology, 260*, 284-289.

Nakamura, Y., Egami, Y., & Shimizu, K. (1996). *Development of an assembled camshaft by mechanical bonding* (0148-7191). Retrieved from

Neville, A., Morina, A., Haque, T., & Voong, M. (2007). Compatibility between tribological surfaces and lubricant additives—how friction and wear reduction can be controlled by surface/lube synergies. *Tribology International, 40*(10), 1680-1695.

Pawlak, Z. (2003). Lubrication chemistry *Tribochemistry of lubricating oils* (Vol. 45): Elsevier.

Podgornik, B., Jacobson, S., & Hogmark, S. (2003). DLC coating of boundary lubricated components—advantages of coating one of the contact surfaces rather than both or none. *Tribology International, 36*(11), 843-849.

Priest, M. (2012). Impact of ethanol biofuel on automotive piston ring friction. Retrieved from https://institutes.engineering.leeds.ac.uk/thermofluids/research/tribology-surface-engineering/current-research/impact-of-ethanol-biofuel.shtml

Quazi, M., Fazal, M., Haseeb, A., Yusof, F., Masjuki, H., & Arslan, A. (2016a). Laser-based surface modifications of aluminum and its alloys. *Critical Reviews in Solid State and Materials Sciences, 41*(2), 106-131.

Quazi, M., Fazal, M., Haseeb, A., Yusof, F., Masjuki, H., & Arslan, A. (2016b). A review to the laser cladding of self-lubricating composite coatings. *Lasers in Manufacturing and Materials Processing, 3*(2), 67-99.

Rahimi, B., Semnani, A., Nezamzadeh-Ejhieh, A., Shakoori Langeroodi, H., & Hakim Davood, M. (2012). Monitoring of the physical and chemical properties of a gasoline engine oil during its usage. *Journal of analytical methods in chemistry, 2012*.

Rahman, M. N., Atan, N., Mokhtar, A., & Khalid, A. (2014). Influences of intake temperature and bio-petrol fuel temperature on SI engine: an overview.

REBEL. (2011). Bioenergy-Renewable Energy. *Bioethanol Processing.* Retrieved from http://www.responsiblebusiness.eu/display/rebwp7/PDF

Rejowski, E. D., Mordente Sr, P., Pillis, M. F., & Casserly, T. (2012). *Application of DLC coating in cylinder liners for friction reduction* (0148-7191). Retrieved from

Richardson, D. E. (2000a). Review of power cylinder friction for diesel engines. *Journal of engineering for gas turbines and power, 122*(4), 506-519.

Richardson, D. E. (2000b). Review of power cylinder friction for diesel engines. *TRANSACTIONS-AMERICAN SOCIETY OF MECHANICAL ENGINEERS JOURNAL OF ENGINEERING FOR GAS TURBINES AND POWER, 122*(4), 506-519.

Rizvi, S. Q. A. (2009). Dispersants. In L. R. Rudnick (Ed.), *Lubricant additives: chemistry and applications*: CRC press.

Robinson, J. W., Zhou, Y., Bhattacharya, P., Erck, R., Qu, J., Bays, J. T., & Cosimbescu, L. (2016). Probing the molecular design of hyper-branched aryl polyesters towards lubricant applications. *Scientific Reports, 6*, 18624. doi:10.1038/srep18624

https://www.nature.com/articles/srep18624#supplementary-information

Sagawa, T., Fujimoto, H., & Nakamura, K. (2002). *Study of Fuel Dilution in Direct-Injection and Multipoint Injection Gasoline Engines*. Retrieved from

Schamel, A., Grischke, M., & Bethke, R. (1997). *Amorphous carbon coatings for low friction and wear in bucket tappet valvetrains* (0148-7191). Retrieved from

Schwartz, S. E., Smolenski, D. J., & Clark, S. L. (1988). *Entry and retention of methanol fuel in engine oil*. Retrieved from

Shahabuddin, M., Masjuki, H., Kalam, M., Bhuiya, M., & Mehat, H. (2013). Comparative tribological investigation of bio-lubricant formulated from a non-edible oil source (Jatropha oil). *Industrial Crops and Products, 47*, 323-330.

Shanta, S., Molina, G., & Soloiu, V. (2011). Tribological effects of mineral-oil lubricant contamination with biofuels: a pin-on-disk tribometry and wear study. *Advances in Tribology, 2011*.

Shanta, S. M. (2011). *Investigations of the tribological effects of engine oil dilution by vegetable and animal fat feedstock biodiesel on selected surfaces.* (Master), Georgia Southern University. Retrieved from http://digitalcommons.georgiasouthern.edu/etd/776 (776)

Smith, O., Priest, M., Taylor, R., Price, R., & Cantley, A. (2005). *In-cylinder fuel and lubricant effects on gasoline engine friction.* Paper presented at the World Tribology Congress III.

Song, H.-J., & Li, N. (2011). Frictional behavior of oxide graphene nanosheets as water-base lubricant additive. *Applied Physics A: Materials Science & Processing, 105*(4), 827-832.

Spikes, H., & Costa, H. (2016). Impact of ethanol on the formation of antiwear tribofilms from engine lubricants. *Tribology International, 93,* 364-376.

Stachowiak, G., & Batchelor, A. W. (2005). *Engineering tribology* (3 rd ed.). Butterworth-Heinemann: Oxford: Elsevier.

SUDZUCKERGroup. (2016). Bioethanol as a growth market. Retrieved from http://www.cropenergies.com/en/Bioethanol/Markt/Dynamisches_Wachstum/

Tandon, A., Kumar, A., Mondal, P., Vijay, P., Bhangale, U., & Tyagi, D. (2011). Tribological Issues Related to the Use of Biofuels: A New Environmental Challenge. *British Journal of Environment & Climate Change, 1*(2), 28-43.

Tasdemir, H. A., Tokoroyama, T., Kousaka, H., Umehara, N., & Mabuchi, Y. (2014). Influence of zinc dialkyldithiophosphate tribofilm formation on the tribological performance of self-mated diamond-like carbon contacts under boundary lubrication. *Thin Solid Films, 562*, 389-397.

Tasdemir, H. A., Wakayama, M., Tokoroyama, T., Kousaka, H., Umehara, N., Mabuchi, Y., & Higuchi, T. (2014). The effect of oil temperature and additive concentration on the wear of non-hydrogenated DLC coating. *Tribology International, 77,* 65-71.

Taylor, B. J., & Eyre, T. S. (1979). A review of piston ring and cylinder liner materials. *Tribology International, 12*(2), 79-89.

Tippayawong, N., & Sooksarn, P. (2010). Assessment of lubricating oil degradation in small motorcycle engine fueled with gasohol. *MAEJO INTERNATIONAL JOURNAL OF SCIENCE AND TECHNOLOGY, 4*(2), 201-209.

Torres-Jimenez, E., Jerman, M. S., Gregorc, A., Lisec, I., Dorado, M. P., & Kegl, B. (2011). Physical and chemical properties of ethanol–diesel fuel blends. *Fuel, 90*(2), 795-802.

Tung, S. C., & Gao, H. (2003). Tribological characteristics and surface interaction between piston ring coatings and a blend of energy-conserving oils and ethanol fuels. *Wear, 255*(7), 1276-1285.

Tung, S. C., & McMillan, M. L. (2004). Automotive tribology overview of current advances and challenges for the future. *Tribology International, 37*(7), 517-536. doi:http://dx.doi.org/10.1016/j.triboint.2004.01.013

Tze-Chi Jao, C. A. P. (2008). Application of Surfactants in Lubricants and Fuels. In U. Zoller (Ed.), *Handbook of detergents, part F: Production* (Vol. 142): CRC Press.

Uy, D., Simko, S. J., Carter Iii, R. O., Jensen, R. K., & Gangopadhyay, A. K. (2007). Characterization of anti-wear films formed from fresh and aged engine oils. *Wear, 263*(7–12), 1165-1174.

Uy, D., Zdrodowski, R. J., O'neill, A. E., Simko, S. J., Gangopadhyay, A. K., Morcos, M., . . . Parsons, G. (2011). Comparison of the effects of biodiesel and mineral diesel fuel dilution on aged engine oil properties. *Tribology Transactions, 54*(5), 749-763.

Vengudusamy, B., Green, J. H., Lamb, G. D., & Spikes, H. A. (2011). Tribological properties of tribofilms formed from ZDDP in DLC/DLC and DLC/steel contacts. *Tribology International, 44*(2), 165-174.

Veselá, K., Pexa, M., & Mařík, J. (2009). The effect of biofuels on the quality and purity of engine oil. *Agronomy Research, 12*(2), 425-430.

Wattrus, M. (2013a). Fuel property effects on oil dilution in diesel engines. *SAE International Journal of Fuels and Lubricants, 6*(3), 794-806.

Wattrus, M. (2013b). *Fuel Property Effects on Oil Dilution in Diesel Engines*. Retrieved from

Windholz, M. (1979). *an encyclopedia of chemicals, drugs, and biologicals* (9 th ed.): Rahway (N.J.) : Merck.

Woo, C. (2017). Biofuels in Asia. Retrieved from http://www.acfa.org.sg/pdf/ACFA%20ARTC%202017_final_no%20text.pdf

Wu, Tsui, W., & Liu, T. (2007). Experimental analysis of tribological properties of lubricating oils with nanoparticle additives. *Wear, 262*(7), 819-825.

Wu, Y., Li, W., Zhang, M., & Wang, X. (2013). Oxidative degradation of synthetic ester and its influence on tribological behavior. *Tribology International, 64*, 16-23.

Xie, H., Jiang, B., He, J., Xia, X., & Pan, F. (2016). Lubrication performance of MoS 2 and SiO 2 nanoparticles as lubricant additives in magnesium alloy-steel contacts. *Tribology International, 93*, 63-70.

Xu, B., Qi, Y., Zhang, W., & Cai, S. (2007). Fuel properties and emissions characteristics of ethanol-diesel blend on small diesel engine. *International journal of automotive technology, 8*(1), 9-18.

Yasuda, Y., Kano, M., Mabuchi, Y., & Abou, S. (2003). *Research on diamond-like carbon coatings for low-friction valve lifters* (0148-7191). Retrieved from

Yoshida, H., Kusama, K., & Sagawa, J. (1990). *Effects of surface treatments on piston ring friction force and wear* (0148-7191). Retrieved from

Yücesu, H. S., Topgül, T., Cinar, C., & Okur, M. (2006). Effect of ethanol–gasoline blends on engine performance and exhaust emissions in different compression ratios. *Applied Thermal Engineering, 26*(17), 2272-2278.

Yusoff, M. N. A. M., Zulkifli, N. W. M., Masum, B. M., & Masjuki, H. H. (2015). Feasibility of bioethanol and biobutanol as transportation fuel in spark-ignition engine: a review. *RSC Advances, 5*(121), 100184-100211. doi:10.1039/C5RA12735A

Zahid, R., Hassan, M. B. H., Varman, M., Mufti, R. A., Kalam, M. A., Zulkifli, N. W. B. M., & Gulzar, M. (2016). A Review on Effects of Lubricant Formulations on Tribological Performance and Boundary Lubrication Mechanisms of Non-Doped DLC/DLC Contacts. *Critical Reviews in Solid State and Materials Sciences*, 1-28.

Zahid, R., Masjuki, H., Varman, M., Mufti, R. A., Kalam, M. A., & Gulzar, M. (2015). Effect of lubricant formulations on the tribological performance of self-mated doped DLC contacts: A review. *Tribology Letters, 58*(2), 32.

Zheng, D., Wu, Y.-p., Li, Z.-y., & Cai, Z.-b. (2017). Tribological properties of WS 2/graphene nanocomposites as lubricating oil additives. *RSC Advances, 7*(23), 14060-14068.

Zulkifli, N. W. M., Kalam, M. A., Masjuki, H. H., Shahabuddin, M., & Yunus, R. (2013). Wear prevention characteristics of a palm oil-based TMP (trimethylolpropane) ester as an engine lubricant. *Energy, 54*, 167-173.

B.1. List of publication

Journal Article

1. Khuong, L. S., Zulkifli, N. W. M., Masjuki, H. H., Mohamad, E. N., Arslan, A., Mosarof, M. H., & Azham, A. (2016). A review on the effect of bioethanol dilution on the properties and performance of automotive lubricants in gasoline engines. *RSC Advances, 6*(71), 66847-66869. **[ISI Journal, Q2]**

2. Khuong, L. S., Masjuki, H. H., Zulkifli, N. W. M., Mohamad, E. N., Kalam, M. A., Abdullah Alabdulkarem, Arslan, A., Mosarof, M. H., Syahir, A. Z., & Jamshaid, M. (2017). Effect of gasoline–bioethanol blends on the properties and lubrication characteristics of commercial engine oil. *RSC Advances*, *7*(25), 15005-15019. **[ISI Journal, Q2].**